

**THE UNIVERSITY OF HULL**

**Synthesis and characterization of new ring opening  
polymerization (ROP) catalysts based on aluminium or  
tungsten complexes.**

being a Thesis submitted for the Degree of  
Master of Science by Research  
in the University of Hull

By  
**Xinsen Sun, B.Sc.**  
February 2014

© 2014

This copy of the thesis has been supplied on condition that anyone who consults it is understood to recognise that its copyright rests with the author and that no quotation from thesis, nor any information derived therefrom, may be published without the author's prior, written consent.

## Abstract

Cyclic esters provide versatile biocompatible and biodegradable polymers possessing good mechanical properties. These polymers are also models for studying the kinetics, thermodynamics, and mechanisms of many elementary reactions in polymerization. Both organoaluminium and tungsten complexes for ring opening polymerization have received increasing attention over the last few years. The aim of this study is to investigate a series of new complexes incorporating aluminium and tungsten metals in combination of various ligands, and assess their ability as catalysts for the ring opening polymerization of  $\epsilon$ -caprolactone and *rac*-lactide.

Reaction of  $\text{Me}_3\text{Al}$  (two equivalents) with anisidines formed a family of organoaluminium complexes, viz  $\{[1,2-(\text{OMe}),\text{N-C}_6\text{H}_4(\mu\text{-Me}_2\text{Al})](\mu\text{-Me}_2\text{Al})\}_2$  (**1**),  $[1,3-(\text{Me}_3\text{AlOMe}),\text{NHC}_6\text{H}_4(\mu\text{-Me}_2\text{Al})]_2$  (**2**) and  $[1,4-(\text{Me}_3\text{AlOMe}),\text{NHC}_6\text{H}_4(\mu\text{-Me}_2\text{Al})]_2$  (**3**). Complexes **1** - **3** were found to be highly active for the ring opening polymerization (ROP) of  $\epsilon$ -caprolactone either with or without benzyl alcohol present; at various temperatures, the activity order **1** > **2**  $\approx$  **3** was observed. For the ROP of *rac*-lactide results for **1** - **3** were poor (Chapter 2).

By varying the reaction conditions, the reaction of  $[\text{W}(\text{eg})_3]$  ( $\text{eg} = 1,2\text{-ethanediolato}$ ) with *p-tert*-butylcalix[*n*]areneH<sub>*n*</sub> (*n* = 6 or 8) in refluxing toluene affords different tungstocalixarene complexes. Complexes  $\{[\text{W}(\text{eg})]_2(\mu\text{-O})p\text{-tert-butylcalix}[6]\text{arene}\}$  (**1**),  $\{[\text{W}(\text{eg})]_2p\text{-tert-butylcalix}[8]\text{arene}\} \cdot \text{MeCN}$  (**3**),  $\{1,2\text{-}[\text{W}(\text{eg})_2]_2p\text{-tert-butylcalix}[8]\text{areneH}_4\} / \{1,3\text{-}[\text{W}(\text{eg})_2]_2p\text{-tert-butylcalix}[8]\text{areneH}_4\}$  (**4a**)/(**4b**)  $\cdot 3.5\text{MeCN}$  and  $\{[\text{WO}(\text{eg})]_2p\text{-tert-butyltetrahomodioxacalix}[6]\text{areneH}_2\}$  (**5**) have been screened for their ability to ring open polymerize (ROP)  $\epsilon$ -caprolactone; conversion rates were poor at temperatures below 110 °C. All tungsten complexes have similar conversion rates, yet ROP using complex **3** has outstanding polymerization weight compared with other co-catalysts (Chapter 3).

## **Acknowledgement**

First and foremost thanks to the Almighty God of Chemistry, who gave me challenges, joys and ability to accomplish this research work.

I wish to express my profound sense of gratitude towards my principal supervisor, Prof. Carl Redshaw, who enlightened my way with his valuable guidance, suggestions and continuous encouragement, during the research work and the preparation of this thesis. The opportunity he gave to me to study in Hull has been really fantastic.

I am also thankful to my associate supervisors, Dr. Timothy J. Prior, for his advice. He has been great help for me to settle into a new environment, and his strict reminder of safety helps me form good experimental habits. Also Dr Mark Elsegood (Loughborough University) is thanked for some of the X-ray crystallography.

I would also like to thank David Miller and Shanyan Mo for being great people to have worked alongside and for the great laughs and memories as part of the Team. Adam, Liam and Rhiannon have brought fresh air to our lab. They maximized the happy atmosphere in our group!

I would also like to thanks many researchers and staff involved with me at University of Hull for their help and support during my research.

Lastly, I owe my family members an expression of my gratitude for their patience, understanding, support and encouragement during the completion of this research work. I am especially grateful to Jessie Du; thank you for seeing me through the ups and downs. The life in UK has been fascinating with you. You have been amazing!

## List of Abbreviation

<b>ABS</b>	Acrylonitrile Butadiene Styrene
<b>ASA</b>	Acrylonitrile Styrene Acrylate
<b>atm</b>	The standard atmosphere
<b>BnOH</b>	Benzyl alcohol
<b><i>t</i>Bu</b>	Butyl
<b>Cp</b>	cyclopentadienyl
<b>DLA</b>	<i>D, D</i> -lactide
<b>LCD</b>	Liquid-crystal-display
<b>LLA</b>	<i>L, L</i> -lactide
<b>h</b>	hour
<b>M</b>	metal
<b><i>meso</i>- LA</b>	<i>meso</i> -lactide
<b><i>rac</i>- LA</b>	<i>racemic</i> lactide
<b>MAO</b>	Methylaluminoxane
<b>min</b>	Minutes
<b><math>M_n</math></b>	Number-averaged molecular weight
<b><math>M_w</math></b>	Weight-averaged molecular weight
<b>NMR</b>	Nuclear magnetic resonance
<b>PA</b>	Polyamide
<b>PC</b>	Polycarbonate
<b>PDI</b>	Polydispersity index
<b>PE</b>	Polyethylene
<b>PE- HD</b>	Polyethylene, high density



<b>PE- LD</b>	Polyethylene, low density
<b>PE- LLD</b>	Polyethylene, linear low density
<b>PE- MD</b>	Polyethylene, medium density
<b>PET</b>	Polyethylene terephthalate
<b>PCL</b>	Poly $\epsilon$ - caprolactone
<b>PLA</b>	Poly lactide
<b>PUR</b>	Polyurethane
<b>PMMA</b>	Polymethyl methacrylate
<b>PP</b>	Polypropylene
<b>ppm</b>	Parts per million
<b>PS</b>	Polystyrene
<b>PS- E</b>	Polystyrene, expandable
<b>PVC</b>	Polyvinyl chloride
<b>ROP</b>	Ring opening polymerization
<b>SAN</b>	Styrene-acrylonitrile
<b>THF</b>	Tetrahydrofuran
<b>TMA</b>	Trimethylaluminium
<b>Å</b>	angstrom
<b>°C</b>	Degree Celsius

## List of Figures

<b>Figure 1.</b>	World plastics production 1950-2012.	P4
<b>Figure 2.</b>	European plastics demand* by segment and resin type 2012	P5
<b>Figure 3.</b>	Activation of metallocene with TMA. Ti can be substitute with Zr,	P10
<b>Figure 4.</b>	Molecular structure of <b>1</b> showing the atom numbering scheme.	P47
<b>Figure 5.</b>	Molecular structure of <b>2</b> showing the atom numbering scheme.	P48
<b>Figure 6.</b>	Molecular structure of <b>3</b> showing the atom numbering scheme.	P49
<b>Figure 7.</b>	$M_n$ and $M_w/M_n$ vs. monomer conversion in the ROP of $\epsilon$ -CL initiated by <b>1</b> / <i>o</i> -anisidine aluminium complex (Table 1, entries 1–5).	P51
<b>Figure 8.</b>	Plots of $M_n$ values vs. CL/Al molar ratio in the ROP of $\epsilon$ -CL initiated by <b>1</b> (Table 1, entries 2, and 8–11).	P52
<b>Figure 9.</b>	Monomer conversion and $M_n \times 10^{-4}$ vs different Al-anisidine Compound <b>1</b> , <b>2</b> and <b>3</b> in the ROP of $\epsilon$ -CL (Table 2, entries 1-6 and 10-12).	P55
<b>Figure 10.</b>	Two views to emphasize the calix conformation of <b>1</b> .	P63
<b>Figure 11.</b>	Molecular structure of <b>2</b> showing the atom numbering scheme.	P64
<b>Figure 12.</b>	Bi-layer packing of <b>2</b> .	P65
<b>Figure 13.</b>	Molecular structure of compound <b>3</b> .	P66
<b>Figure 14.</b>	Top, Molecular structure of the major isomer of <b>4a</b> ; bottom, molecular structure of minor isomer of <b>4b</b> .	P67
<b>Figure 15.</b>	Two views of the molecular structure of <b>5</b> .	P69
<b>Figure 16.</b>	$^1\text{H}$ NMR of $\{[1,4-(\text{Me}_3\text{AlOMe}),\text{NH}-\text{C}_6\text{H}_4](\mu-\text{Me}_2\text{Al})\}_2$ ( <b>3</b> ).	P76
<b>Figure 17.</b>	$^1\text{H}$ NMR of $\epsilon$ -caprolactone.	P78

- Figure 18.** Figure 18.  $^1\text{H}$  NMR of  $\epsilon$ -caprolactone after ring opening polymerization using **1** 80°C for 30 minutes. P78
- Figure 19.**  $^1\text{H}$  NMR of calix[8]arene P80
- Figure 20.**  $^1\text{H}$  NMR of p-*tert*-butyltetrahomodioxacalix[6]areneH<sub>6</sub> P84
- Figure 21.** Figure 21. Partial  $^1\text{H}$  NMR of W(eg)<sub>3</sub> indicates 12 H have observed for OCH<sub>2</sub>. P85

## List of Schemes

<b>Scheme 1.</b>	Simple schematic retranslation for polymerization.	P6
<b>Scheme 2.</b>	Simple schematic retranslation for Initiation step.	P6
<b>Scheme 3.</b>	Simple schematic retranslation for propagation step.	P6
<b>Scheme 4.</b>	Simple schematic retranslation for termination step.	P7
<b>Scheme 5.</b>	Simple Schematic demonstration of Ziegler –Natta heterogeneous Catalyst.	P8
<b>Scheme 6.</b>	Structures of monomers and their polymers for lactide (PLA) and $\epsilon$ -Caprolactone (PCL).	P10
<b>Scheme 7.</b>	Structures of stereoisomers for lactide.	P11
<b>Scheme 8.</b>	Two types of bond cleavage for $\beta$ -butyrolactone ring.	P13
<b>Scheme 9.</b>	Scheme 9. Simple schematic translation of Ring Opening Polymerization mechanism for $\epsilon$ -CL	P15
<b>Scheme 10.</b>	Normal coordination insertion.	P15
<b>Scheme 11.</b>	Intra- molecular lactone switching.	P16
<b>Scheme 12.</b>	Inter- molecular lactone switching.	P16
<b>Scheme 13.</b>	Aluminium Complexes from Lin <b>1</b> and Chisholm <b>2</b> groups.	P18
<b>Scheme 14.</b>	Aluminium Complex <b>3</b> of Hsueh's research.	P19
<b>Scheme 15.</b>	Aluminium Complexes <b>4-6</b> from Chisholm's research	P20
<b>Scheme 16.</b>	Oxygen (sulfur) coordinated organic aluminium complexes.	P21
<b>Scheme 17.</b>	Nitrogen coordinated organic aluminium complexes form Inoue and Emig's research.	P22
<b>Scheme 18.</b>	Simple schematic retranslation of nitrogen coordinated organic aluminium complexes from Chen, Wang, Mu and Sun's research.	P23
<b>Scheme 19.</b>	Simple schematic retranslation of nitrogen coordinated organic aluminium complexes from Wang's research.	P25
<b>Scheme 20.</b>	Simple schematic retranslation of oxygen and nitrogen coordinated organic aluminium complexes from N. Nomura and K. Nomura's research.	P26
<b>Scheme 21.</b>	Simple schematic retranslation of oxygen, nitrogen coordinated	P27

	organic aluminium Salen complexes.	
<b>Scheme 22.</b>	Simple schematic retranslation of oxygen, nitrogen coordinated organic aluminium Salen complexes from Chen and Carpentier's research.	P28
<b>Scheme 23.</b>	Simple schematic retranslation of oxygen, nitrogen coordinated organic aluminium complexes from Wang, Darensbourg, Getzler and Ko's research.	P30
<b>Scheme 24.</b>	Simple schematic retranslation of tungstocalix [5] complexes from Lattman's research. L= NH <i>t</i> Bu <b>41</b> , SO <sub>3</sub> CF <sub>3</sub> <b>42</b> .	P31
<b>Scheme 25.</b>	Simple schematic retranslation of tungstocalix complexes. Upper left <b>43</b> ; upper right <b>44</b> R= <i>t</i> Bu , S= MeCN; Bottom <b>45</b> .	P32
<b>Scheme 26.</b>	Scheme 26. Chelating ligands used in this study. <i>o</i> , <i>m</i> , <i>p</i> - anisidines and calixarenes.	P34
<b>Scheme 27.</b>	Reported organometallic ring opening polymerization pre-catalyst.	P45
<b>Scheme 28.</b>	Simple schematic retranslation of tungstocalix complexes <b>1-5</b> .	P62
<b>Scheme 29.</b>	Schematic retranslation of synthesis tetrahomodioxacalix[6]arene.	P82
<b>Scheme 30.</b>	Scheme 30. Schematic retranslation of W(eg) <sub>3</sub> ( <b>d</b> ) and its by-products ( <b>a</b> ), ( <b>b</b> ) and ( <b>c</b> ).	P85

## List of Tables

<b>Table 1.</b>	Ring Opening Polymerization screening of $\varepsilon$ -CL by pre-catalysts <b>1</b> . <sup>a</sup>	P50
<b>Table 2.</b>	Ring Opening Polymerization screening of $\varepsilon$ -CL by pre-catalysts <b>1</b> to <b>3</b> . <sup>a</sup>	P53
<b>Table 3.</b>	Screening of the known [1, 2] complexes Me <sub>2</sub> Al[O-2- <i>t</i> Bu-6-(RN=CH)C <sub>6</sub> H <sub>3</sub> ] (R = <i>t</i> Bu ( <b>4</b> ), C <sub>6</sub> F <sub>5</sub> ( <b>5</b> ))	P55
<b>Table 4.</b>	Ring Opening Polymerization screening of <i>rac</i> -LA by pre-catalysts <b>1</b> to <b>3</b> . <sup>a</sup>	P56
<b>Table 5.</b>	Ring Opening Polymerization screening of $\varepsilon$ -CL by tungsten pre-catalysts <b>1</b> , <b>3-5</b> .	P71

# Contents

	page
<b>Abstract</b>	<b>i</b>
<b>Acknowledgement</b>	<b>ii</b>
<b>List of Abbreviation</b>	<b>iii</b>
<b>List of Figures</b>	<b>v</b>
<b>List of Schemes</b>	<b>vii</b>
<b>List of Tables</b>	<b>ix</b>
<b>Contents</b>	<b>ix</b>
<b>Chapter 1: General Introduction</b>	
1.1. Introduction	2
1.1.1 Plastics	2
1.1.2 Polymers	6
1.1.2.1 Ziegler- Natta Catalyst	8
1.1.2.2 Metallocene Catalyst	9
1.1.3 Poly Cyclic Esters	10
1.1.3.1 Poly Lactide and Poly $\epsilon$ -caprolactone	12
1.1.4 Aluminium Catalysts	17
1.1.4.1 Oxygen (sulfur) coordinated organic aluminium complexes	18
1.1.4.2 Nitrogen coordinated organic aluminium complexes	21
1.1.4.3 Oxygen, nitrogen coordinated organic aluminium complexes	25
1.1.5 Tungsten Calixarene Complexes	30
1.2 Characterization of GPC	33
1.3 Aim of Study	34
1.4 Thesis overview	36
1.5 References	37

## **Chapter 2. Organoaluminium complexes of *ortho*-, *meta*-, *para*-anisidines**

2.1 Introduction	44
2.1.1 Organoaluminium complexes and its ring opening polymerization	44
2.2 Result and Discussion	46
2.2.1 Ring Opening Polymerization (ROP) of $\epsilon$ -Caprolactone ( $\epsilon$ -CL).	50
2.2.2 Ring Opening Polymerization (ROP) of <i>rac</i> -lactide ( <i>rac</i> -LA).	56
2.2.3 Conclusion	57
2.3 References	58

## **Chapter 3. Organotungsten complexes of calix[6 and 8]arenes**

3.1 Introduction	61
3.1.1 Tungstocalixarene complexes and its ring opening polymerization	61
3.2 Result and Discussion	62
3.2.1 Ring Opening Polymerization (ROP) of $\epsilon$ -Caprolactone ( $\epsilon$ -CL).	69
3.2.2 Conclusion	72
3.3 References	73

## **Chapter 4. Experiment Section**

4.1 General Consideration	75
4.2 Organoaluminium complexes of <i>ortho</i> -, <i>meta</i> -, <i>para</i> -anisidines	75
4.2.1 Synthesis of {[1,4-(Me <sub>3</sub> AlOMe),NH-C <sub>6</sub> H <sub>4</sub> ]( $\mu$ -Me <sub>2</sub> Al)} <sub>2</sub> ( <b>3</b> )	75
4.2.2 Ring opening polymerization.	77



4.2.3 Crystallography	79
4.3 Organotungsten complexes of calix[6 and 8]arenes	80
4.3.1 Synthesis of calixarene.	80
4.3.1.1 Synthesis of calixarene[8]	80
4.3.1.2 Synthesis of calixarene[6]	81
4.3.1.3 Synthesis of p- <i>tert</i> -butyltetrahomodioxacalix[6]areneH <sub>6</sub>	82
4.3.2 Synthesis of [W(eg) <sub>3</sub> ]	84
4.3.3 Synthesis of Tungstocalixarene complexes	86
4.3.3.1 Synthesis of {[W(eg) <sub>2</sub> ] <sub>2</sub> p- <i>tert</i> -butylcalix[6]areneH <sub>2</sub> }·MeCN	86
4.3.3.2 Synthesis of {1,2-[W(eg) <sub>2</sub> ] <sub>2</sub> p- <i>tert</i> -butylcalix[8]areneH <sub>4</sub> }/ {1,3-[W(eg) <sub>2</sub> ] <sub>2</sub> p- <i>tert</i> -butylcalix[8]areneH <sub>4</sub> }·3.5MeCN	86
4.3.3.3 Synthesis of {[WO(eg) <sub>2</sub> ] <sub>2</sub> p- <i>tert</i> -butyltetrahomodioxacalix[6] areneH <sub>2</sub> }	86
4.3.4 Ring Opening Polymerization	88
4.3.5 Crystallography	88
<b>4.4 References</b>	
<b>Appendix</b>	<b>90</b>

# **Chapter 1**

## **Introduction**

# **1. 1 Introduction**

## **1.1Plastics**

A plastic is a type of synthetic or man-made polymer, similar in many ways to natural products found in plants and animal parts. Webster's Dictionary defines polymers as "any of various complex organic compounds produced by polymerization, capable of being molded, extruded, cast into various shapes and films, or drawn into filaments and then used as textile fibres"

Although natural polymers, such as amber, tortoise shells and animal horns, have been established for thousands of years, and the history of manufactured plastics goes back more than 100 years, when compared to other materials, plastics are relatively modern. Alexander Parkes produce the first artificial plastic at the 1862 Great International Exhibition in London. This material was an organic material, which came from cellulose, could be molded when heat was applied and retained its shape when the temperatures cooled off. The creator of this material claimed that this new material could do anything that rubber was capable of, but at a cheaper price. He had discovered a material that moved the entire human civilization to move from the age of iron into a new era. <sup>1</sup>

In 1907, chemist Leo Hendrik Baekland, while striving to produce a synthetic varnish, stumbled upon the formula for a new synthetic polymer originating from coal tar. He subsequently named the new substance "Bakelite." Bakelite, once formed, could not be melted. Because of its properties as an electrical insulator, Bakelite was used in the production of high-tech objects including cameras and telephones. It was also used in the production of ashtrays and as a substitute for jade, marble and amber. By 1909, Baekland had coined "plastics" as the term to describe this completely new category of materials.

The first patent for polyvinyl chloride (PVC), a substance now used widely in vinyl siding and water pipes, was registered in 1914. Cellophane was also discovered during this period.<sup>1</sup>

Plastics did not really take off until after the First World War, with the use of petroleum, a substance easier to process than coal into raw materials. Plastics served as substitutes for wood, glass and metal during the hardship times of World War's I & II. After World War II, newer plastics, such as polyurethane, polyester, silicones, polypropylene, and polycarbonate joined poly methyl methacrylate and polystyrene and PVC in widespread applications. Many more would follow and by the 1960s, plastics were within everyone's reach due to their inexpensive cost. Plastics had thus come to be considered 'common'—a symbol of the consumer society.

Since the 1970s, we have witnessed the advent of 'high-tech' plastics used in demanding fields such as health and technology. New types and forms of plastics with new or improved performance characteristics continue to be developed. With continuous growth for more than 50 years, global production in 2012 rose to 288 million tonnes, with a 2.8 % increase compared to 2011 (Figure 1).<sup>2</sup> We now use and produce almost 175 times as much plastic as we did in 1950. The expected plastic consumption in 2016 will be over 400 million tonnes.<sup>3</sup>

Plastics usage over the past century has enabled society to make huge technological advances. Although the largest area of using plastic is within the packaging sector, which represents 39.4 % of the total plastics demand, there is huge demand from different sectors for various kinds of plastics (Figure 2).<sup>2</sup> Plastics have become an important part of our modern lifestyle. Without the introduction of plastics, commodity products of

modern life, LCD flat screen television or touch screen smartphones would not be possible! We would not be able to practice most sports as well, since most of sports equipment and outfits are made of plastics. In the medical and safety area, plastics directly lead to breakthroughs. Therefore, some people even claim post 20<sup>th</sup> century is the age of plastic.

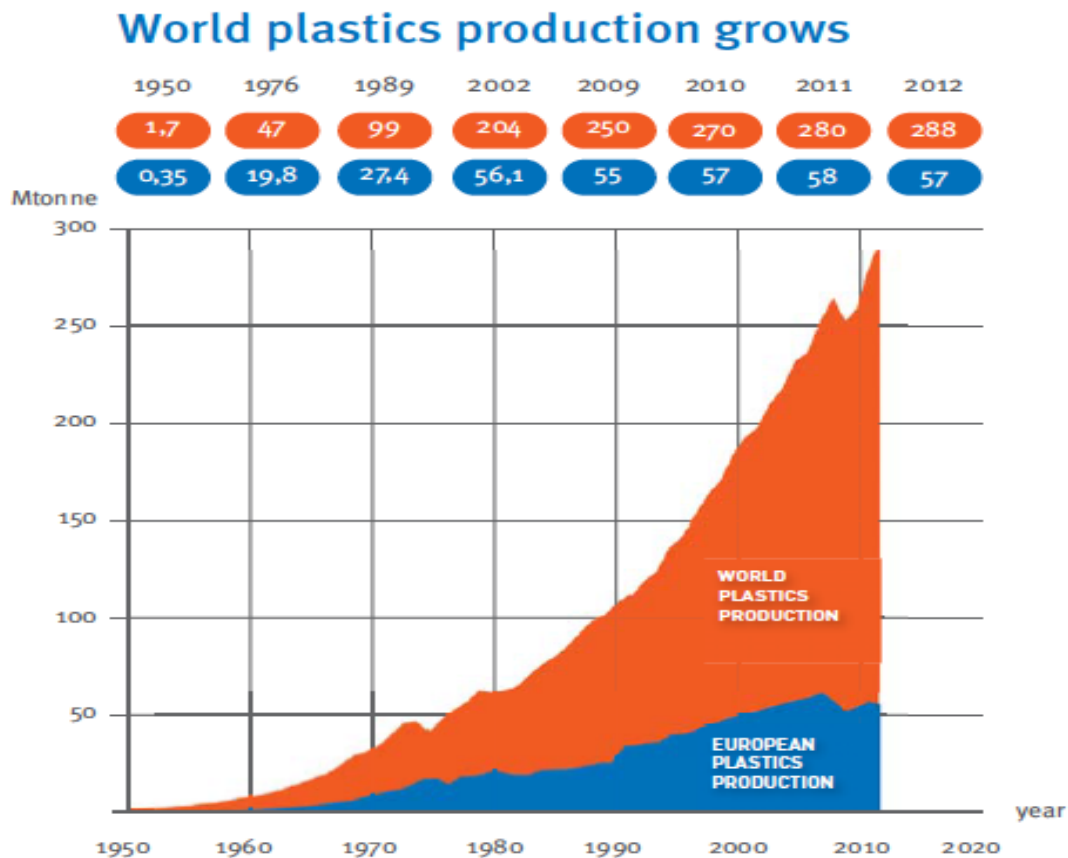


**Figure 1.** World plastic production with Europe plastics production 1950-2012. Includes thermoplastics, polyurethanes, thermosets, elastomers, adhesives, coatings and sealants and PP-fibres. Not included PET-, PA- and polyacryl-fibers. (Picture reproduce from Plastic Europe, *Plastics- the Fact 2013*, 2013) <sup>2</sup>

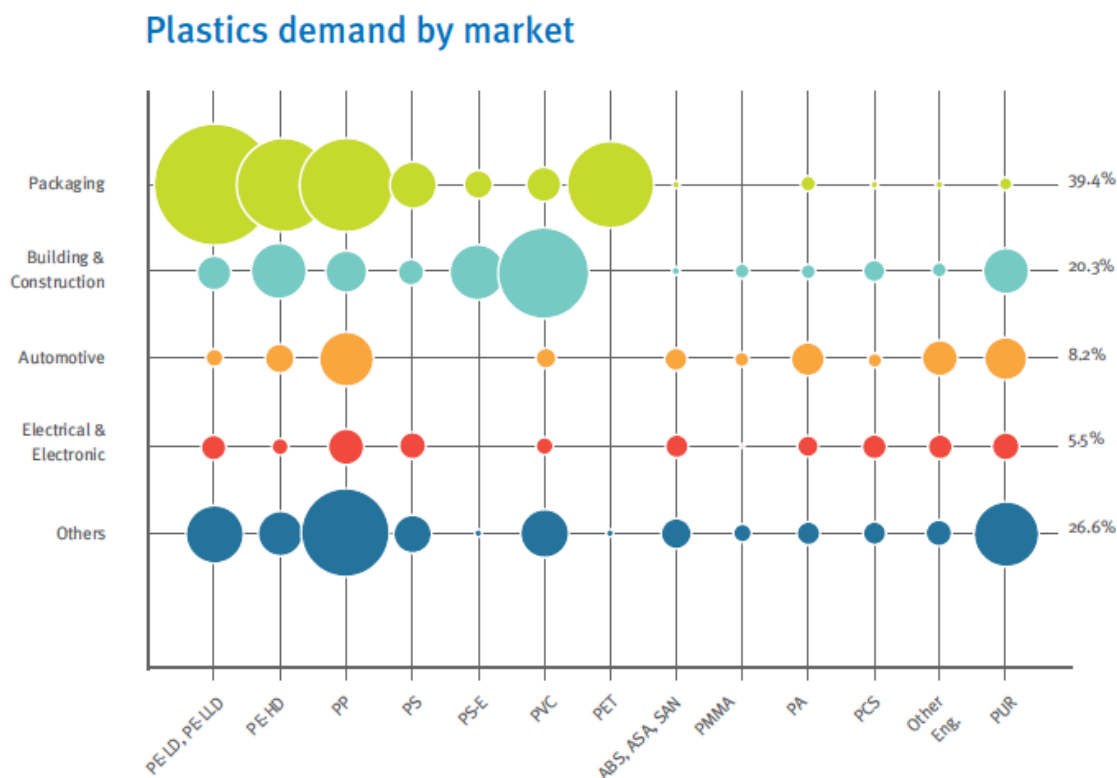


**Figure 2.** European plastics demand\* by segment and resin type 2012 Picture reproduce from Plastic Europe, *Plastics- the Fact 2013*, 2013)<sup>2</sup>

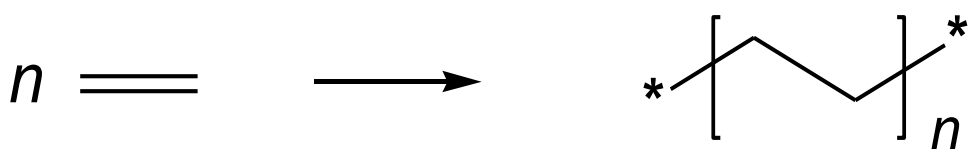
The polymerization conditions required for producing the polymer consisted of high temperatures (80 – 230 °C) and pressures (1000 – 3000 atm.). With such high standard manufacturing conditions and the economical demand from industry, there is a necessity for increasing the process efficiency and material effectiveness. These requirements initiate the study of new catalysts with higher activity, lower cost and synthesis of new types of polymer.

### 1.1.2 Polymer

Polymers are large molecules that composed of many repeated subunits in a reduplicative pattern. Each small molecule (subunit) that constitutes the polymer is a monomer.

Although each monomer has a fixed molecular weight, it is hard to measure the exact synthetic materials weight. A polymeric material commonly consists of huge amount of polymer chains with different number of monomers.

Polymerization is the reaction of an unsaturated organic reactant, commonly a C=C, combining itself over and over again to generate a polymer chain (Scheme 1)

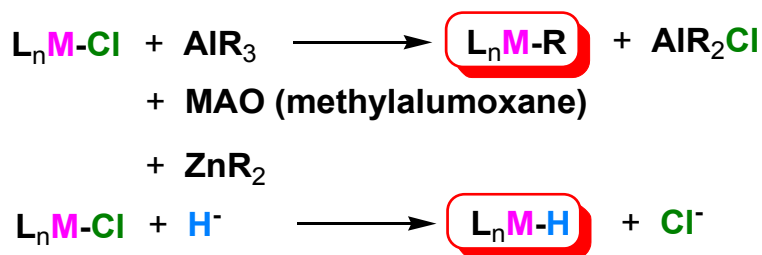


**Scheme 1.** A simple schematic retranslation for polymerization.

When only a few subunits combine together to produce a short chain, it is usually referred as oligomerisation. In the other words, oligomers are very short polymers.

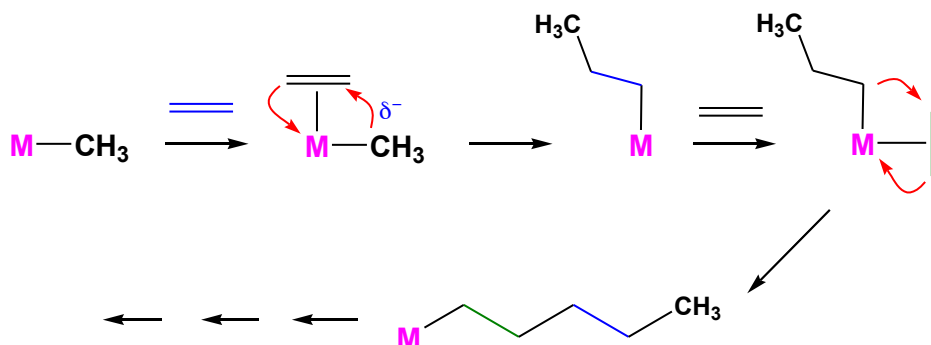
There are generally three components for most polymerizations:

**Initiation:** generating the active catalyst from a less active catalyst precursor.



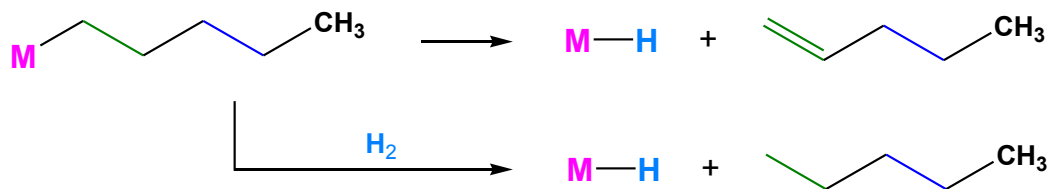
**Scheme 2.** A simple schematic retranslation for Initiation step.

**Propagation:** the polymer chain growth portion of the reaction that occurs over and over again.



**Scheme 3.** A simple schematic representation for propagation step.

**Termination:** a reaction step that stops the polymer chain growth.



**Scheme 4.** A simple schematic representation for termination step.

In a good polymerization catalyst, the initiation step generates as much active catalyst as possible and the propagation step occurs as often as possible, while the termination step is unlikely to happen. For early transition metal catalysts, the  $\beta$ -hydride elimination step that can cause termination is not that favourable.

A Living Catalyst is typically a polymerization catalyst in which all the transition metal complexes present are the same and already in an active catalytic state (no initiation step).

When the substrate is added all the catalyst molecules start the polymer chain growing

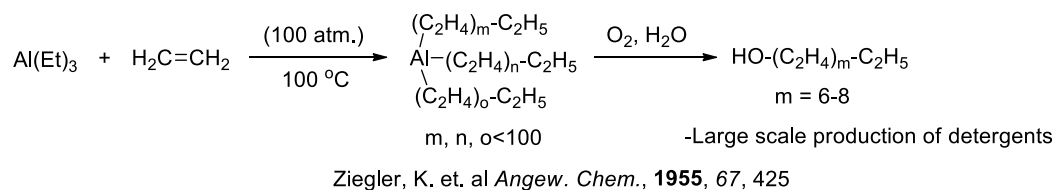


steps at the same time and same rate. This means that at any point the polymer chains growing off each and every catalyst are all essentially the same length. This leads to polymers that have an  $M_w/M_n$  value very close to 1.0.

### 1.1.2.1 Ziegler- Natta Catalyst

The German chemist Karl Ziegler (1898-1973) discovered in 1953 that when  $\text{TiCl}_4(\text{s})$  and  $\text{AlEt}_3$  are combined together they produced an extremely active heterogeneous catalyst for the polymerization of ethylene at atmospheric pressure.<sup>4</sup> Giulio Natta (1903-1979), an Italian chemist, extended the method to other olefins like propylene and developed variations of the Ziegler catalyst based on his findings on the mechanism of the polymerization reaction.<sup>5</sup> The Ziegler-Natta catalyst family includes halides of titanium, chromium, vanadium, and zirconium, typically activated by alkyl aluminium compounds. Ziegler and Natta received the Nobel Prize in Chemistry for their work in 1963.

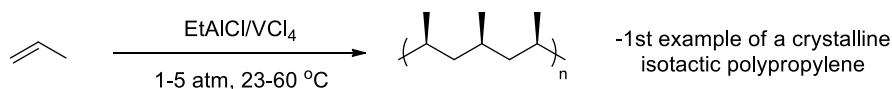
### Early polymerization w/ aluminum: The "Aufbaureaktion"



## Polymerization of ethylene



## Nattas Contribution



Natta, G. et. al. *J. Am. Chem. Soc.*, **1955**, 77, 1708

**Scheme 5.** Simple Schematic demonstration of Ziegler –Natta heterogeneous Catalyst.

### 1.1.2.2 Metallocene Catalysis

In 1952, Fischer and Wilkinson reported an organometallic complex of a transition metal connected by a  $\pi$  bond of two aromatic rings with the formation of a structure which was similar to a sandwich.<sup>6</sup> That was the first report of metallocene compound. Since then, these metallocene compounds have had extensive application in various research topics, Fischer and Wilkinson received the Nobel Prize in Chemistry for their work in 1963. However, the earliest homogeneous metallocene catalyst  $\text{Cp}_2\text{TiCl}_2/\text{Et}_2\text{AlCl}$  for ethylene polymerization had very low activity.

In the 1970s, Kaminsky and Sinn found that the  $\text{Cp}_2\text{ZrCl}_2/\text{MAO}$  system was capable of high activity olefin polymerization catalysis, and thus opened up a new area for olefin polymerization catalysts.<sup>7</sup> A metallocene catalyst is a catalyst system which has a metallocene compound as a main complex and a Lewis acid such as methylaluminoxane (MAO) or a boron-containing cation activator/co-catalyst. Compared with the conventional Ziegler-Natta catalyst, a metallocene catalyst has the following characteristics: (1) very high catalytic activity; (2) single active centre, thus resulting polymer molecular weight distribution is narrower; (3) by changing the structure of the metallocene catalyst, the catalyst performance can be regulated as well as the characteristic of the resulting polymer. The inadequacy of the metallocene catalyst could be: (1) difficult to synthesis with low yield rate; (2) unsuitable for gas phase and slurry polymerization; (3) high cost of co-catalyst MAO; (4) poor thermal stability.<sup>8</sup>

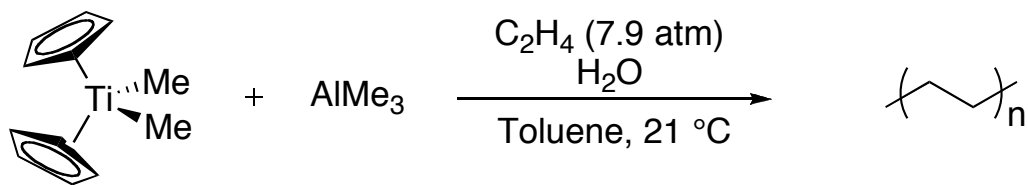
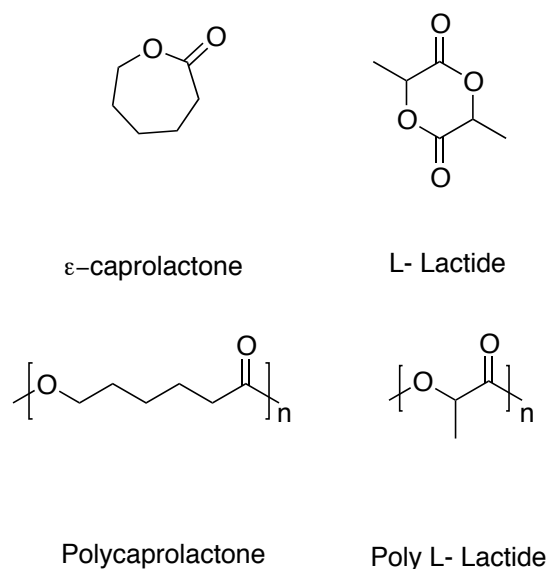


**Figure 3.** Activation of a metallocene with TMA (Ti can be substitute with Zr).<sup>9</sup>

### 1.1.3 Poly Cyclic Esters

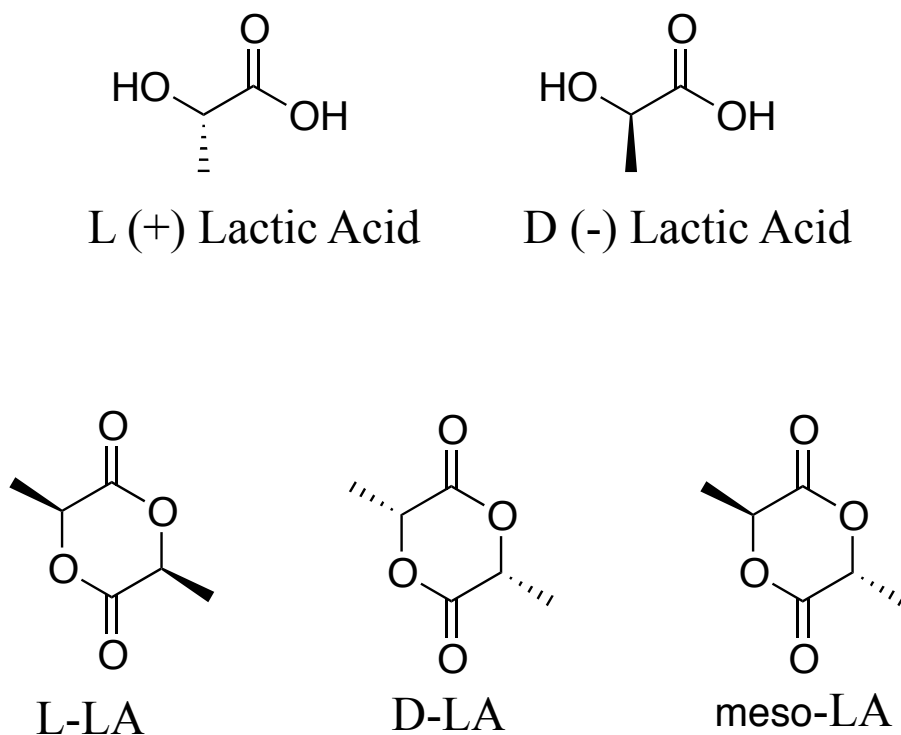
Cycle esters, which are also known as lactones or lactides, are normally polymerized by ROP (Ring Opening Polymerization). The most frequently reported cycle esters' polymerizations in the peer reviewed literature are poly lactide (PLA) and poly  $\epsilon$ -Caprolactone (PCL) (Scheme 6.).



**Scheme 6.** Structures of monomers and their polymers for lactide (PLA) and  $\epsilon$ -Caprolactone (PCL).

Poly lactide can be generated by direct condensation or by conducting ring opening polymerization on the cyclic dimer of lactic acid (Lactide). Lactic acid is an intermediate

metabolites of Krebs cycle, and the absorption and metabolism mechanism had been well studied. Based on its high bio- safety properties, poly lactide was selected as one of earliest biodegradable absorbent material for clinical use. It is also the most widely studied and used biodegradable materials so far. Lactic acid contains a methyl group on  $\alpha$ -position, hence it can be divided into *L* (+) and *D* (-) two optical isomers. Moreover, lactide contains two chiral centres, thus various stereoisomers exist. Those stereoisomers are *L*, *L*-lactide (LLA), *D*, *D*-lactide (DLA) and *meso*-lactide (*meso*-LA) three stereoisomers; racemic lactide (*rac*-LA) is the DLA and an equal mixture of LLA (Scheme 7).



**Scheme 7.** Structures of stereoisomers for lactide.

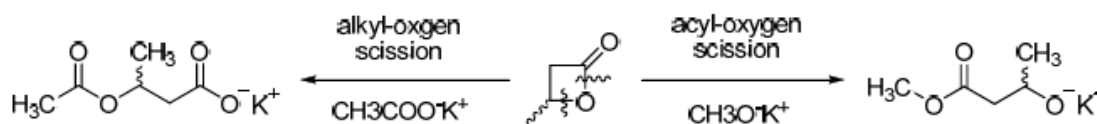
Characteristics of poly lactide such as mechanical, physical and degradation are widely different based on the configuration of lactide monomer. Polymerization of optically pure *D*-LA and *L*-LA can generate poly-*L*-lactide (PLLA) and poly-*D*-lactide (PDLA). A catalytic isotactic crystalline polymer with 180 ° C melting point, which has excellent mechanical strength, can be obtained under suitable conditions;<sup>10</sup> while under the same conditions, the racemic lactide (*meso*-LA and *rac*-LA) is a polymerization product and is atactic non-crystalline poly lactide, which with a low mechanical strength. When it comes to terms of degradation performance, PLLA degradation absorption time is about 3-3.5 years, which is suitable for the production of the bone fixation device; *meso*-lactide and *rac*- lactide absorption speed is only 3-6 months, thus very suitable for applications such as a drug carrier controlled release.<sup>11</sup>

Poly  $\epsilon$ -caprolactone (PCL), generally polymerized by ring opening polymerization of  $\epsilon$ -caprolactone, is a semi-crystalline linear aliphatic polyester having a comparably low melting point (59-64 °C). PCL has a repeating unit structure of five non-polar methylene “-CH<sub>2</sub>-“groups and an ester of a polar “-COO-“group. This structural property makes the mechanical properties of PCL similar to polyolefins, with good flexibility and process-ability. However, there is a serious flaw for PCL due to its very low melting point, therefore impossible to use as a heat resistance material.

#### **1.1.3.1 Ring Opening Polymerization for Poly Lactide (PLA) and Poly $\epsilon$ -caprolactone (PCL).**

Condensation polymerization reaction has a long history, which goes back to 1930s. Carothers began a systematically study by using aliphatic polyester to synthetic stable

fibres.<sup>12</sup> However, the polycondensation reaction has a serious limitation. In order to obtain a high molecular weight product, condensation polymerization reaction requires high reaction temperature and long reaction time. Moreover, during condensation polymerization reaction, it sometimes produces water or other small molecule by-products, thus the product is difficult to obtain as high molecular weight polymer. For Lactide or lactone monomer, ring opening polymerization is an important method for the synthesis of biodegradable aliphatic polyesters. Compared to polycondensation, ring opening polymerization for cyclic esters could achieve high molecular weight polymers readily, and is also easier to control the polymerization. The ring opening polymerization method therefore attracted much attention; it is a very active area of research.<sup>13, 14</sup> How likely ring opening polymerization reaction is to occur is based on cyclic monomer's nature of itself, the strength of the monomer's strain determines whether they can provide enough free energy for ring opening reaction. Therefore, the pentaheterocyclic lactone is difficult to start ring opening polymerization under mild conditions. Depending on the open loop manner, the ring opening reaction can occur through the scission of alkyl-oxygen bond or acyl-oxygen bond. For a large tension ring, such as  $\beta$ -butyrolactone ring, both scission patterns could occur under different initiate conditions.<sup>15, 16</sup> For the larger ester rings, the ring opening reaction generally occurs in the acyl-oxygen bond cleavage position.

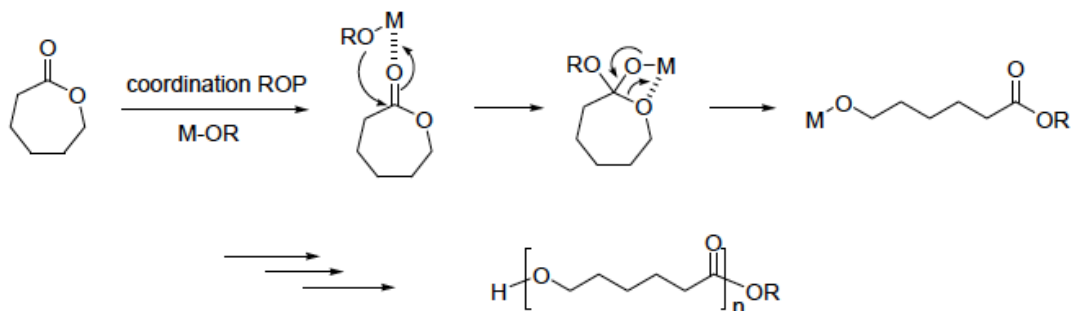


**Scheme 8.** Two types of bond cleavage for  $\beta$ -butyrolactone ring.

Most ring opening polymerization is conducted in the presence of a catalyst or initiator.

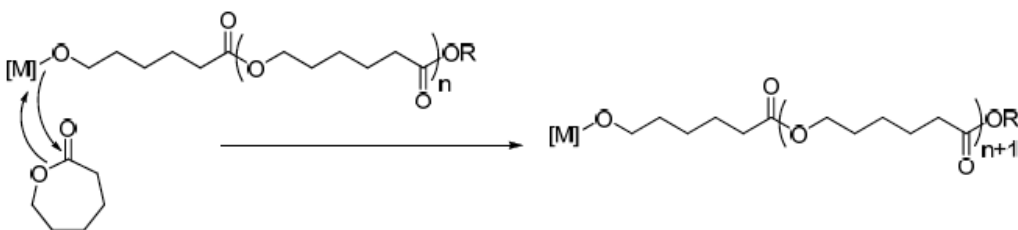
Many organometallic complexes, such as metal oxides, carboxylate, alkoxides and phenolate are effective catalysts for ring opening polymerization.<sup>17, 18, 19</sup> Based on initiation steps, there are three primary ring opening polymerization mechanism: cationic polymerization, anionic polymerization and "coordination - insertion" polymerization.<sup>20</sup> Among the three of them, coordination - insertion ring opening polymerization seized most attention and has become a hot research topic due to the reasons that it can lead to polymers with clear structures and controllable molecular weight.

In the synthesis of high molecular weight homopolymer/copolymers, the most common coordination - insertion polymerization are metal alkoxides and metal carboxylic catalysts. There are many different types of these catalysts, such as early transition metals (Ti, V and W etc.), late transition metals (Fe, Co and Zn etc.) and main group elements (Al). In compounds with the presence of L-M bond (M: metal ion, L: anion substituent, typically RO<sup>-</sup>), when catalyse the polymerization of CL, L<sup>δ-</sup> and M<sup>δ+</sup> are participate in the reaction: the first monomer activated on metal ion M<sup>δ+</sup>, then L<sup>δ-</sup> nucleophile attack the activated monomer, then monomer having a ring opening and insert into L- M bond (Scheme 9).



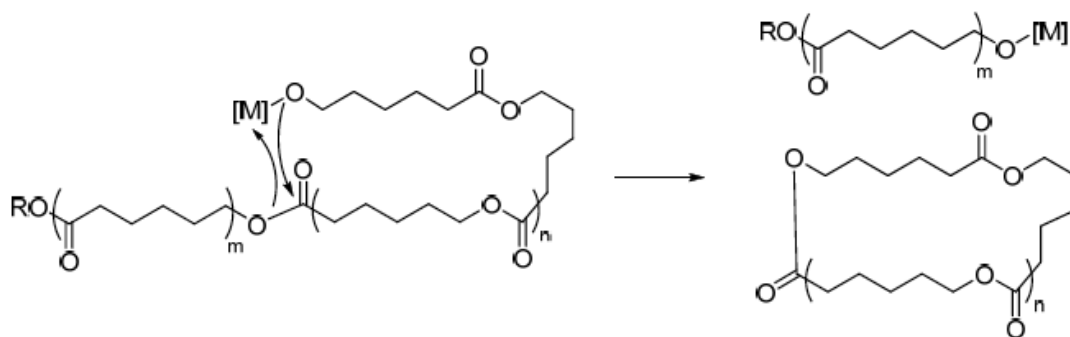
**Scheme 9.** Simple schematic translation of the Ring Opening Polymerization mechanism of  $\epsilon$ -CL.

Kricheldorf studied several metal alkoxide catalyst systems. During each polymerization process, he found that, in addition to the normal coordination – insertion (Scheme 10.), some of the active M-OR might also cause intra- molecular and inter- molecular lactones to switch, which can lead to cyclic oligomers. Therefore, the polymer molecular weight distribution is broader (Scheme 11, 12).<sup>21,22</sup> Polydispersity index (PDI), which can indicate polymer molecular weight distribution, is dependent on the type and amount of the catalyst used, and is also affected by the reaction temperature, reaction time and other factors such as the chemical structure of the monomer. Unsuitable temperature, lengthy reaction time and excessive flexibility etc. could increase the possibility of the occurrence of unnecessary polymerization or oligomerization reactions.<sup>23, 24</sup>

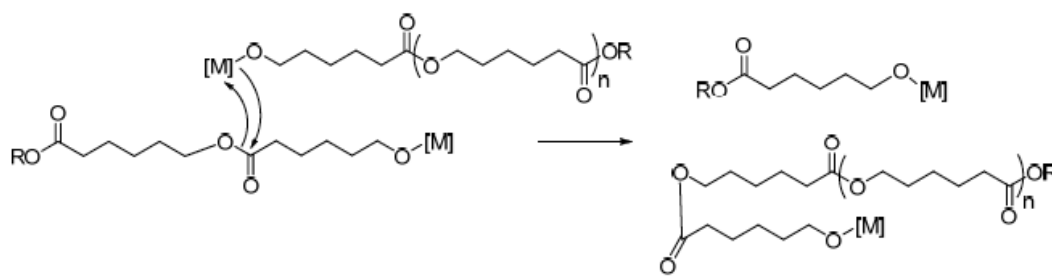


**Scheme 10.** Normal coordination insertion.





**Scheme 11.** Intra-molecular lactone switching.



**Scheme 12.** Inter-molecular lactone switching.

The core of “Coordination- Insertion “ring opening polymerization of a cyclic ester is the catalyst. The polymer produced by different catalysts may have different microstructures, which in turn will bring different physical, mechanical, chemical properties and biodegradation rates. People may design different polymers with various characteristics by selecting the appropriate metals and different ligand binding.<sup>23</sup> Currently, the ring opening polymerization of cyclic esters catalyst research focus on the following aspects: (1) finding a highly active catalyst system; (2) being able to control polymerization activity; (3) being able to form a high molecular weight polymers with narrow molecular weight distribution polymers; (4) trying to proceed stereoselective monomers’ polymerization such as certain lactide; (5) gathering knowledge of catalytic polymerization’s mechanism to better understand polymerization and to guide the design of new catalysts.

#### 1.1.4 Aluminium Catalysts

The following briefly describes organoaluminium catalyst systems for ring opening polymerization of cyclic esters in recent research.

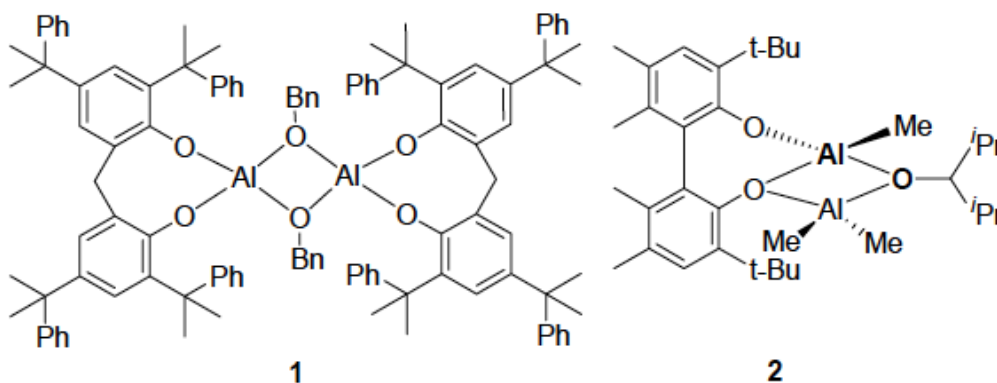
For aluminium catalyst systems, aluminium alkoxide can be used as a catalyst; an aluminium alkyl complex with alcohol may also work as a catalyst (aluminium alkoxide generated *in situ*). Due to the reason that aluminium catalytic activity is lower than other metals in general, therefore to some extent it reduces the occurrence of intra-molecular and inter-molecular lactone switching, which facilitates better control of the polymerization process, and thus control the molecular weight.

Teyssie reported an  $\text{Al}(\text{OiPr})_3$  catalyst for *L*-lactide (LLA) ring opening polymerization, which has significance in aluminium catalyst research.<sup>20, 21</sup> He found that  $\text{Al}(\text{OiPr})_3$  in toluene at 70 ° C acted as a catalyst for ring opening polymerisation, and they were able to summarize a fixed relationship between rate of polymerization, the cyclic ester monomer concentration and initiator concentrations. Each of the alkoxy group in  $\text{Al}(\text{OiPr})_3$  can act as a polymerization initiator. The resultant polymer has a very narrow molecular weight distribution ( $\text{PDI} = 1.1\text{-}1.4$ ). Subsequently, academic and industrial sectors have generated great interest towards aluminium catalysts. This makes the organo-aluminium complexes one of the most commonly used catalysts for lactone ring opening polymerization.

##### 1.1.4.1 Oxygen (sulfur) coordinated organic aluminium complexes

The Lin group reported the compound **1** (Scheme 13.) to be highly effective for ring opening polymerization for both  $\epsilon$ -caprolactone and *L*-lactide.<sup>26</sup> For the ring opening polymerization of  $\epsilon$ -caprolactone, benzyl alcohol was added as a chain transfer agent. Chain growth proceeds in the chain transfer between alkoxy species with alcohol. This complex can also catalyse LLA polymerization; the resultant polymer has narrow molecular weight distribution (PDI = 1.06-1.11).

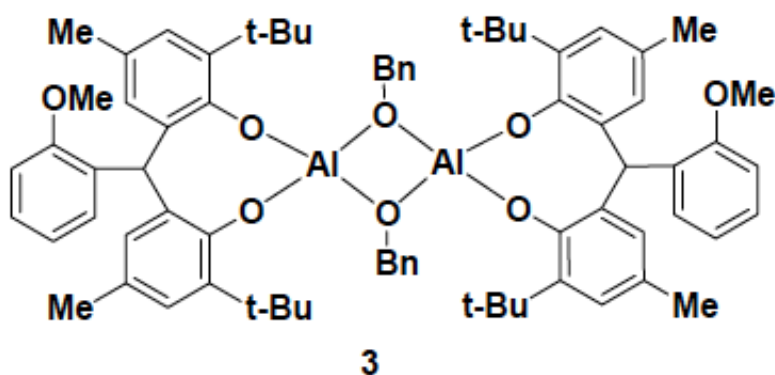
Chisholm reported compound **2** (Scheme 13.), which could catalyse racemic lactide ring opening polymerization. However, this needs to use the aluminium catalyst for polymerization of the monomer at higher temperatures. The reaction at 80 ° C for 40 h reached a 40 % conversion rate. When the reaction was refluxed in toluene for 20 h, the conversion rate can be increased to 82 %. The ligands were also reacted with lithium or zinc. The conversion rate for ring opening polymerization of the Li and Zn complexes are both higher than Al species.



**Scheme13.** The Aluminium Complexes from Lin **1** and Chisholm's **2** research.

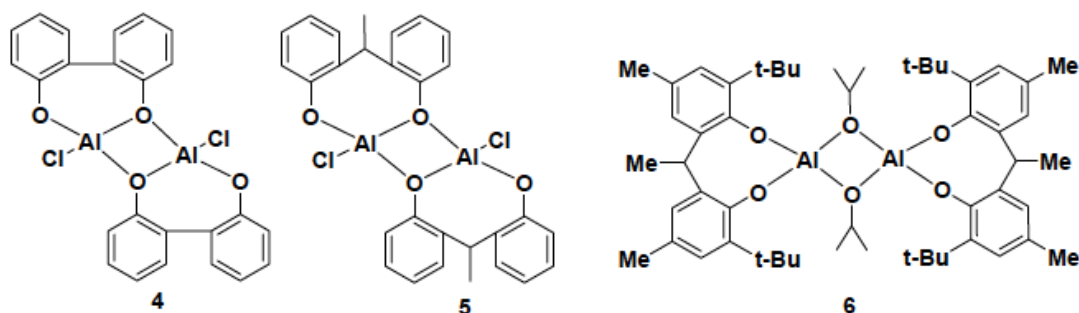
Hsueh *et al.* reported an aluminium compound **3** (Scheme 14.) has catalytic activity for ring opening polymerization of  $\epsilon$ -caprolactone. The resulting polymer molecular weight

distribution is very narrow; additionally the molecular weight and monomer conversion has a linear relationship. Hsueh studied the reaction mechanism by NMR tracking, indicating that the initiation step is induced by monomer being inserted into the PhCH<sub>2</sub>O-Al bond. Catalyst **3** can realize the same  $\epsilon$ -caprolactone copolymerized with other monomers.  $\epsilon$ -Caprolactone copolymerized with styrene to obtain block copolymers, which has very narrow molecular weight distribution.<sup>28</sup>



**Scheme 14.** Aluminium Complex of Hsueh's research.

The Chisholm group also reported similar catalysts **4-6** (Scheme 15) in later studies. In their work, the catalysts **4-6** are capable of catalysing copolymerization reaction of lactide with ethylene oxide. However, throughout the polymerization, the polymerization rate is too slow, and the catalysts were found to be poorly active for polymerization and the resulting polymer structure is not a clear A-B-A-B type block polymer.<sup>29</sup>



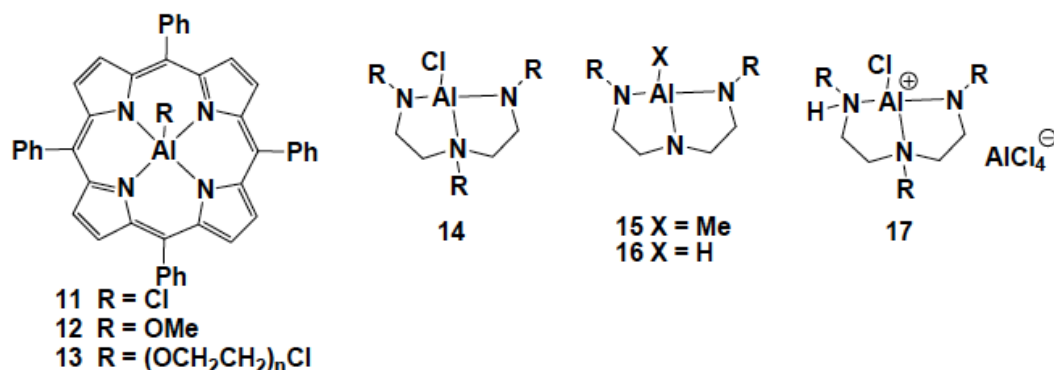
**Scheme 15.** The aluminium complexes **4-6** from Chisholm's research.

Chen *et al.* introduced some similar ligand skeletons with electron-withdrawing substituents **7,8** (Scheme 16). These complexes can efficiently catalyse  $\epsilon$ -caprolactone ring-opening polymerization. The resulting molecular weight distributions are between 1.08-1.25. Moreover, there is a linear relationship between conversion rate and molecular weight, which indicated a living polymerization process.<sup>30</sup>

The structure/binding of some bidentate sulfur compounds are similar to the bidentate oxygen ligands, and the properties of them are also very similar. Huang *et al.* reported complexes **9,10** (Scheme 16.), which can efficiently catalyse the ring opening polymerization of  $\epsilon$ -caprolactone at room temperature. The complex **9** may also lead to ring opening polymerization of *L*-lactide, yet complex **10** have no catalytic activity for *L*-lactide. The ring opening polymerization for  $\epsilon$ -caprolactone by using **9** is a living polymerization. To study the mechanism of the catalytic process by NMR tracking, they found that the monomer insertion occurs between the S-Al bonds. After the formation of the active centre, the monomer is further inserted into the chain growth phase. The result of catalyst **10** for  $\epsilon$ -caprolactone ring opening polymerization has wide polymer



conditions. In contrast, the compounds **15** and **16** can lead to polylactide under these conditions. Moreover, the hydride compound **16** had higher activity than the alkyl compound **15**, but the two catalytic products obtained by polymerization of lactide polymers had a relatively wide molecular weight distribution (about 1.7).<sup>33, 34</sup>



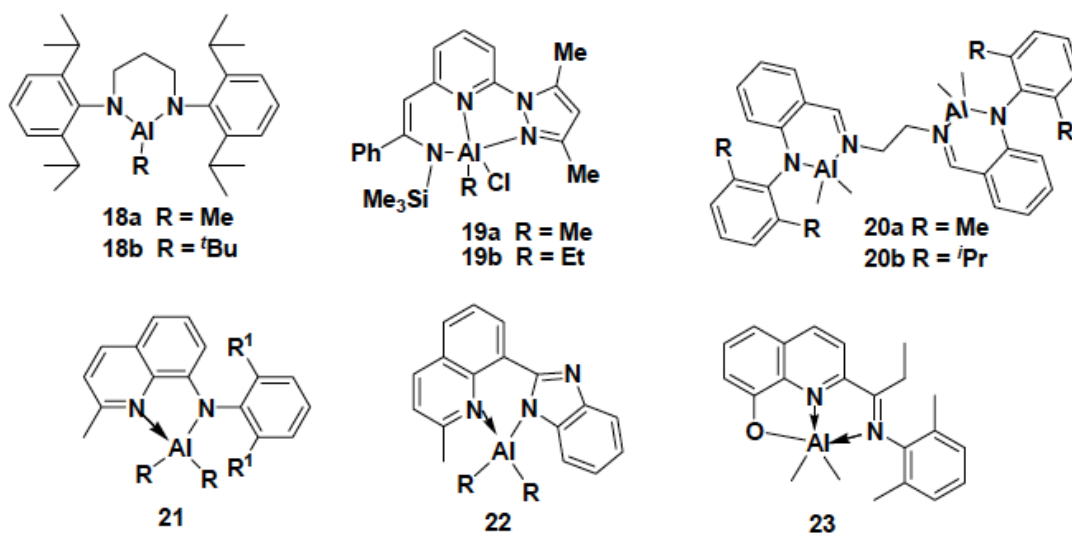
**Scheme 17.** Nitrogen coordinated organo aluminium complexes from Inoue and Emig's research.

In 2002, Chen *et al.* synthesized three coordinated two aluminium alkyl amine complexes **18a** and **18b** by reaction of ArNH(CH<sub>2</sub>)<sub>3</sub>NHAr and AlMe<sub>3</sub> (Scheme 18). Tracing catalytic process of compound **18** for ring opening polymerization by NMR, they found the methyl group is still attached to the aluminium centre, and the monomer inserts into N-Al bond to form an active centre to initiate. After that, monomers are continuously inserted into the Al-O bond to generate a polymer. Compounds **18a** and **18b** have prosaic catalytic activity, uncontrollable molecular weight and broad molecular weight distribution (PDI = 3.19).<sup>35</sup>

In recent years, Wang *et al.* have done a lot of work on the development of the organo-aluminium compounds. They reported a series of nitrogen coordinated aluminium metal

complexes, such as compound **19a** and **19b** (Scheme 18). With the addition of benzyl alcohol, the molecular weight distribution for ring opening polymerization of  $\epsilon$ -caprolactone is narrower; without the addition of benzyl alcohol, the conditions can lead to  $\epsilon$ -caprolactone ring opening polymerization, but the molecular weight distribution is wider. The same identical ligands were studied with zinc complexes; a similar catalytic activity of  $\epsilon$ -caprolactone has been shown.<sup>36</sup>

The Mu group reported a series of amine-imide dual-core complexes **20a** and **20b** (Scheme 18), which also achieved high catalytic activity for the ring opening polymerization of  $\epsilon$ -caprolactone. Among the catalytic polymerization processes, the polymerization rate, monomer concentration and initiator concentrations constitute a linear relationship. Moreover, the molecular weight and conversion rate also formed a linear relationship; the resultant polymer molecular weight distribution was very narrow, which indicated that the polymerization was a living polymerization. Similar binuclear zinc complexes also have catalytic activity for ring opening polymerization of  $\epsilon$ -caprolactone.<sup>37</sup>



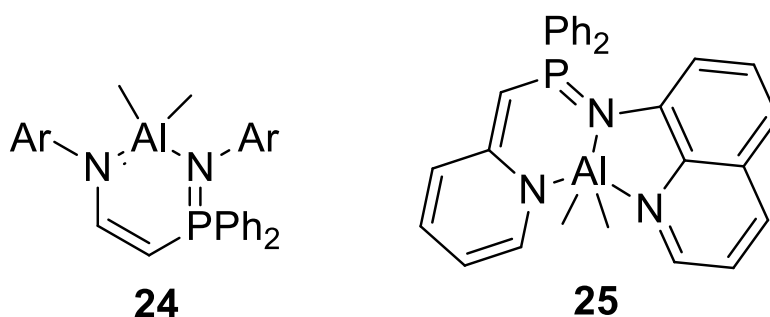


**Scheme 18.** Simple schematic retranslation of nitrogen coordinated organic aluminium complexes from Chen, Wang, Mu and Sun's research.

Sun *et al.* designed and developed a series of N ^ N, N ^ N ^ O coordinated catalysts, and they have shown good catalytic activity for ring opening polymerization of  $\epsilon$ -caprolactone. For example, compound **21** (Scheme 18) was found to be highly active for ring opening polymerization of  $\epsilon$ -caprolactone. The resultant polycaprolactone's molecular weight could reach as high as  $M_n = 139000\text{g/mol}$ .<sup>38</sup> Complex **22** (Scheme 18) was found to be highly active for ring opening polymerization of  $\epsilon$ -caprolactone either with or without benzyl alcohol present. Among the catalytic polymerization processes, the polymerization rate, monomer concentration and initiator concentrations constitute a linear relationship. Moreover, the molecular weight and conversion rate also formed a linear relationship; the resultant polymer molecular weight distribution was very narrow (PDI 1.08-1.25), which indicated that the polymerization was a living polymerization.<sup>39</sup> Compound **23** (Scheme 18) was found to be highly active for ring opening polymerization of  $\epsilon$ -caprolactone only in the presence of benzyl alcohol. This polymerization was a living polymerization, and exhibited high thermal stability at 90 °C.<sup>40</sup>

Wang *et al.* reported a bidentate N ^ N ligand chloric compound **24** (Scheme 19). The compound can efficiently catalyse ring opening polymerization of  $\epsilon$ -caprolactone in the presence of one equivalent of benzyl alcohol. Kinetic studies showed that the rate of the polymerization reaction and the monomer concentration affected each other; molecular weight of the resulting poly caprolactone and the monomer conversion rate had a linear

relationship. Thus, it was possible to control the polymerization of caprolactone.<sup>41</sup> In addition, they also synthesized a series of N ^ N ^ N tridentate aluminium quinoline complexes of catalyst type **25** (Scheme 19.), which were was found to be highly active for ring opening polymerization of  $\epsilon$ -caprolactone only in the presence of benzyl alcohol. This polymerization can lead to a poly caprolactone that has a controllable molecular weight, and the molecular weight distribution was very narrow (PDI = 1.06-1.33).<sup>42</sup>



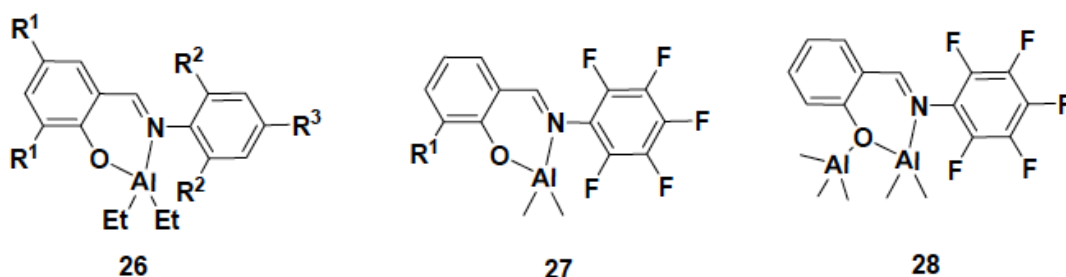
**Scheme 19.** Simple schematic retranslation of nitrogen coordinated organic aluminium complexes from Wang's research.

#### 1.1.4.3 Oxygen and nitrogen coordinated organic aluminium complexes

N. Nomura reported a series of aluminium salicylaldehyde imine compounds **26** (Scheme 20) which can be efficiently catalyse  $\epsilon$ -caprolactone ring-opening polymerization. The process is further initiator by the reaction of aluminium complexes and benzyl alcohol. The molecular weight of the obtained polymer matched with structures measured by NMR spectroscopy, and showed that such catalysts may be obtained by direct reaction of salicylaldiminato with triethylaluminium *in situ*.<sup>43</sup>

K. Nomura *et al* have done similar work. When the imine substituent is an electron-withdrawing group, the catalytic activity increased **27** (Scheme 20). The study found that the substituents for the salicylaldehyde hydroxyl group at the *ortho* position are necessary for the preparation of mononuclear species. When no substituent is at the *ortho* position to a hydroxyl group, a binuclear compound **28** was formed (Scheme 20).

44-46

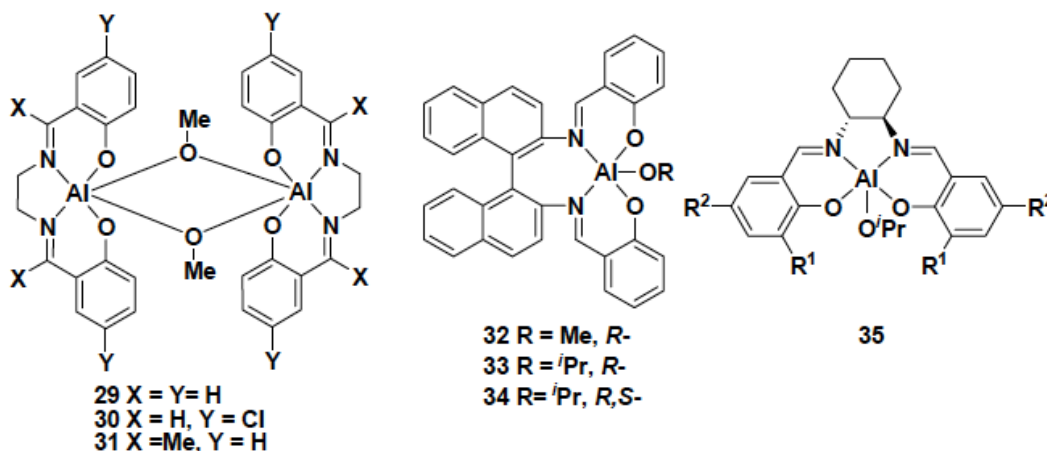


**Scheme 20.** Simple schematic retranslation of oxygen and nitrogen coordinated organic aluminium complexes from N. Nomura and K. Nomura's research.

Salen ligands have been widely studied. Chiral and non-chiral Salen ligands' catalytic performance may be completely different. Non-chiral aluminium compounds **29-31** (Scheme 21) were found to be highly active for ring opening polymerization of lactide (LA), and the polymerizations are living. By analysis of each single crystal structure, the structure in the solid state shows a dimeric structure, which was bridged by Me-O. It presents a monomeric and dimeric equilibrium in solution. Compounds **29-30** in the catalytic process also show a clear effect of the solvent. The conversion rate of lactide was significantly higher in dichloromethane than that of toluene under the same conditions. Compound **29** is the optical purity for the catalytic LA, to obtain optically

clear polymers. Although there is no chiral ligand, the catalysis of racemic LA showed some stereoselectivity of PLLA and PDLA presence of small cell in the resulting block polymer chain. The mechanism is generally considered as a "terminal control mechanism", the end of the growing chain will affect the next monomer insertion. The catalyst shows a perspective view of the selectivity.<sup>47-51</sup>

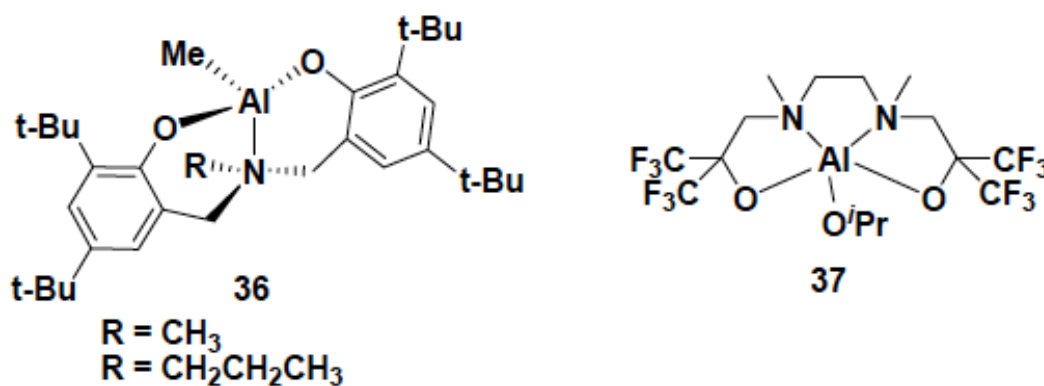
Chiral Salen aluminium compounds **32-34** (Scheme 21) show good stereoselectivity in the polymerization of *rac*-LA. Studies shows modifying the ligand substituents can improve the selectivity of the catalytic perspective. For example, for the polymerization *rac*-LA, an increase in the steric hindrance at the *ortho* phenolic hydroxyl group can improve the optical selectivity. Increasing the electronegativity at the *ortho* position can improve the catalytic activity. For ring opening polymerization of lactide by complexes **32-35**, the activities are significantly higher activity than **29-31** bridged achiral compounds, which achieve higher conversion rates in the same amount of time.<sup>52-55</sup>



**Scheme 21.** Simple schematic retranslation of oxygen, nitrogen coordinated organic aluminium Salen complexes.

C.-T. Chen reported a similar complex **36** (Scheme 22) which also showed high catalytic activity. For the catalytic processes "active" and "immortal" features have also been observed. Moreover, side arms do not contain heteroatom ligands, which can better control centre aluminium atoms steric effects can not contain Lewis acidic side arm heteroatom ligands, can better control catalyst.<sup>56</sup>

In 2005, the Carpentier group reported the synthesis of a poly fluorinated alkoxy aluminium complex **37** (Scheme 22), wherein five-coordinated aluminium atoms, which has a similar structure to other Salen aluminium complexes. Complex **37** is stable at room temperature in air, which is a highly active catalyst for ring opening polymerization of  $\epsilon$ -caprolactone.<sup>50</sup> In dichloromethane solvent, with a monomer and catalyst ratio of 100, the monomer conversion rate was 100 % after one hour, and the molecular weight of 11400 was achieved. Moreover, the molecular weight distribution was very narrow (PDI = 1.11). In 2010, relevant review articles for Salen aluminium complexes have described the polymerization behaviour in detail.<sup>58,59</sup>

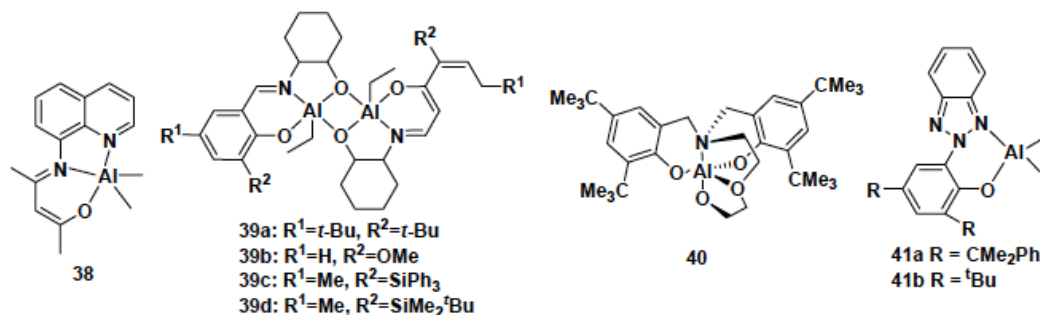


**Scheme 22.** Simple schematic retranslation of oxygen, nitrogen coordinated organic aluminium Salen complexes from Chen and Carpentier's research.

The Wang group recently reported a class of *N,N,O*-tridentate aluminium complex catalyst of type **38** (Scheme 23). The aluminium complex was found to efficiently catalyse ring opening polymerization of  $\epsilon$ -caprolactone (95 °C, 40 min, 100 % conversion rate); the molecular weight of the resulting poly caprolactone was 33300 g / mol, PDI = 1.24. They also studied the polymerization kinetics; the study found the rate of polymerization and monomer concentration to be a linear relationship, and the polymerization reaction is a controllable polymerization.<sup>60</sup>

Darensbourg reported a class of dual-core aluminium tridentate complex catalysts **39** (Scheme 23), and studied the catalytic ring-opening polymerization of cyclic esters. The study found that such catalysts could be efficient catalysts for controlled *rac*-lactide ring-opening polymerization. The resulting poly lactide was an isotactic polymer.<sup>61</sup>

Getzler reported a class of *O,N,O*-tridentate dianion aluminium complex catalysts **40** (Scheme 23), and studied the catalytic ring opening polymerization of lactide. The study found, either melt polymerization or solution polymerization conversion rate has a linear relationship with the amount of catalyst and reaction time, indicating that the polymerization was a controlled polymerization. The resulting physical properties of the poly lactide were compared with the same molecular weight linear polymer, and a cyclic polymer is more likely the case here.<sup>62</sup> Ko *et al.* synthesized a novel *N,O*-bidentate ligand for the aluminum compound **41** (Scheme 23), which was found to be active for ring opening polymerization of *L*-lactide in the presence of 9 -9 -anthracenemethanol. The polymerization was a controlled polymerization.<sup>63</sup>



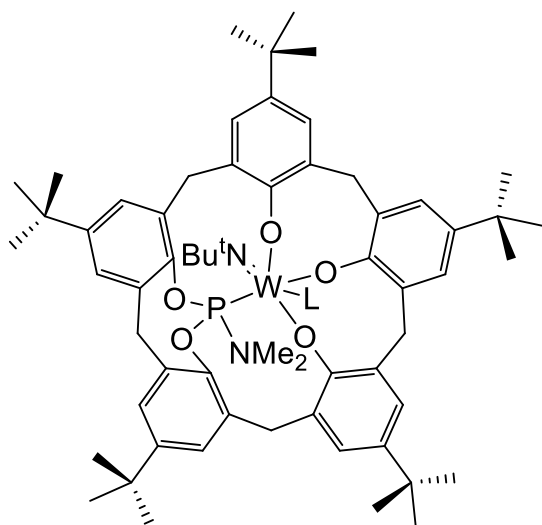
**Scheme 23.** Simple schematic retranslation of oxygen, nitrogen coordinated organic aluminium complexes from Wang, Darensbourg, Getzler and Ko's research.

### 1.1.5 Tungsten Calixarene Complexes

The coordination chemistry of the simplest of the calix[ $n$ ]arenes, the calix[4]arene, is well studied as highlighted by a number of recent reviews.<sup>64</sup> On the other hand, metal compounds containing the larger ring ( $n \geq 5$ ) are still quite rare. The larger calix[ $n$ ]arenes ( $n > 4$ ) continue to be of interest, primarily due to their ability to simultaneously accommodate multiple metal centres.<sup>65</sup> This is desirable since metals in close proximity have the potential to communicate, which in turn may lead to beneficial effects in areas such as magnetism or catalysis.<sup>66</sup>

Moreover, for larger calixarene systems, more people are focusing on the study of late transition metal groups and some of early transition metals (titanium, zirconium, niobium and vanadium), but not much attention is being paid to tungstocalixarene systems.

Lattman has studied the ability of the calix[5]arene ligand to accommodate both a main group ligand,  $\text{Me}_2\text{NP}$ , as well as a functionalised transition metal,  $[\text{W}(\text{N}t\text{Bu})\text{L}]$  ( $\text{L} = \text{NH}t\text{Bu}$  **41**,  $\text{SO}_3\text{CF}_3$  **42**) (Scheme 24).<sup>67</sup>



**Scheme 24.** Simple schematic retranslation of tungstocalix[5] complexes from Lattman's research (L= NH<sup>t</sup>Bu **41** , SO<sub>3</sub> CF<sub>3</sub> **42**).

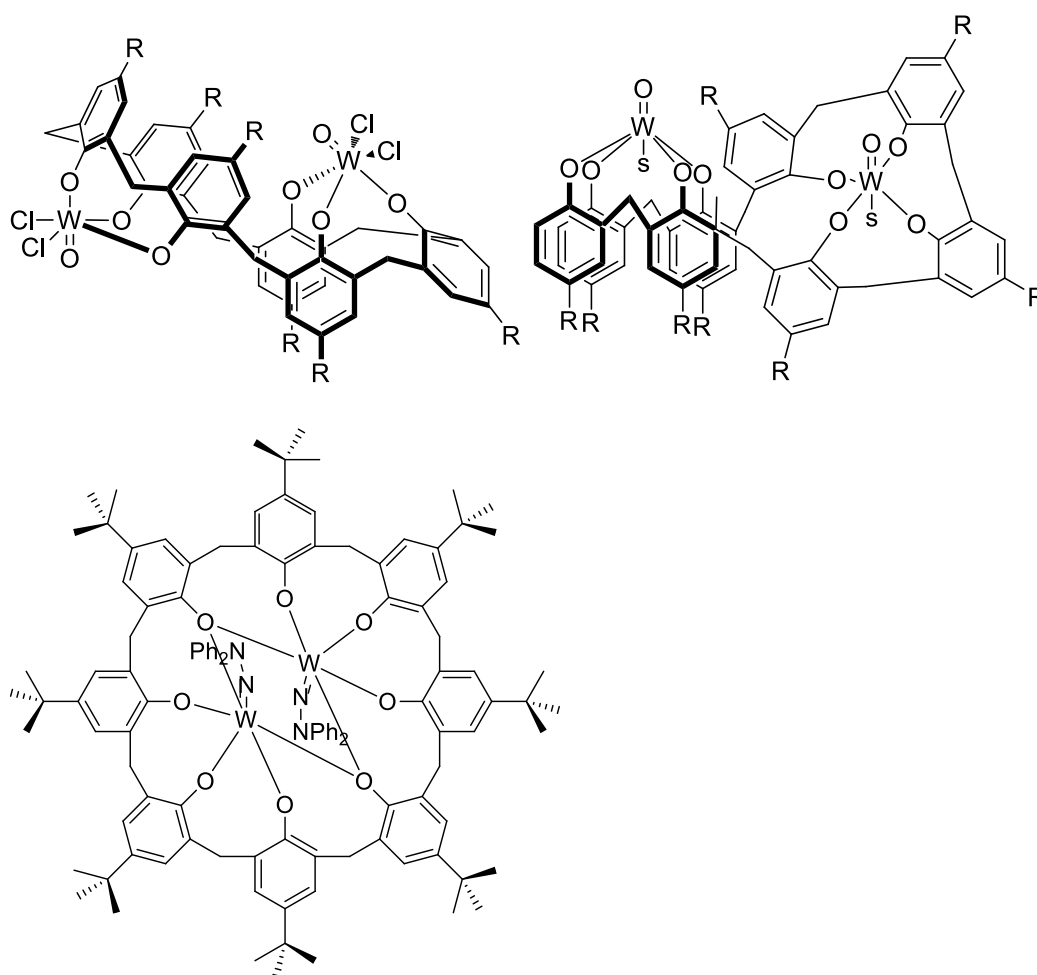
For the smaller calix[*n*]arenes (*n*= 3 and 4), metal oxo species have attracted interest due to their tendency to self-assemble into columnar structures and when multiple dodecyloxy groups are present liquid crystalline phases form.<sup>68</sup> For the larger ring systems studies are rare and only discrete molecules have been derived from the *p-tert*-butylcalix[6 and 8]areneH<sub>6,8</sub> ligands.<sup>69</sup> Reaction of 2 equivalents of WOCl<sub>4</sub> with *p-tert*-butylcalix[6]areneH<sub>6</sub> in toluene affords, via the loss of two molecules of HCl per tungsten, the complex **43** (Scheme 25). The ligand remains doubly protonated and adopts a pinched conformation to accommodate the two facially coordinated metal centres. The geometry about each tungsten centre is best described as pseudo octahedral with the oxo ligand lying trans to an elongated W-O bond.

A similar reaction using *p-tert*-butylcalix[8]areneH<sub>8</sub> and 2 equivalents of WOCl<sub>4</sub> gave the complex **44** (Scheme 25), formed by loss of four molecules of HCl per tungsten. The ring twists to accommodate the two W-O fragments. A molecule of the solvent (MeCN)



binds to each tungsten centre *trans* to the oxo function and each is encapsulated by three calixarene sub-units.<sup>70</sup>

One other tungsten complex of p-*tert*-butylcalix[8]areneH<sub>8</sub> is known and was obtained via treatment of the ligand with the hydrazido-tetraalkoxide [W(NNPh<sub>2</sub>)(OtBu)<sub>4</sub>] (2 equivalents) results in elimination of eight molecules of *t*BuOH and formation **45** (Scheme 25).<sup>72</sup>



**Scheme 25.** Simple schematic representation of tungstocalix complexes. Upper left **43**; upper right **44** R= *t*Bu , S= MeCN; Bottom **45**.

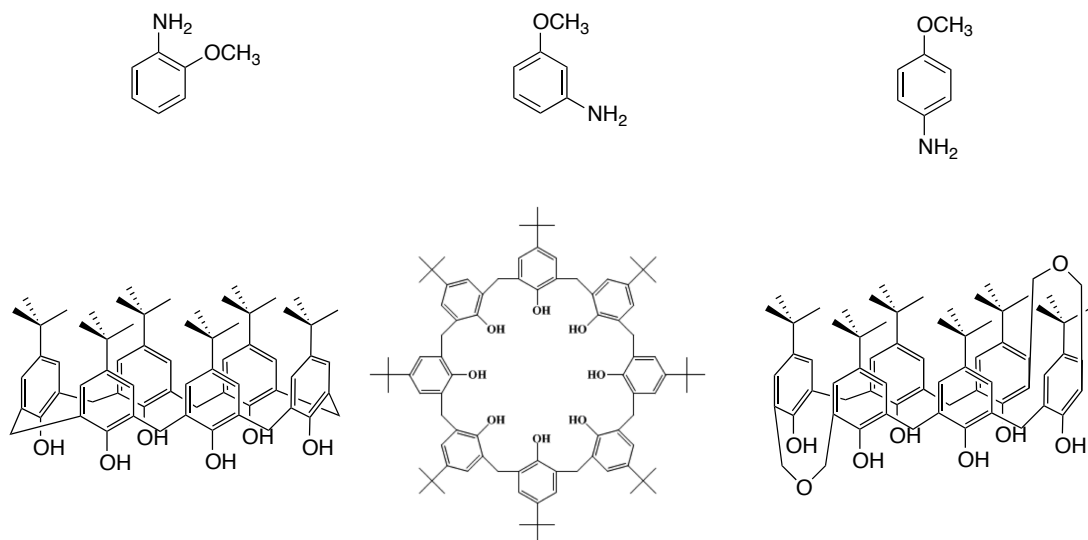
## 1.2 Characterization of GPC

As mentioned earlier, since polymerizations produce materials with a broad distribution of molecular weights (MWs), it can be very misleading to report a single quantity for MW. Rather, it is much more useful to know something about the average and overall distribution of chain lengths in a polymer sample. Thus, MWs are reported as several values: the number average molecular weight,  $M_n$ , the weight average molecular weight  $M_w$ , as well as several others.<sup>72, 73</sup> The  $M_n$  value reported for a polymer states the average number of repeat units (monomers) times the monomer's MW for all of the polymer chains in the sample, while the  $M_w$  represents a weighted average whereby the longer chains bias the value. A measure of the distribution of a polymer's MW is termed polydispersity index (PDI) and is a ratio of two MW averages. The most common value of PDI is the ratio of  $M_w/M_n$ . As  $M_w$  is always  $> M_n$ , the PDI of a polymer is always  $> 1$ . The PDIs of polymers made by step growth polymerizations are between 1 and 2 and are a function of conversion. On the other hand, the PDI of polymers made by chain growth polymerizations can vary greatly; controlled, "living" polymers can be made with PDIs of 1.01 while some metal-catalyzed or un-controlled free radical polymers have PDIs  $> 10.2$ . Material properties can vary greatly depending on MW and PDI; therefore, the ability to control these values through synthetic methodology is highly valued. Furthermore, much information about the polymerization mechanism can be obtained by evaluating trends observed in MW and PDI data. There are many ways to measure  $M_n$ ,  $M_w$ , and PDI values for synthetic polymers. These include size exclusion chromatography (SEC, also known as gel permeation chromatography, GPC), end group analysis (integration of  $^1\text{H}$  NMR spectrum), light scattering, and matrix-assisted laser desorption ionization time-of-flight

mass spectrometry (MALDI-TOF MS), are just a few of the common methods and are all used in the chapters that follow. Unfortunately, the structure and functionality in many polymers can make their detailed characterization extremely difficult and in certain instances, impossible. For example, most conducting polymers are intractable materials and cannot be characterized in the solution state. Thus, developing methods of solubilizing such materials to enable detailed characterization is an active area of research.<sup>74–78</sup>

### 1.3 Aim of Study

The aim of this study is to investigate a series of new complexes incorporating aluminium and tungsten metals in combination of various ligands (Scheme 26), and assess their ability as catalysts for the ring opening polymerization of  $\epsilon$ -caprolactone and *rac*-lactide.



**Scheme 26.** Chelating ligands used in this study. *o*, *m*, *p*-anisidines and calixarenes.

We have decided to focus our efforts on aluminium and tungsten. Aluminium species have proven their efficiency as catalysts for ring opening polymerization. As we discussed in section 1.4, several researchers have reported organoaluminium complexes. However, we believe there is some room for unstudied systems. We wish to investigate their potential for improving upon previously studies by controlling/manipulating polymerization conditions and chelating ligands.

For tungsten complexes, we want to investigate the potential for the synthesis of different tungstocalixarene complexes to build upon this scarce literature field. We also want to study ring opening polymerization of  $\epsilon$ -caprolactone by tungsten complexes, since almost no investigations for this polymerization have been reported.

All complexes have been fully characterized spectroscopically and wherever possible their molecular structures has been confirmed by single crystal X-ray diffraction studies. These complexes have all been screened for their ability to ring opening polymerization of  $\epsilon$ -caprolactone, and where appropriate for their ability for ring opening polymerization of *rac*-lactide. When deemed necessary, known complexes from the literature have also been synthesized to enable comparative studies under our specific conditions to be achieved. Some unpublished complexes have been done by other colleagues in our group, experiments themselves have been repeated, but no characterization has been included in this report.

## 1.4 Thesis overview

This study focuses on ring opening polymerization of  $\epsilon$ -caprolactone and *rac*-lactide.

Various multi-nuclear pro-catalysts have been synthesized and spectroscopically characterized, and then tested for their abilities as polymerization catalysts.

In the first results and discussion chapter, **Chapter 2**, the synthesis of binuclear aluminium complexes have been screened for their ability for ring opening polymerization of  $\epsilon$ -caprolactone and *rac*-lactide.

In the second part of the study, **Chapter 3**, the focus is on tungsten complexes supported by larger calix[*n*]arenes (*n*=6 and 8). These systems have also been screened for their ability produce poly caprolactone.

All synthetic procedures, characterization data and polymerization methods are presented in the experiment section (**Chapter 4**).

## 1.5 References

1. The Plastic Industry Trade Association, *History of Plastics*, 2014
2. Plastic Europe, *Plastics- the Fact 2013*, 2013
3. P. Bjacek, *Oil and Gas*, 2008, **106**
4. K. Ziegler, E. Hozkamp, H. Briel, H. Martin, *Angew. Chem.*, 1955, **67**, 541
5. G. Natta, P. Pino, G. Mazzanti, U. Giannini, *J. Am. Chem. Soc.*, 1957, **79**, 2975
6. G. Wilkinson, I.M. Birmingham, *J. Am. Chem. Soc.*, 1954, **76**, 4281-4284.
7. H. Sinn, W. Kaminsky, H. J. Vollmer, R. Woldt, *Angew. Chem. Int. Ed. Engl.*, 1980, **19**, 390-392.
8. H. G. Alt, A. Köppl, *Chem. Rev.*, 2000, **100**, 1205-1221.
9. W. Kaminsky, *Angew. Chem. Int. Ed. Engl.*, 1976, **15**, 630.
10. S. A. Krouse, R. R. Schrock, R. E. Cohen, *Macromolecules*, 1987, 903-904.
11. A. Belbella, C. Vauthier, H. Fessi, J. P. Devissaguet, F. Puisieux, *International Journal of Pharmaceutics*, 1996, 95-102.
12. W. H. Carothers, *Chem. Rev.*, 1931, 353-426.
13. O. Dechy-Cabare, B. Martin-Vaca, D. Bourissou, *Chem. Rev.*, 2004, 6147-6176.
14. D. Mecerreyes, R. Jerome, P. Dubois, *Macromolecular Architectures*, 1999, 1-59.
15. Z. Grobelny, A. Stolarzewicz, B. Morejko, W. Pisarski, A. Maercker, A. Skibinski, S. Krompiec, J. Rzepa, *Macromolecules*, 2006, 6832-6837.
16. A. Stolarzewicz, Z. Grobelny, W. Pisarski, B. Losiewicz, B. Piekarnik, A. Swinarew, *Eur. J. Org. Chem.*, 2006, 2485-2497. *Chem.*, 1999, 2447-2455.
17. D. Mecerreyes, D. Dahan, P. Lecomte, P. Dubois, A. Demonceau, A. F. Noels, R. Jerome, *J. Polym. Sci., Part A: Polym. Chem.*, 1999, 2447-2455.

18. D. Mecerreyes, P. Dubois, R. Jerome, J.L. Hedrick, *Macromolecular Chemistry and Physics*, 1999, 156-165.
19. D. Mecerreyes, P. Dubois, R. Jerome, J.L. Hedrick, C. J. Hawker, *J. Polym. Sci., Part A: Polym. Chem.*, 1999, 1923-1930.
20. D. Mecerreyes, R. Jerome, P. Dubois, *Macromolecular Architectures*, 1999, 1-59.
21. J. Baran, A. Duda, A. Kowalski, R. Szymanski, S. Penczek, *Macromolecular Symposia*, 1997, 93-101.
22. J. Baran, A. Duda, A. Kowalski, R. Szymanski, S. Penczek, *Macromol. Rapid Commun.*, 1997, 325-333.
23. K. M. Stridsberg, M. Ryner, A.C. Albertsson, *Controlled ring-opening polymerization: Polymers with designed macromolecular architecture, in Degradable aliphatic polyesters*. 2002, Springer-Verlag Berlin: Berlin. p. 41-65.
24. P. Dubois, C. Jacobs, R. Jerome, P. Teyssie, *Macromolecules*, 1991, 2266-2270
25. C. Jacobs, P. Dubois, R. Jerome, P. Teyssie, *Macromolecules*, 1991, 3027-3034.
26. Y. C. Liu, B. T. Ko, C.C. Lin, *Macromolecules*, 2001, **27**, 6196-6201.
27. M. H. Chisholm, M. H.; C. C. Lin, J. C. Gallucci, B. T. Ko, *Dalton Trans.*, 2003, 406-412.
28. M. L. Hsueh, B.H. Huang, C. C. Lin, *Macromolecules*, 2002, 5763-5768.
29. M. H. Chisholm, D. Navarro-Llobet, W. J. Simonsick, *Macromolecules*, 2001, 8851-8857
30. H. L. Chen, B. T. Ko, B. H. Huang, C. C. Lin, *Organometallics*, 2001, 5076-5083.
31. C. H. Huang, F. C. Wang, B. T. Ko, T. L. Yu, C. C. Lin, *Macromolecules*, 2001, 356-361.

32. T. Aida, S. Inoue, *Accounts of Chemical Research*, 1996, 39-48.
33. N. Emig, H. Nguyen, H. Krautscheid, R. Reau, G. Bertrand, *Organometallics*, 1998, 3599-3608.
34. N. Emig, R. Reau, H. Krautscheid, D. Fenske, G. Bertrand, *J. Am. Chem. Soc.*, 1996, 5822-5823.
35. D. Chakraborty, E. Y. X. Chen, *Organometallics*, 2002, 1438-1442.
36. Z. Y Chai, C. Zhang, Z. X. Wang, *Organometallics*, 2008, 1626-1633.
37. W. Yao, Y. Mu, A. Gao, W. Gao, L. Ye, *Dalton Trans.*, 2008, 3199-3206.
38. M. Shen, W. Zhang, K. Nomura, W. -H. Sun, *Dalton Trans.*, 2009, 9000-9009.
39. M. Shen, W. Huang, W. Zhang, X. Hao, W. -H. Sun, C. Redshaw, *Dalton Trans.*, 2010, 39, 9912-9922.
40. W. -H. Sun, M. Shen, W. Zhang, W. Huang, S. Liu, C. Redshaw, *Dalton Trans.*, 2011, 40, 2645-2653.
41. W. -A. Ma, L. Wang, Z. -X. Wang, *Dalton Trans.*, 2011, 40, 4669-4677.
42. W. -A. Ma, Z. -X. Wang, *Organometallics*, 2011, 30, 4364-4373.
43. N. Nomura, T. Aoyama, R. Ishii, T. Kondo, *Macromolecules*, 2005, 5363-5366.
44. N. Iwasa, M. Fujiki, K. Nomura, *J. Mol. Catal. A: Chem.*, 2008, 67-75
45. S. Iwasa, Y. Furukawa, K. Nomura, *Novel aluminum compound is used as ring-opening polymerization catalyst for polymerizing lactone, lactide and cyclic anhydride for manufacturing polyester.*, 2009, Daiso Co Ltd; Univ Nara.
46. M. Shen, W. J. Zhang, K. Nomura, W. -H. Sun, *Dalton Trans.*, 2009, 9000-9009.
47. D. A. Atwood, J. A. Jegier, D. Rutherford, *Inorg. Chem.*, 1996, 63-70.



48. D. A. Atwood, J. A. Jegier, D. Rutherford, *Bulletin of the Chemical Society of Japan*, 1997, 2093-2100
49. A. Bhaw-Luximon, D. Jhurry, N. Spassky, *Polymer Bulletin*, 2000, 31-38.
50. P. A. Cameron, D. Jhurry, V. C. Gibson, A. J. P. White, D. J. Williams, S. Williams, *Macromol. Rapid Commun.*, 1999, 616-618.
51. G. Montaudo, M. S. Montaudo, C. Puglisi, F. Samperi, N. Spassky, A. LeBorgne, M. Wisniewski, *Macromolecules*, 1996, 6461-6465.
52. N. Spassky, M. Wisniewski, C. Pluta, A. LeBorgne, *Macromol. Chem. Phys.*, 1996, 2627-2637.
53. T. M. Ovitt, G. W. Coates, *J. Am. Chem. Soc.*, 1999, 4072-4073
54. C. P. Radano, G. L. Baker, M. R. Smith, *J. Am. Chem. Soc.*, 2000, 1552-1553.
55. T. M. Ovitt, G. W. Coates, *J. Polym. Sci. Pol. Chem.*, 2000, 4686-4692.
56. C. T. Chen, C. A. Huang, B. H. Huang, *Macromolecules*, 2004, 7968-7973.
57. A. Amgoune, L. Lavanant, C. M. Thomas, Y. Chi, R. Welter, S. Dagorne, J. F. Carpentier, *Organometallics*, 2005, 6279-6282.
58. C. M. Thomas, *Chem. Soc. Rev.*, 2010, 39, 165–173.
59. M. J. Stanford, A. P. Dove, *Chem. Soc. Rev.*, 2010, 39, 486–494.
60. W. -A. Ma, Z. -X. Wang, *Dalton Trans.*, 2011, 40, 1778-1786.
61. D. J. Darensbourg, O. Karroonnirun, S. J. Wilson, *Inorg. Chem.*, 2011, **50**, 6775-6787.
62. J. Weil, R. T. Mathers, Y. D. Y. L. Getzler, *Macromolecules* 2012, **45**, 1118-1121.
63. C. -Y. Li, C. -Y. Tsai, C. -H. Lin, B. -T. Ko, *Dalton Trans.*, 2011, **40**, 1880-1887.
64. M. Fan, H. Zhang, M. Lattman, *Chem. Commun.*, 1998, 99.

65. (a) C.D. Gutsche, *Calixarenes*, Royal Society of Chemistry, Cambridge, 1989; (b) D.M. Roundhill, *Prog. Inorg. Chem.* **43**, 1995, 553; (c) C. Wieser, C.B. Dielman, D. Matt, *Coord., Chem. Rev.* 1997, **165**, 93; (d) A. Ikeda, S. Shinkai, *Chem. Rev.*, 1997, **97**, 1713; (e) C.D. Gutsche, *Calixarenes Revisited*, Royal Society of Chemistry, Letchworth, 1988.; (f) J.L. Atwood, L.J. Barbour, M.J. Hardie, C.L. Raston, *Coord., Chem. Rev.*, 2001, **222**, 3; (g) Z. Asfari, V. Böhmer, J. Harrowfield, J. Vicens (Eds.), *Calixarenes*, 2001, Kluwer, Dordrecht, 2001; (h) W. Sliwa, *Croatica Chem. Acta*, 2002, **75**, 131; (i) P.D. Harvey, *Coord. Chem. Rev.*, 2002, **233/234**, 289.
66. C. Redshaw *Coord. Chem. Rev.* **2003**, 244, 45.
67. (a) D.H. Homden and C. Redshaw, *Chem. Rev.* **2008**, 108, 5086. (b) Scott paper
68. (a) M. Aoki, K. Murata, S. Shinkai, *Chem. Lett.*, 1991, 1715; (b) M. Aoki, K. Nakashima, H. Kawabata, S. Tsutsui, S. Shinkai, *Perkin Trans.*, 1993, **2**, 347.
69. (a) G. E. Hofmeister, F. Ekkehardt, S. F. Pedersen, *J. Am. Chem. Soc.*, 1989, **111**, 2318; (b) G. E. Hofmeister, E. Alvarado, J. A. Leary, D. I. Yoon, S. F. Pedersen, *J. Am. Chem. Soc.*, 1990, **112**, 8843.
70. W. Clegg, R. J. Errington, P. Kraxner, C. Redshaw, *Dalton Trans.*, 1992, 1443
71. C. Redshaw, M.R.J. Elsegood, *Inorg. Chem.*, 2000, **39**, 5164.
72. G. Odian, *Principles of Polymerization*; Wiley & Sons: New York, 3<sup>rd</sup> ed., 1991.
73. J. M. G. Cowie, *Polymers: Chemistry and physics of modern materials*; Chapman and Hall: New York, 2<sup>nd</sup> ed., 1991.
74. F. Stelzer, R. H. Grubbs, G. Leising, *Polymer*, 1991, **32**, 1851–1856.
75. M. W. Wagaman, R. H. Grubbs, *Macromolecules*, 1997, **30**, 3978–3985.
76. K. Knoll, R. R. Schrock, *J. Am. Chem. Soc.*, 1989, **111**, 7989–8004.

77. S. A. Krouse, R. R. Schrock, *Macromolecules*, 1988, **21**, 1885–1888.
78. O. A. Scherman, California Institute of Technology, *PhD. Thesis*, 2004, 3-4.

## Chapter 2

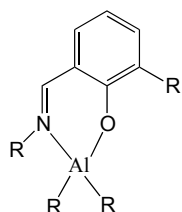
### Organoaluminium complexes of *ortho*-, *meta*-, *para*-anisidines

## 2.1. Introduction

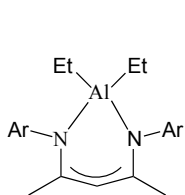
### 2.1.1 Organoaluminium complexes and its ring opening polymerization

The ring opening polymerization (ROP) of cyclic esters to produce biodegradable polymers continues to be an area of immense academic interest. A variety of metal-based initiators have been employed, which operate via a coordination-insertion mechanism. Aluminium complexes too have attracted attention in this area, primarily due to their beneficial toxicity (low) and Lewis acidity (high).<sup>1</sup> Of the previously reported organoaluminium systems, most studies have centred around the use of *N,O*-phenoxyimine (salicylaldimine) type ligand sets (see **I**, chart 1).<sup>2</sup> For example, Nomura and co-workers studied the series of dimethylaluminium complexes  $[\text{Me}_2\text{Al}[\text{O}-2-\text{R}^1-6-(\text{R}^2\text{N}=\text{CH})\text{C}_6\text{H}_3]]$  ( $\text{R}^1 = \text{Me}, t\text{Bu}$ ;  $\text{R}^2 = t\text{Bu}, \text{cyclohexyl}, \text{adamantyl}, \text{Ph}, 2,6\text{-Me}_2\text{C}_6\text{H}_3, 2,6\text{-}i\text{Pr}_2\text{C}_6\text{H}_3$ ), for which it was found that the imine bound substituent ( $\text{R}^2$ ) had a significant influence on the observed catalytic activity.<sup>[2a,d]</sup> As well as other systems derived from other bi-dentate chelates, for example the *N,N*- and *O,O*-chelate systems **II** – **IV**,<sup>3</sup> recent studies have also focussed on the use of tri- (eg. **V** and **VI**),<sup>1c, 4</sup> and tetra-dentate ligand sets (eg. **VII** and **VIII**);<sup>5</sup> macro-cyclic ligands have also been studied.<sup>6</sup> These multi-dentate ligands, which are usually derived from amines/anilines, have been shown to yield complexes capable of the ROP of  $\epsilon$ -caprolactone in a living manner, allowing for control over the molecular weight and distribution of the resulting polymer product.<sup>3</sup> We have also found that remote dialkylaluminium centres present in the same complex can have beneficial cooperative effects on the catalytic activity as long as they are not linked by aluminoxane type bonding.<sup>6</sup>

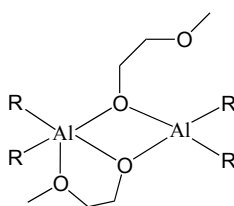
With this in mind, we are exploring the potential of functionalised anilines as ancillary ligands at aluminium in the ROP of  $\epsilon$ -caprolactone or *rac*-lactide, where there is the potential for binding multiple organoaluminium centres in relatively close proximity.



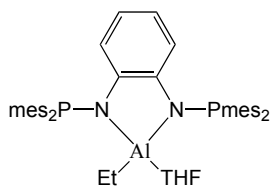
I. K. Nomura *et al*  
Zhang and Wang  
N. Nomura *et al*  
Pappalardo *et al*



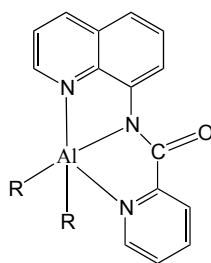
II. Gong and Ma



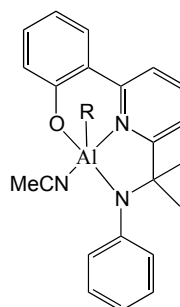
III. Lewinski *et al*



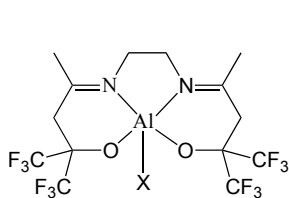
IV. Eisen and Hey-Hawkins



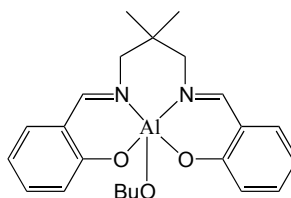
V. Sun *et al*



VI. Solan *et al*



VII. Carpentier *et al*



VIII. N. Nomura *et al*

**Scheme 27.** Reported organometallic ring opening polymerization pre-catalyst.

In this chapter, we present our findings on systems derived from the interaction of *o*-, *m*-, *p*-anisidines with trimethylaluminium and explore the effect of the structures of the resulting organoaluminium derived species on catalytic activity in the ROP of  $\epsilon$ -caprolactone; activities for the ROP of *rac*-lactide were very and so further studies were discontinued.

## 2. 2. Result and Discussion

Interaction of *o*-anisidine with two equivalents of Me<sub>3</sub>Al in toluene afforded the complex  $\{[1,2-(\text{OMe}),\text{N}-\text{C}_6\text{H}_4(\mu\text{-Me}_2\text{Al})](\mu\text{-Me}_2\text{Al})\}_2$  (**1**) in good isolated yield. Slow cooling of the reaction to 0 °C led to the formation of colourless crystals suitable for a single crystal X-ray diffraction study. The molecular structure of **1** is shown in Figure 4. X-ray data is attached in appendix but no further discussion due to the reason that other member in our group completes it.

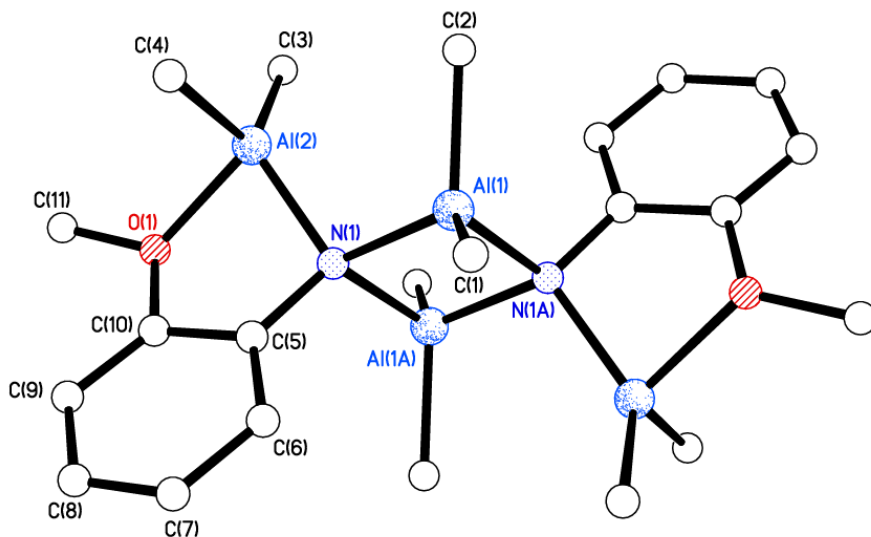


**Figure 4.** Molecular structure of **1** showing the atom numbering scheme.

Similar use of *m*-anisidine failed to produce any crystalline product on cooling of a saturated toluene solution, instead it proved necessary to add an equal volume of *n*-hexane and cool the resulting toluene/hexane solution to -78 °C, whereupon a while crystalline product formed, albeit in much lower isolated yield. Use of solely toluene tended to result in the formation of sticky (off-white) oil, which more often than not would fail to crystallize. The molecular structure of **2** is shown in Figure 5. X-ray data is attached in appendix but no further discussion due to the reason that other member in our group completes it.

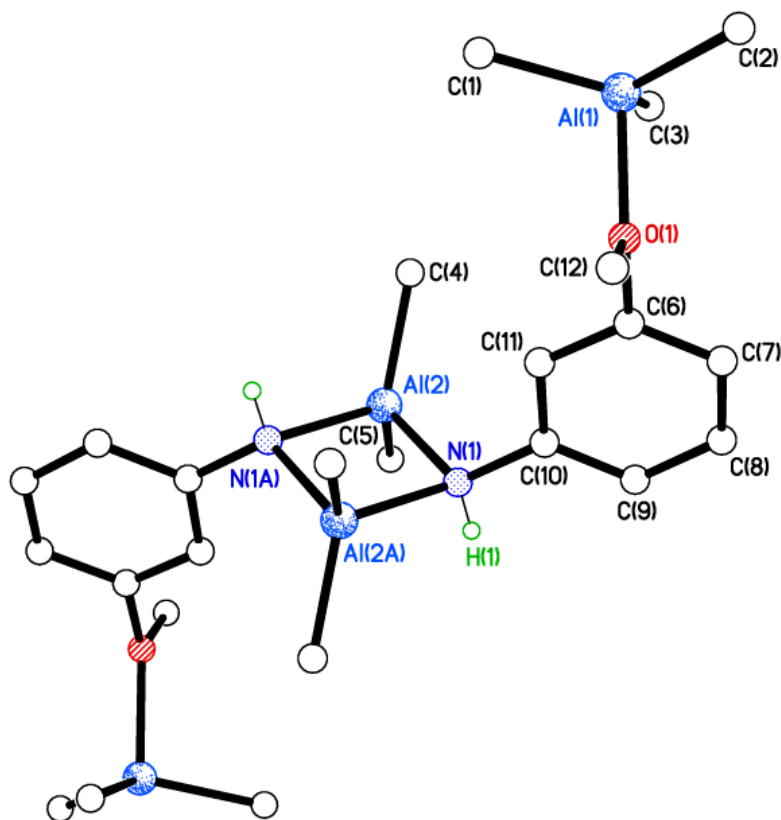


**Figure 5.** Molecular structure of **2** showing the atom numbering scheme.



An analogous product to **2** was obtained when employing *p*-anisidine as starting material, viz  $[p\text{-(Me}_3\text{AlOMe),NHC}_6\text{H}_4(\mu\text{-Me}_2\text{Al})]_2$  (**3**), which can be readily recrystallized from a saturated toluene solution on prolonged standing at ambient temperature (isolated yield ~ 48 %). The molecular structure of **3** is shown in Figure 6., with selected bond lengths and angles given in the caption. The molecular arrangement of **3** is very similar to that present in **2**; a centrosymmetric dimer is formed from the two *p*-anisidine derived groups and two Me<sub>2</sub>Al bridges. The OMe function of each *p*-anisidine is bound to a terminal Me<sub>3</sub>Al group.

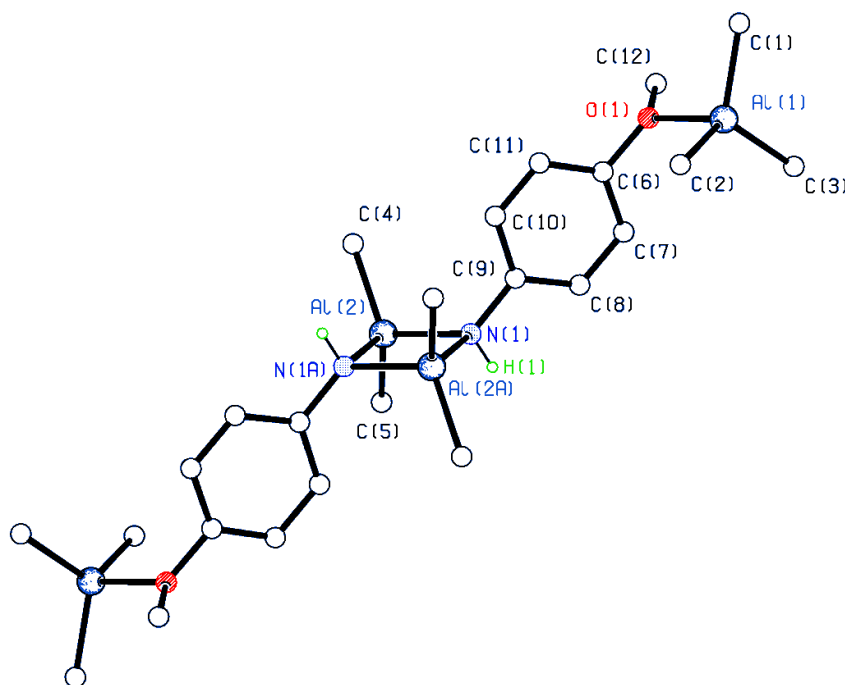


**Figure 6.** Molecular structure of **3** showing the atom numbering scheme. Selected bond lengths (Å) and angles (°): Al(1) – O(1) 1.9582(19), Al(2) – N(1) 1.9851 (15), Al(2) – N(1A) 1.9809 (15); Al(1) – O(1) – C(6) 120.28(10), N(1) – Al(2) – N(1A) 87.24(6), Al(2) – N(1) – C(10) 120.62(14).

### 2.2.1 Ring-Opening Polymerization (ROP) of $\epsilon$ -Caprolactone ( $\epsilon$ -CL).

Aluminium compounds are often reported as efficient catalysts for ring-opening polymerization (ROP) of cyclic esters.<sup>1</sup> The catalytic behaviour of **1** - **3** was explored toward the ROP of  $\epsilon$ -CL. Generally these complexes exhibited good activity for the ROP of  $\epsilon$ -CL. Runs were observed over 30 min, results for which are summarized in Table 1. Moreover, the detailed investigations for the optimization of the conditions were conducted by employing **1** as the initiator, the results for which are collected in Table 1.

The pre-catalyst **1** was effective in the ROP of  $\epsilon$ -CL both in the presence and absence of benzyl alcohol (BnOH) (Table 1, entries 1–7) though lower activities was observed in the absence of benzyl alcohol, although such conditions produced polymers with a similar molecular weight distribution. Given that the aluminium complex, in the presence of benzyl alcohol, exhibited better activity, detailed investigations of complex **1–3** have been carried out in the presence of BnOH (Table 1).

According to entries 1–5 in Table 1, a linear relationship between the monomer conversions and  $M_n$  values was observed with narrow molecular weight distributions [1.47–1.80], indicating the classical feature of a living polymerization process (Fig. 7). The molecular weight distributions [PDI] values of the resultant polymers became a little broader with increased monomer conversions [e.g., PDI: 1.47 (conversion 31.9 %), 1.41 (conversion 43.9 %), 1.73 (conversion 82.0 %), and 1.80 (conversion 98.7 %) in Table 1].

Entry	Cat.	CL:X <sup>b</sup> :Bn	T/°C	t/min	m/g	Yield (%)	$M_n \cdot 10^{-4c}$	PDI
<b>OH</b>								
<b>1</b>	1	250:01:01	110	30	2.26	82.0	1.84	1.73
<b>2</b>	1	250:01:01	80	30	2.72	98.7	2.04	1.80
<b>3</b>	1	250:01:01	60	30	1.37	49.7	1.41	1.62
<b>4</b>	1	250:01:01	40	30	1.21	43.9	1.37	1.55
<b>5</b>	1	250:01:01	25	30	0.88	31.9	0.96	1.47
<b>6</b>	1	250:01:00	110	30	2.02	73.3	1.65	1.72
<b>7</b>	1	250:01:00	80	30	2.54	92.2	1.98	1.85
<b>8</b>	1	62.5:01:01	80	30	2.08	75.6	0.53	1.88
<b>9</b>	1	125:01:01	80	30	2.16	78.4	0.90	1.98
<b>10</b>	1	500:01:01	80	30	2.56	93.1	2.16	1.88
<b>11</b>	1	1000:01:01	80	30	0.32	11.6	2.74	1.98

<sup>a</sup> Conditions: 20  $\mu$ mol of cat.; 1.0 M  $\epsilon$ -CL toluene solution. <sup>b</sup> X = Al-anisidine complexes

<sup>c</sup> GPC data in THF vs polystyrene standards.

**Table 1.** Ring Opening Polymerization screening of  $\epsilon$ -CL by pre-catalysts **1**.<sup>a</sup>

Table 1 displays result for elevation of the temperature (Table 1, entries 1–5), which resulted in higher molecular weight polymer and a higher conversion rate until 85 °C, and decreased at higher temperatures for **1**.

As high-molecular-weight polyesters possess better mechanical properties for subsequent utilization, high-molecular-weight PCL is an attractive target. An increase of the

monomer/Al ratio often leads to higher molecular weights; however, this is usually to the detriment of the monomer conversion rate. Here, we also investigated the effect of the  $\epsilon$ -CL/Al molar ratio on the catalytic behaviour, and the results are given in Table 1 (entries 2, and 8–11). When the mole ratio CL: Al was increased from 62.5 to 1000, the molecular weight increased from  $0.53 \times 10^4$  to  $2.74 \times 10^4$  with little change of molecular weight distribution (1.88–1.98), but the conversion rate significantly decreased, producing polymers with lower molecular weight than the calculated  $M_n$  values (Figure 8).

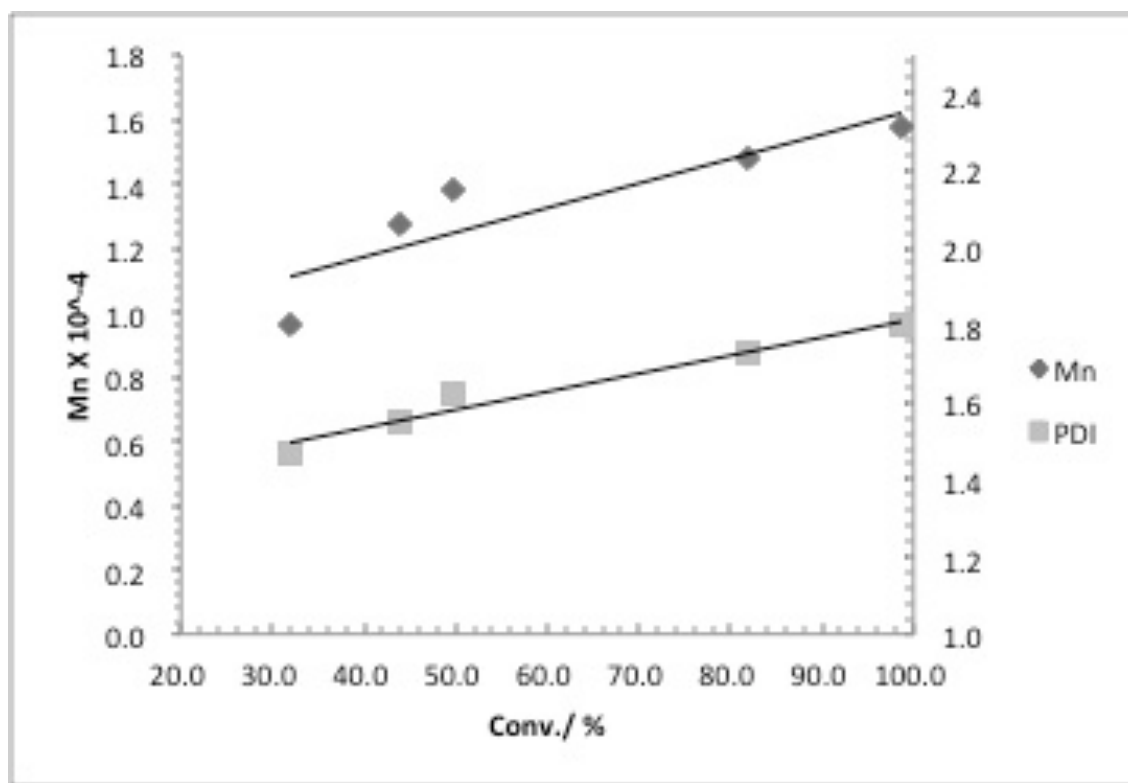


**Figure 7.**  $M_n$  and  $M_w/M_n$  vs. monomer conversion in the ROP of  $\epsilon$ -CL initiated by **1**/*o*-anisidine aluminium complex (Table 1, entries 1–5).

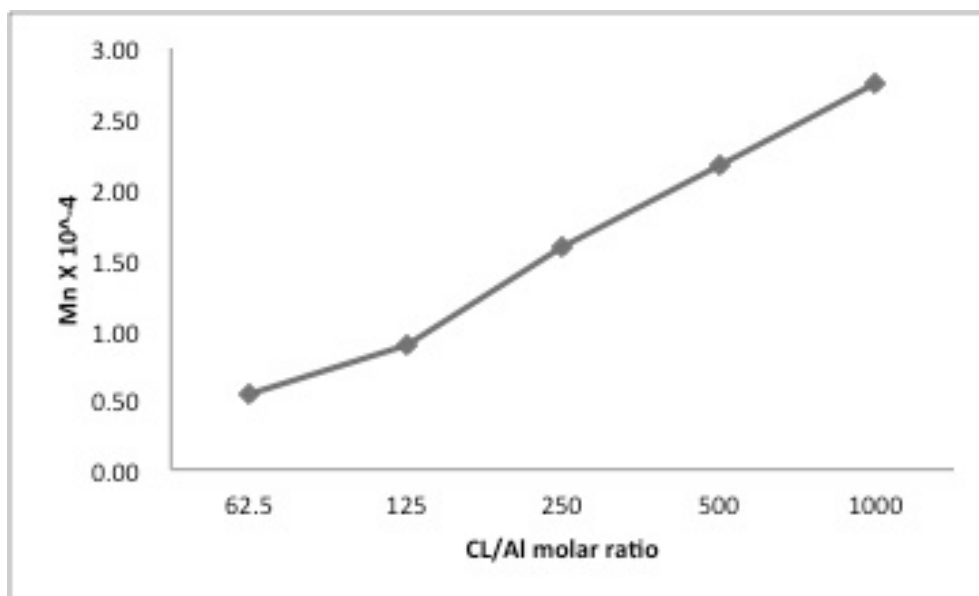


**Figure 8.** Plots of  $M_n$  values vs. CL/Al molar ratio in the ROP of  $\epsilon$ -CL initiated by **1** (Table 1, entries 2, and 8–11).

In addition, we investigated the behaviour of the other complexes herein toward the ROP of  $\epsilon$ -CL. Generally, the anisidine aluminium complexes showed good catalytic activity with high conversion ( $> 90\%$ ). The activity order **1**  $>$  **2**  $\approx$  **3** was observed, with **1** clearly out-performing **2** and **3** at  $110\text{ }^{\circ}\text{C}$ . The effect on the molecular weight of the polymer also exhibited the same order. Despite the similar conversion rates and molecular weights obtained using **2** and **3** at different temperatures (Table 2, entries 2, 3, 5, 6, 8 and 9), the molecular weight distributions using **3** were somewhat smaller, compared with **2** [e.g., PDI:  $110\text{ }^{\circ}\text{C}$  (1.73 vs 1.10),  $85\text{ }^{\circ}\text{C}$  (1.95 vs 1.37), and  $25\text{ }^{\circ}\text{C}$  (1.53 vs 1.16) in Table 2]. This is attributed to the ease with which **3** can be reproducibly crystallized on a large scale.

Entry	Cat	CL:X <sup>b</sup> :BnOH	T/°C	t/min	m/g	Yield (%)	M <sub>n</sub> *10 <sup>-4</sup> <sup>c</sup>	PDI
1	1	250:01:01	110	30	2.26	82.0	1.84	1.73
2	2	250:01:01	110	30	1.79	64.9	1.16	1.73
3	3	250:01:01	110	30	1.71	62.0	1.02	1.10
4	1	250:01:01	80	30	2.72	98.7	2.04	1.80
5	2	250:01:01	80	30	2.56	92.9	1.06	1.95
6	3	250:01:01	80	30	2.67	96.9	1.16	1.37
7	1	250:01:01	25	30	0.88	31.9	0.96	1.47
8	2	250:01:01	25	30	0.79	28.7	0.70	1.53
9	3	250:01:01	25	30	0.8	29.0	0.69	1.16

<sup>a</sup> Conditions: 20 μmol of cat.; 1.0 M ε-CL toluene solution. <sup>b</sup> X = Al-anisidine

complexes <sup>c</sup> GPC data in THF vs polystyrene standards.

**Table 2.** Ring Opening Polymerization screening of ε-CL by pre-catalysts **1** to **3**.<sup>a</sup>

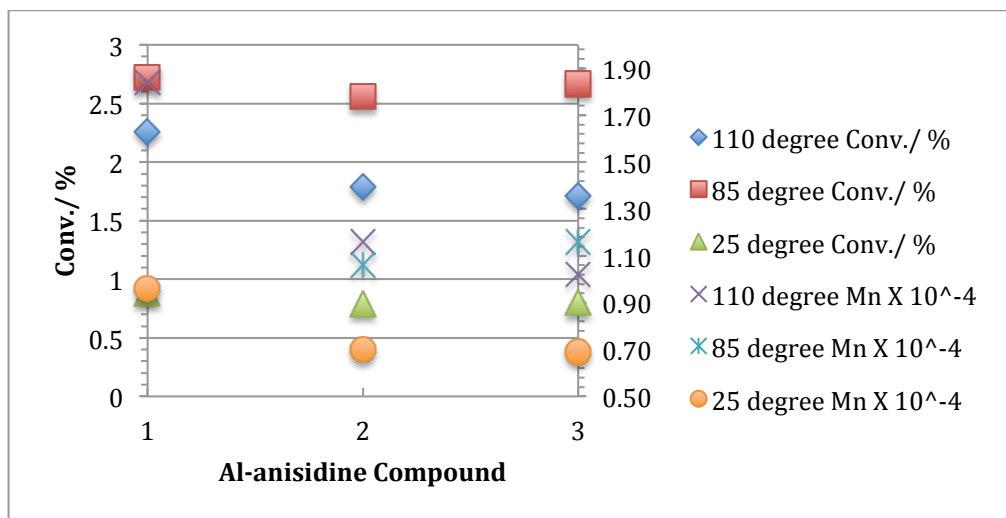


**Figure 9.** Monomer conversion and M<sub>n</sub> X 10<sup>-4</sup> vs. Different Al-anisidine Compound **1**, **2** and **3** in the ROP of ε-CL (Table 2, entries 1-6 and 10-12).

In order to compare the systems herein with others in the literature, we screened the complexes  $\text{Me}_2\text{Al}[\text{O}-2-t\text{Bu}-6-(\text{RN}=\text{CH})\text{C}_6\text{H}_3]$  ( $\text{R} = t\text{Bu}, \text{C}_6\text{F}_5$ ) under the same conditions. <sup>[2a,d]</sup> For  $\text{R} = \text{C}_6\text{F}_5$ , the system exhibited a yield of 94.7 % at 60 °C over 60 min, whereas for  $\text{R} = t\text{Bu}$ , the systems was virtually inactive (yield < 10 %) – see Table 3.

Entry	Cat.	CL:X <sup>b</sup> :Bn	T/°C	t/min	m/g	Yield (%)	M <sub>n</sub> *10 <sup>-4</sup>	PDI
OH								
c								
Entry	Cat.	CL:X <sup>b</sup> :Bn	T/°C	t/min	m/g	Yield (%)	M <sub>n</sub> *10 <sup>-4</sup>	PDI
2	4	250:01:01	60	30	0.00	00.0	N/A	N/A
1	4	250:01:01	50	30	0.00	00.0	N/A	N/A
2	4	250:01:01	60	30	0.00	00.0	N/A	N/A
3	4	250:01:01	60	60	0.27	9.0	1.77	1.22
4	5	250:01:01	60	60	2.23	98.0	3.03	1.89
5	5	250:01:01	60	30	2.71	94.2	3.89	1.53
6	5	250:01:01	60	60	2.73	94.7	5.01	1.89

<sup>a</sup> Conditions: 20 μmol of cat.; 1.0 M ε-CL toluene solution. <sup>b</sup> X=Al-anisidine complexes <sup>c</sup> GPC data in THF vs polystyrene standards.

**Table 3.** Screening of the known<sup>[1, 2]</sup> complexes  $\text{Me}_2\text{Al}[\text{O}-2-t\text{Bu}-6-(\text{RN}=\text{CH})\text{C}_6\text{H}_3]$  ( $\text{R} = t\text{Bu}$  (**4**),  $\text{C}_6\text{F}_5$  (**5**))

### 2.2.2 Ring-Opening Polymerization (ROP) of *rac*-Lactide (LA).

The ROP of *rac*-Lactide (LA) using **1–3** was conducted both in the presence and absence of BnOH. Disappointingly, these aluminium compounds exhibited very low activity (see Table 3) and therefore further investigations were discontinued.

Entry	Cat.	CL:X <sup>b</sup> : BnOH	T/°C	t/min	m/g	Yield (%)
<b>1</b>	1	250:01:01	80	30	0.13	4.7
<b>2</b>	3	250:01:01	80	30	0.08	2.9
<b>3</b>	1	250:01:01	110	30	0	0.0
<b>4</b>	3	250:01:01	110	30	0	0.0
<b>5</b>	1	250:01:01	80	24h	0.19	6.9
<b>6</b>	3	250:01:01	80	24h	0.13	4.7
<b>7</b>	1	250:01:00	80	24h	0	0.0
<b>8</b>	3	250:01:00	80	24h	0	0.0
<sup>a</sup> Conditions: 20 μmol of cat.; 1.0 M ε-CL toluene solution. <sup>b</sup> X = Al-anisidine complexes						

**Table 4.** Ring Opening Polymerization screening of *rac*-LA by pre-catalysts **1** to **3**.<sup>a</sup>



### 2.2.3 Conclusion

In conclusion, we have treated *o*-, *m*- and *p*-anisidine each with two equivalents of trimethylaluminium. Crystal structure analyses of the products revealed that in the case of the *ortho*-anisidine, a complex containing two types of Me<sub>2</sub>Al bridge is formed, namely {[1,2-(OMe),N-C<sub>6</sub>H<sub>4</sub>(μ-Me<sub>2</sub>Al)](μ-Me<sub>2</sub>Al)}<sub>2</sub> (**1**). By contrast, as a result of the increased distance between the methoxy and amino functionalities, both the *meta*- and *para*-anisidines react to form dimeric complexes containing an Me<sub>3</sub>Al group bound to each methoxy group, namely {[1,3-(Me<sub>3</sub>AlOMe),NH-C<sub>6</sub>H<sub>4</sub>](μ-Me<sub>2</sub>Al)}<sub>2</sub> (**2**) and {[1,4-(Me<sub>3</sub>AlOMe),NH-C<sub>6</sub>H<sub>4</sub>](μ-Me<sub>2</sub>Al)}<sub>2</sub> (**3**), respectively. In terms of the ROP of ε-caprolactone, complexes **1** - **3** can efficiently promote the ROP of ε-caprolactone both in the presence and absence of BnOH. Complex **1** afforded highest activity, particularly at 110 °C, and, given the molecular structures, this is tentatively attributed to the close proximity of the two Me<sub>2</sub>Al bridging groups in **1**. It is noteworthy that we have previously observed beneficial cooperative effects for two Me<sub>2</sub>Al groups positioned 5.7818(10) Å apart in a macrocyclic system,<sup>[6]</sup> closer Al – Al interactions in such systems (< 3.2270(14) Å) hindered the polymerization process. Herein, the Al(1) ... Al(2) distance in the best performing system, namely the ‘*ortho*’ complex **1** is 3.394 Å, whereas in the ‘*meta*’ and ‘*para*’ complexes, the distance is somewhat shorter, for example in **2**, the Al(2) – Al(2A) distance is 2.8573(8) Å.

## References

1. (a) C. K. Williams, *Chem. Soc. Rev.*, 2007, **36**, 1573. (b) A. Arbaoui and C. Redshaw, *Polymer Chem.*, 2010, **1**, 801. (c) W. Alkarekshi, A. P. Armitage, O. Boyron, C. J. Davies, M. Govere, A. Gregory, K. Singh and G. A. Solan, *Organometallics*, 2013, **32**, 249 and references therein. (d) Y. Liu, W.-S. Dong, J.-Y. Liu and Y.-S. Li, *Dalton Trans.*, 2014, **43**, 2244.
2. (a) N. Iwasa, M. Fujiki and K. Nomura, *J. Mol. Cat. A, Chem.*, 2008, **292**, 67; (b) C. Zhang and Z.-X. Wang, *J. Organomet. Chem.*, 2008, **613**, 3151; (c) N. Iwasa, J. Liu and K. Nomura, *Catal. Commun.*, 2008, **9**, 1148; (d) J. Liu, N. Iwasa and K. Nomura, *Dalton Trans.*, 2008, 3978; (e) N. Iwasa, S. Katao, J. Liu, M. Fujiki, Y. Furukawa and K. Nomura, *Organometallics*, 2009, **28**, 2179; (f) N. Nomura, T. Aoyama, R. Ishii and T. Kondo, *Macromolecules*, 2005, **38**, 5363; (g) D. Pappalardo, L. Annunziata and C. Pellecchia, *Macromolecules*, 2009, **42**, 6056. (h) X.-F. Yu and Z.-X. Wang, *Dalton Trans.*, 2013, **42**, 3860. (i) T.-L. Huang and C.-T. Chen, *J. Organomet. Chem.*, 2013, **725**, 15. (j) A. Meduri, T. Fuoco, M. Lamberti, C. Pellecchia and D. Pappalardo, *Macromolecules*, 2014, **47**, 534.
1. (a) S. Gong and H. Ma, *Dalton Trans.*, 2008, 3345. (b) J. Lewiński, P. Horeglad, K. Wójcik and I. Justyniak, *Organometallics*, 2005, **24**, 4588. (c) F. Majoumo-Mbe, E. Smolensky, P. Lönnecke, D. Shpasser, M.S. Eisen and E. Hay-Hawkins, *J. Mol. Cat.*, 2005, **240**, 91.
2. (a) M. Shen, W. Zhang, K. Nomura and W.-H. Sun, *Dalton Trans.* 2009, 9000.

3. (a) A. Amgoune, L. Lavanant, C. M. Thomas, Y. Chi, R. Welter, S. Dagorne and J.-F. Carpentier, *Organometallics*, 2005, **24**, 6279; (b) M. Bouyahyi, E. Grunova, N. Marquet, E. Kirillov, C. M. Thomas, T. Roisnel and J.-F. Carpentier, *Organometallics*, 2008, **27**, 5815; (c) M. Bouyahyi, T. Roisnel and J.-F. Carpentier, *Organometallics*, 2012, **31**, 1458. (d) N. Nomura, A. Akita, R. Ishii and M. Mizuno, *J. Am. Chem. Soc.*, 2010, **132**, 1750.
4. A. Arbaoui, C. Redshaw and D.L. Hughes, *Chem. Commun.*, 2008, 4717.
5. SMART (2001), SAINT (2001 & 2008), and APEX 2 (2008) software for CCD diffractometers. Bruker AXS Inc., Madison, USA.
6. G.M. Sheldrick, SHELXTL user manual, version 6.10. Bruker AXS Inc., Madison, WI, USA, (2000).
7. G.M. Sheldrick, *Acta Crystallogr.* 2008, **A64**, 112-122.
8. A.L. Spek, *Acta Crystallogr.* 1990, **A46**, C34.

## **Chapter 3**

### **Organotungsten complexes of calix[6 and 8]arenes**

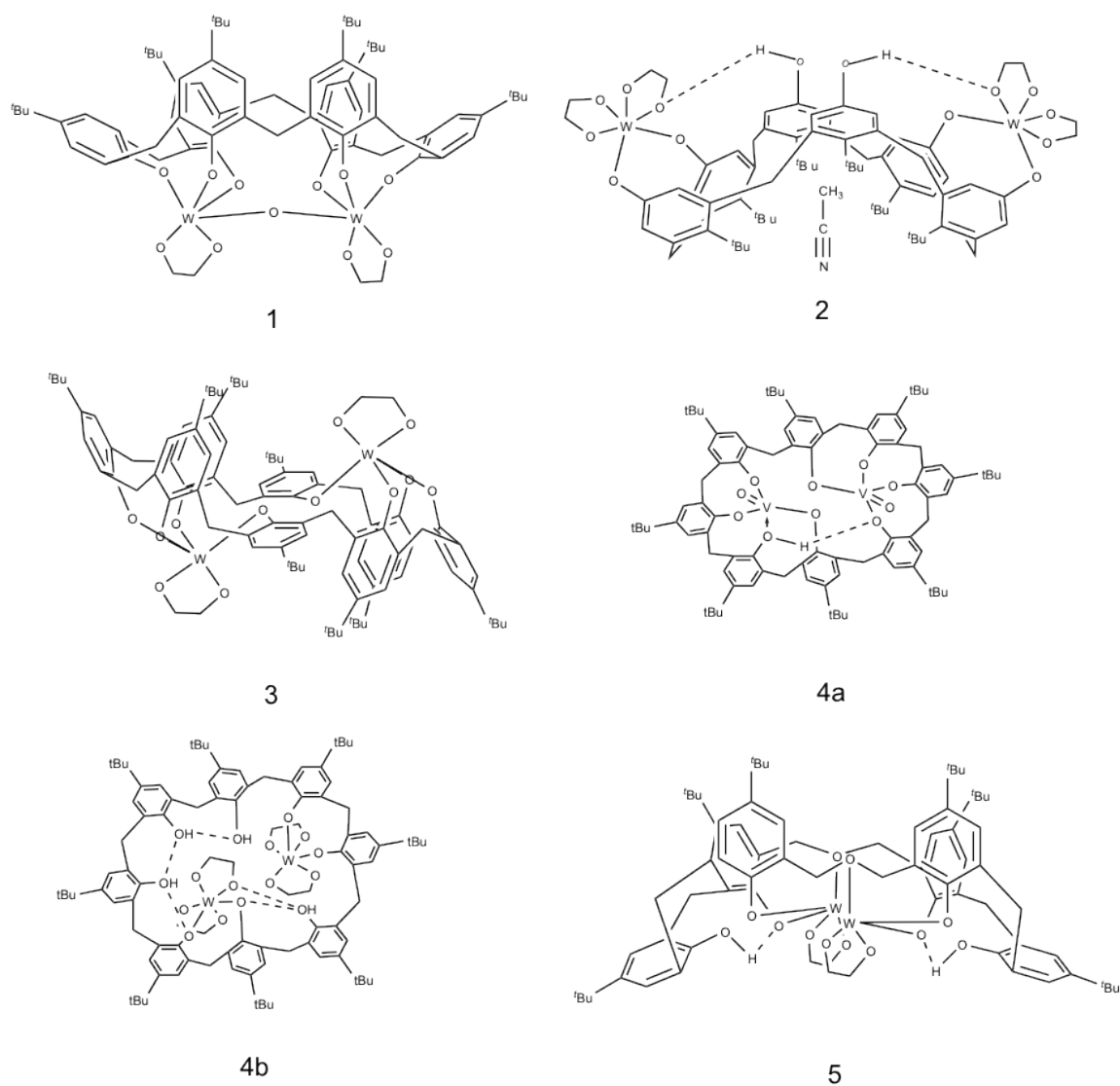
### 3.1 Introduction

The larger calix[*n*]arenes (*n* > 4) continue to be of interest, primarily due to their ability to simultaneously accommodate multiple metal centres.<sup>1</sup> This is desirable since metals in close proximity have the potential to communicate, which in turn may lead to beneficial effects in areas such as magnetism or catalysis.<sup>2</sup> However, the controlled synthesis of specific poly metallic calix[*n*]arenes can be problematic, often complicated by alkali-metal incorporation or fortuitous hydrolysis and/or oxygenation reactions.<sup>3</sup> In the case of tungsten, we have previously shown that by varying the reaction stoichiometry (using WCl<sub>6</sub>), it is possible to control the degree of metallation.<sup>4</sup> The only other tungsten calix[*n*]arenes (*n* > 4) that have been reported are the oxo species

{[WOCl<sub>2</sub>]<sub>2</sub>p-*tert*-butylcalix[6]areneH<sub>2</sub>} and {[WO(NCMe)]<sub>2</sub>p-*tert*-butylcalix[8]arene}<sup>5</sup>, the hydrazido complex {[W(NNPh<sub>2</sub>)]<sub>2</sub>p-*tert*-butylcalix[6]arene}<sup>6</sup> plus the p-*tert*-butylcalix[5]arene complexes prepared by Lattmann *et al.*<sup>7</sup>

In terms of the ring opening polymerization (ROP) of  $\epsilon$ -caprolactone, few group VI systems appear to have been reported.<sup>8</sup>

Herein, we report a number of new tungstocalix[*n*]arene systems (see scheme 28), resulting from the reaction of [W(eg)<sub>3</sub>] (eg = 1,2-ethanediolato) and p-*tert*-butylcalix[6 and 8]areneH<sub>6,8</sub> or p-*tert*-butyltetrahomodioxacalix[6]areneH<sub>6</sub>. The new tungstocalix[6 and 8]arenes have been fully characterized, and their potential as catalysts for the ROP of  $\epsilon$ -caprolactone has been evaluated.



**Scheme 28.** Simple schematic retranslation of tungstocalix complexes **1-5**.

## 3.2 Results and Discussion

### *p*-*tert*-butylcalix[6]areneH<sub>6</sub> chemistry

Reaction of *p*-*tert*-butylcalix[6]areneH<sub>6</sub> with one or two equivalents of [W(eg)<sub>3</sub>] in refluxing toluene, afforded after extraction into hot acetonitrile, the orange/red complex {[W(eg)<sub>3</sub>]<sub>2</sub>(μ-O)*p*-*tert*-butylcalix[6]arene} (**1**) (Figure 10.). X-ray data is attached in appendix but no further discussion due to the reason that another member in our group

conducted the crystal structure determination.

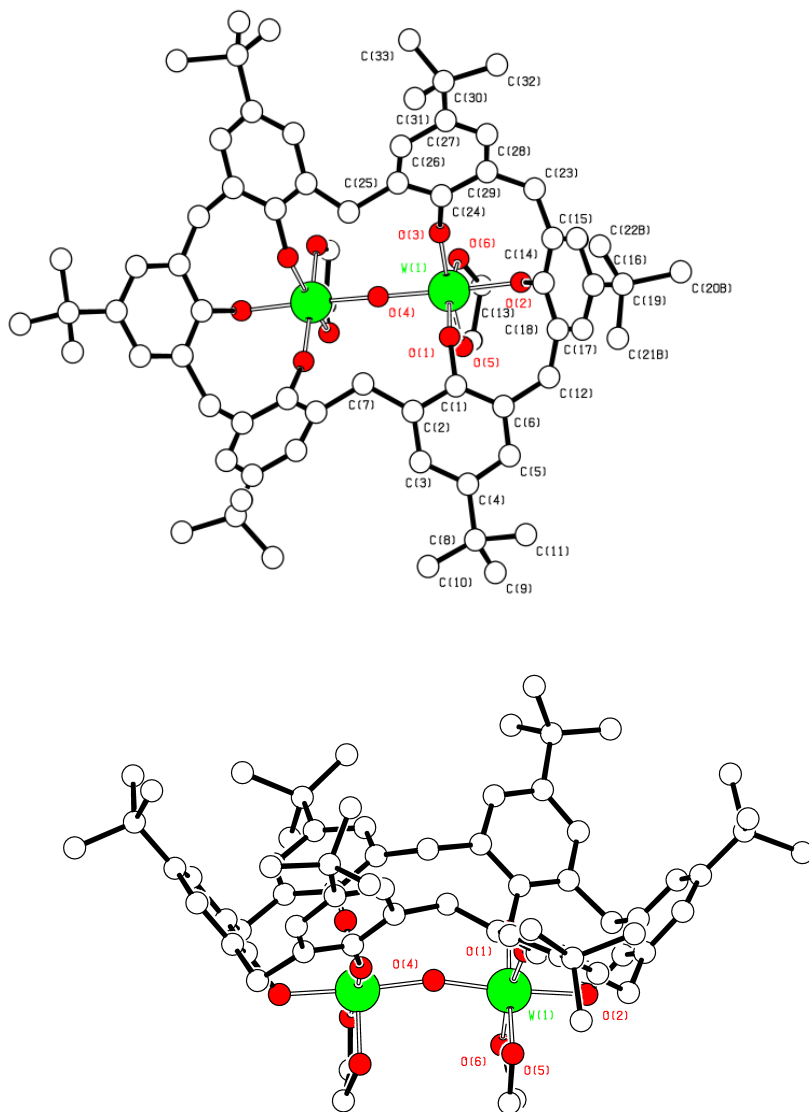


**Figure 10.** Two views to emphasize the calix conformation.

The analogous reaction using four equivalents of  $[\text{W}(\text{eg})_3]$  afforded pale yellow crystals of  $\{[\text{W}(\text{eg})_2]_2\text{p-tert-butylcalix}[6]\text{areneH}_2\} \cdot 1.5\text{MeCN}$  (**2**) in about 45 % isolated yield.

Small crystals of **2**·1.5MeCN suitable for an X-ray structure determination using synchrotron radiation were grown from a hot, saturated solution of acetonitrile on slow cooling and prolonged standing at ambient temperature. The asymmetric unit comprises two molecules of **2** and three molecules of acetonitrile. The molecular structure is shown in Figure 11, with selected bond lengths and angles given in the caption. The geometry about each tungsten is again distorted octahedral, but in this case, each metal only binds to two of the calixarene phenolate oxygen atoms. For each metal, one of the 1,2-ethanediolato ligands is involved in H-bonding to one of the remaining calixarene phenolic groups. The conformation of the calix[6]arene ligand is best described as an enlarged cup, with the phenolic rings bearing O(3) and O(6) forming the base. A molecule of acetonitrile is encapsulated within the cup. Molecules of **2** pack in bi-layers with adjacent *tert*-butyl groups at one interface and inter-digitated *eg* groups at the other (see figure 12).

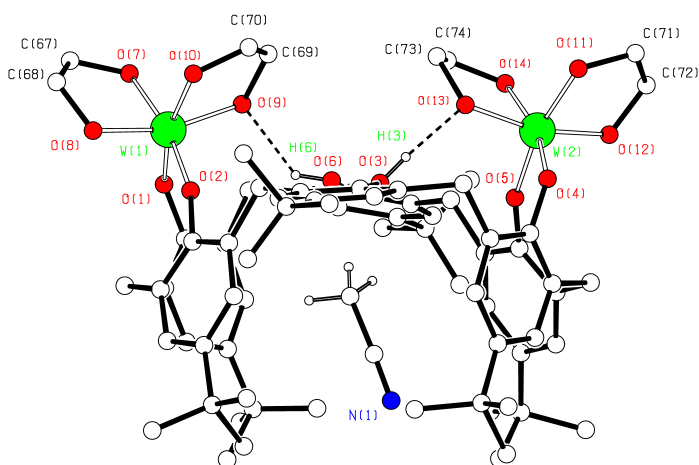




**Figure 11.** Molecular structure of **2** showing the atom numbering scheme. Selected bond lengths (Å) and angles (°): W(1) – O(1) 1.914(3), W(1) – O(2) 1.855(3), W(2) – O(4) 1.923(3), W(2) – O(5) 1.851(3); O(1) – W(1) – O(2) 88.16(15), O(8) – W(1) – O(9)

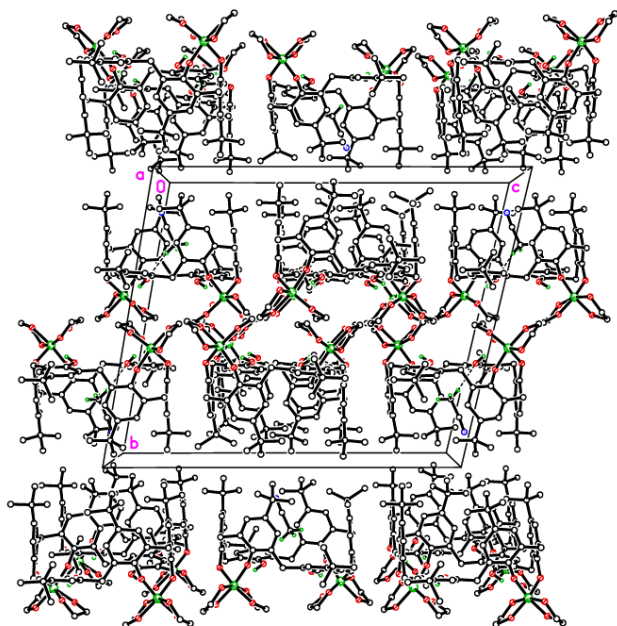


**Figure 12.** Bi-layer packing of **2**.

### **p-tert-butylcalix[8]areneH<sub>8</sub> chemistry**

On extending the synthetic methodology to p-tert-butylcalix[8]areneH<sub>8</sub>, use of one or two equivalents of [W(eg)<sub>3</sub>] led to the isolation of the red complex [W(eg)<sub>2</sub>p-tert-butylcalix[8]arene} (**3**) in good isolated yield. X-ray data is attached in appendix but no further discussion due to the reason that other member in our group completed the structure determination.

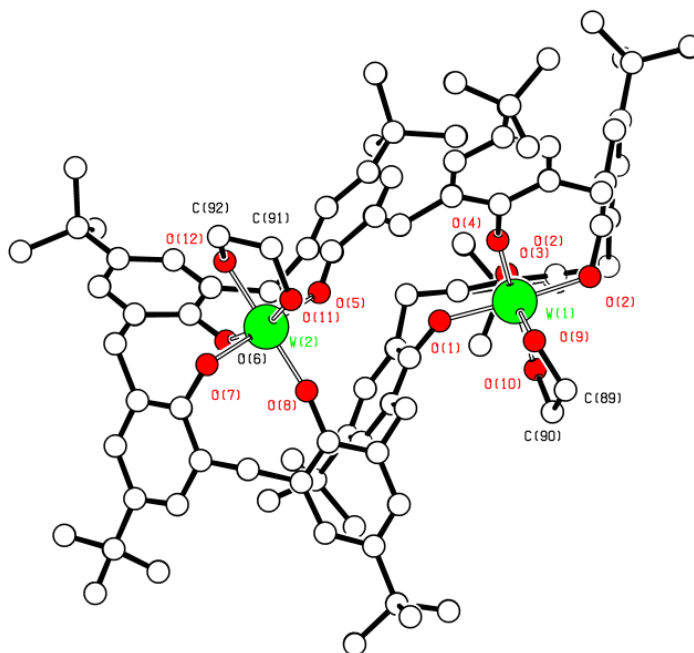


**Figure 13.** Molecular structure of compound **3**.

Increasing the amount of  $[W(eg)_3]$  (to four equivalents) again results in the formation of an orange crystalline solid, however the  $^1H$  NMR spectrum is somewhat different to that of **3**. Interestingly, a crystal structure determination, requiring the use of synchrotron radiation, revealed that the product was a mixture of isomers. In the major isomer (Figure 14), the two tungsten centres bind to neighbouring pairs of phenolate oxygen atoms. For this isomer, all phenolic protons (at O(5), O(6), O(7) and O(8)) were located, but not for O(2) in the minor component. In the minor isomer, this phenolic group O(2) resides between pairs of bonding phenolate oxygens. The tungsten centres and the eg ligands are disordered such that  $W(1):W(1x) = 83.39:16.61(8) \%$  and  $W(2):W(2x) = 62.6:37.4(5) \%$  (same occupancy for the attached eg ligands). The  $W(1):W(1x)$  gives the isomer

ratio, whereas W(2):W(2x) is more of a conformational issue, probably partially depending on the location of W(1) or W(1x).

The acetonitrile containing N(1) lies in the cleft between phenols containing O(5) and O(6). That containing N(3) lies between O(1) and O(2), whilst those containing N(2) and N(4) lie *exo* to the calixarene, between complexes.

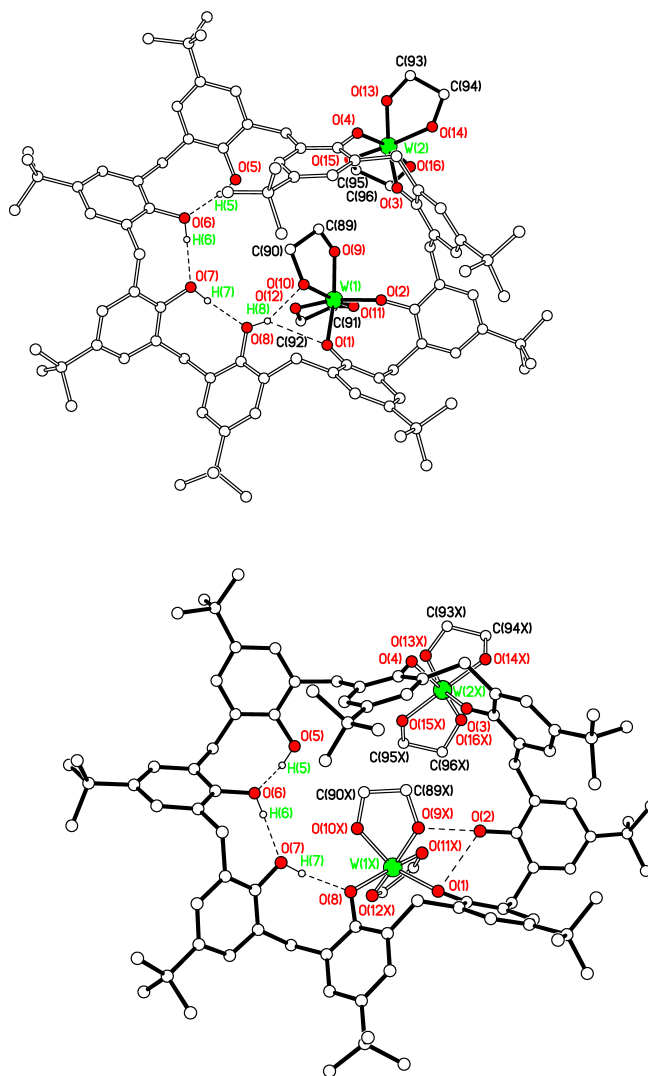


**Figure 14.** Top, Molecular structure of the major isomer of **4a**; bottom, molecular structure of minor isomer of **4b**. Selected bond lengths (Å) and angles (°): Major:

W(1) – O(1) 1.954(4), W(1) – O(2) 1.904(4), W(2) – O(3) 1.912(4), W(2) – O(4) 1.761(6), W(1) – O(9) 1.896(5), W(1) – O(10) 1.942(5); O(1) – W(1) – O(2) 89.58(19), O(1) – W(1) – O(9) 159.5(2), O(3) – W(2) – O(4) 89.3(2). Minor: W(1X) – O(1) 1.855(4), W(2X) – O(3) 1.861(4), W(2X) – O(4) 1.761(6), W(1X) – O(8) 2.150(5), W(1X) – O(9X) 1.88(2), W(1) – O(10X) 1.88(2); O(1) – W(1X) – O(12X) 104.9(8), O(1) – W(1X) – O(9X) 78.8(6), O(3) – W(2X) – O(4) 77.4(2).

### ***p-tert*-butyltetrahomodioxacalix[6]areneH<sub>6</sub> chemistry**

Reaction of *p-tert*-butyltetrahomodioxacalix[6]areneH<sub>6</sub> with two equivalents of [W(eg)<sub>3</sub>] afforded the yellow complex {[WO(eg)]<sub>2</sub> *p-tert*-butyltetrahomodioxacalix[6]areneH<sub>2</sub>} (**5**).

X-ray data is attached in appendix but no further discussion due to the reason that other member in our group completed the structure determination.

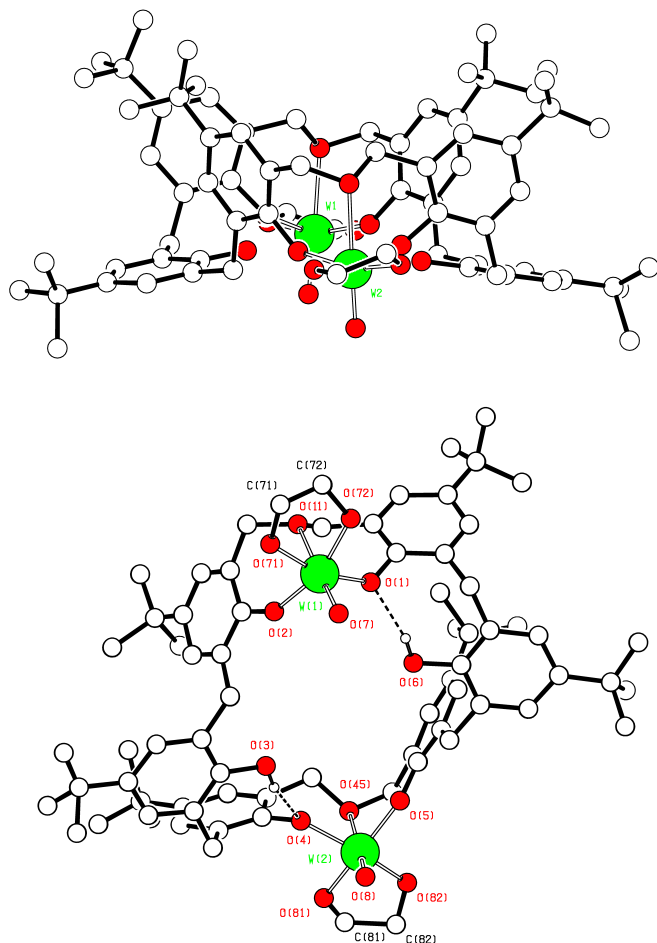


**Figure 15.** Two views of the molecular structure of **5**.

### 3.2.1 Ring Opening Polymerization of $\epsilon$ -caprolactone

The complexes **1** – **5** have been screened for their ability to ring opening polymerization of  $\epsilon$ -caprolactone in the presence of benzyl alcohol (BnOH). Compound **3** was used to optimize the polymerization conditions, and results are tabulated in Table 5. It was necessary to active **3** for the ROP of  $\epsilon$ -caprolactone using BnOH. Good conversion yields were only achieved at temperatures over 100.

According to entries 3, 6 and 7 in Table 5, a linear relationship between the monomer conversions and  $M_n$  values was observed with narrow molecular weight distributions [1.30–1.44], indicating the classical feature of a living polymerization process.

Table 5 displays result for elevation of the temperature (Table 5, entries 3 and 8), which resulted in conversion yields were only achieved at temperatures over 100.

As high-molecular-weight polyesters possess better mechanical properties for subsequent utilization, high-molecular-weight PCL is an attractive target. An increase of the monomer/W ratio should leads to higher molecular weights; however, this is usually to the detriment of the monomer conversion rate. Here, we also investigated the effect of the  $\epsilon$ -CL/W molar ratio on the catalytic behaviour, and the results are given in Table 5 (entries 3, 9 and 10). When the mole ratio CL:W was increased from 200 to 800, the molecular weight increased from  $30.79 \times 10^3$  to  $47.19 \times 10^3$  with little change of molecular weight distribution (1.42–1.52), but the conversion rate decreased (99 % - 64 %).

In addition, we investigated the behaviour of the other complexes herein toward the ROP of  $\epsilon$ -CL. Generally, the anisidine aluminium complexes showed good catalytic activity with high conversion (> 88 %). However, ROP using complex **3** has outstanding polymerization weight compare with other co-catalysts.

Entry	Cat.	CL:X <sup>b</sup> :BnOH	T/°C	t/h	m/g	Yield (%)	M <sub>n</sub> *10 <sup>-3</sup> <sup>c</sup>	PDI
1	1	400:01:01	110	24	2.53	88	1.21	1.0
3	3	400:01:01	110	24	2.82	98	41.40	1.3
4	4	400:01:01	110	24	2.71	94	1.92	1.0
5	5	400:01:01	110	24	2.71	94	7.98	1.1
6	3	400:01:01	110	1	0	0	N/A	N/A
7	3	400:01:01	110	12	2.72	94	9.63	1.44
8	3	400:01:01	80	24	0.32	11	1.83	1.28
9	3	800:01:01	110	24	1.84	64	47.19	1.52
10	3	200:01:01	110	24	2.84	99	30.79	1.42

<sup>a</sup> Conditions: 20 μmol of cat.; 1.0 M ε-CL toluene solution. <sup>b</sup> X=Al-anisidine complexes <sup>c</sup> GPC data in THF vs polystyrene standards.

**Table 5.** Ring Opening Polymerization screening of ε-CL by tungsten pre-catalysts 1, 3-5.

### 3.2.2 Conclusion

In summary, a number of new tungstocalix[6 and 8]arenes have been prepared using the metal precursor [W(eg)<sub>3</sub>] (eg = 1,2-ethanediolato) and the calix[*n*]arenes *p*-*tert*-butylcalix[6 and 8]areneH<sub>6,8</sub> or *p*-*tert*-butyltetrahomodioxacalix[6]areneH<sub>6</sub>. Crystal structure determinations reveal a preference for binding two metal centres, though in the solid-state, the relative positions of the metal centres at the lower rim of the calixarene can vary, for example 1,2-[W(eg)<sub>2</sub>]<sub>2</sub> versus

1,3-[W(eg)<sub>2</sub>]<sub>2</sub>p-*tert*-butylcalix[8]areneH<sub>4</sub>. The syntheses are sensitive to the presence of air and/or moisture, and the work herein includes the characterization of two oxotungsten species. In terms of the ROP In summary, a number of new tungstocalix[6 and 8]arenes have been prepared using the metal precursor [W(eg)<sub>3</sub>] (eg = 1,2-ethanediolato) and the calix[*n*]arenes p-*tert*-butylcalix[6 and 8]areneH<sub>6,8</sub> or p-*tert*-butyltetrahomodioxacalix[6]areneH<sub>6</sub>. Crystal structure determinations reveal a preference for binding two metal centres, though in the solid-state, the relative positions of the metal centres at the lower rim of the calixarene can vary, for example 1,2-[W(eg)<sub>2</sub>]<sub>2</sub> *versus* 1,3-[W(eg)<sub>2</sub>]<sub>2</sub>p-*tert*-butylcalix[8]areneH<sub>4</sub>. The syntheses are sensitive to the presence of air and/or moisture, and the work herein includes the characterization of two oxotungsten species. In terms of the ROP of  $\epsilon$ -caprolactone, only negligible polymer was isolated at temperatures below 100 °C. At 110 °C, all tungstocalix[6 and 8]arenes afforded moderate conversions (88 % to 94 %) over 24 h.



### 3.3 References

- 1 For pre-2003 references, see C. Redshaw *Coord. Chem. Rev.*, 2003, **244**, 45.
- 2 D.H. Homden and C. Redshaw, *Chem. Rev.*, 2008, **108**, 5086.
- 3 (a) C. Redshaw, D.H. Homden, D.L. Hughes, J.A. Wright and M.R.J. Elsegood, *Dalton Trans.*, 2009, 1231. (b) A. Arbaoui, C. Redshaw, M.R.J. Elsegood, V.E. Wright, A. Yoshizawa and T. Yamato, *Chem. Asian J.*, 2010, **5**, 621.
- 4 V.C. Gibson, C. Redshaw and M.R.J. Elsegood, *Chem. Comm.*, 2002, 1200.
- 5 C. Redshaw and M.R.J. Elsegood, *Eur. J. Inorg. Chem.*, 2003, 2071.
- 6 C. Redshaw and M.R.J. Elsegood, *Inorg. Chem.*, 2001, **39**, 5164.
- 7 M. Fan, H. Zhang and M. Lattman, *Chem. Commun.*, 1998, 99.
- 8 (a) M. Labet and W. Thielemans, *Chem. Soc. Rev.*, 2009, **38**, 3484. (b) A. Arbaoui and C. Redshaw, *Polym. Chem*, **2010**, *1*, 801. (c) X. Rong and C. Chunxia, *Progress in Chemistry*, 2012, **24**, 1519.
- 9 C. Redshaw, M. Rowan, D.M. Homden, M.R.J. Elsegood, T. Yamato and C. Pérez-Casas, *Chem. Eur. J.*, 2007, **13**, 10129.
- 10 (a) A. Arduini and A. Casnati in *Macrocyclic Synthesis*, Ed. D. Parker, Oxford University Press, 1996, chapter 7. (b) B. Masci, *J. Org. Chem.*, 2001, **66**, 1497. (c) B. Dhawan and C.D. Gutsche, *J. Org. Chem.*, 1983, **48**, 1536.

## **Chapter 4**

### **Experiment Section**

## 4.1. General Consideration

All manipulations were carried out under an atmosphere of dry nitrogen using conventional Schlenk and cannula techniques or in a conventional nitrogen-filled glove box. Toluene was refluxed over sodium. Acetonitrile were refluxed over calcium hydride. All solvents were distilled and degassed prior to use. IR spectra (nujol mulls, KBr windows) were recorded on a Nicolet Avatar 360 FT IR spectrometer;  $^1\text{H}$  NMR spectra were recorded at room temperature on a Varian VXR 400 S spectrometer at 400 MHz or a Gemini 300 NMR spectrometer or a Bruker Advance DPX-300 spectrometer at 300 MHz. The  $^1\text{H}$  NMR spectra were calibrated against the residual protio impurity of the deuterated solvent. Elemental analyses were performed by the elemental analysis service at the London Metropolitan University and Sichuan Normal University, Chengdu, Sichuan. The anisidine reagents were purchased from Sigma Aldrich and were used as received.

## 4.2. Organoaluminium complexes of *ortho*-, *meta*-, *para*-anisidines

### 4.2.1 Synthesis of $\{[1,4-(\text{Me}_3\text{AlOMe}),\text{NH-C}_6\text{H}_4](\mu\text{-Me}_2\text{Al})\}_2$ (**3**)

$\text{Me}_3\text{Al}$  (16.5 ml, 1.0 M in toluene, 16.5 mmol) was added slowly to *p*-anisidine (1.00 g, 8.2 mmol) at ambient temperature. The system was then refluxed for 12 h, and allowed to cool to room temperature. On prolonged standing (1 – 2 days), crystals of **2** formed, and the resulting residue was extracted into acetonitrile (20 ml) to afford colourless crystals of **3**. MeCN, isolated yield 0.99 g, 48 %. For **3**•MeCN (648.7) Calcd: C 62.9, H 9.0, N 6.5 %. Found: C, 63.0, H 9.0, N 6.9 %. IR: 3259m, 1883w, 1602w, 1506s, 1344m, 1303w, 1257m, 1238s, 1198s, 1153s, 1104m, 1042w, 1014m, 975s, 934w, 860s, 831m,

808m, 765bs, 710bs, 627w. Mass spec (solid, positive ASAP: APCI): 501 ( $M - H$ )<sup>+</sup>, 449 ( $M - H - Al(CH_3)_2$ ), 372 ( $M - H - 2Al(CH_3)_2$ ). ( $C_6D_6$ , 298 K)  $\delta$ : 6.53 – 6.32 (3x m, 8H, arylH), 3.15, 3.13 (2x s, 6H, OMe), 3.11, 3.07 (2x s, 2H, NH), -0.39 (s, 18H, Me<sub>3</sub>Al), -0.48, -0.51, -0.52 (3x s, 12H, Me<sub>2</sub>Al). <sup>13</sup>C NMR: the sample proved to be too insoluble in  $C_6D_6$  to obtain useful spectra; a 12 h acquisition in  $CDCl_3$  allowed us to identify  $\delta$  63.17 (OMe), -8.58 (Me<sub>3</sub>Al), -9.67 (Me<sub>2</sub>Al).

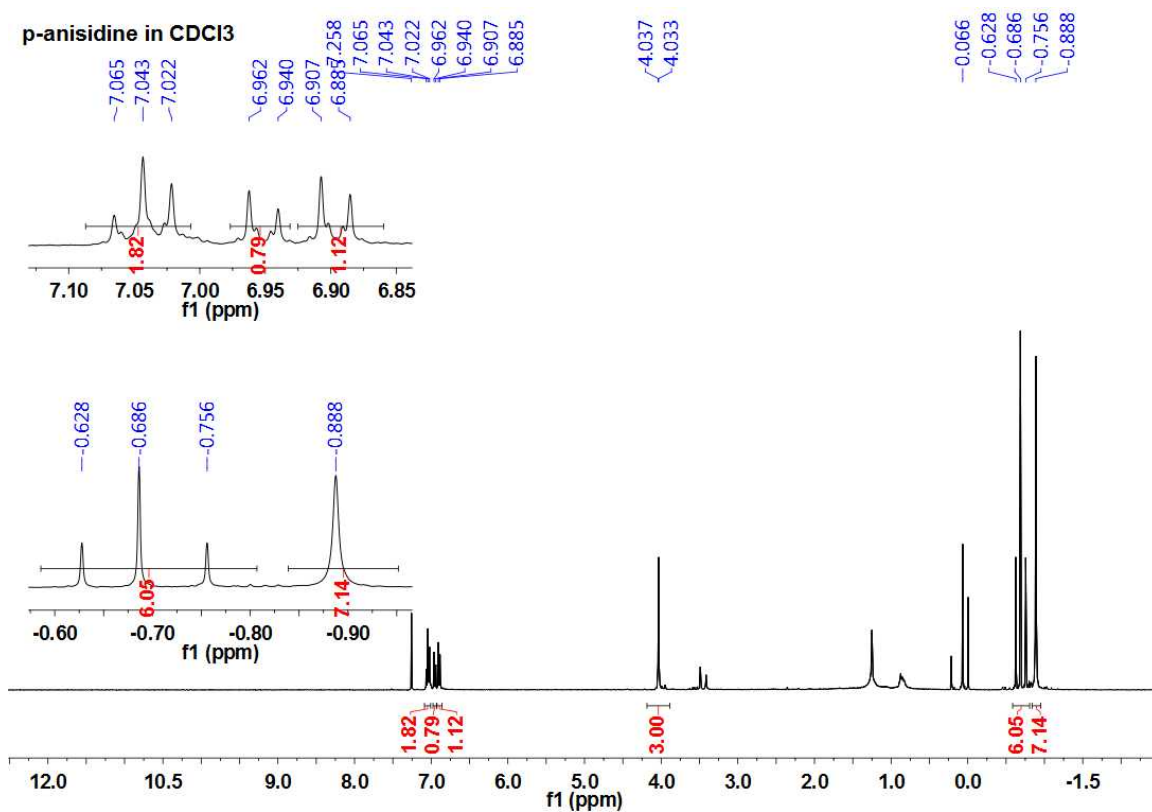


**Figure 16.** <sup>1</sup>H NMR of {[1,4-(Me<sub>3</sub>AlOMe),NH-C<sub>6</sub>H<sub>4</sub>](μ-Me<sub>2</sub>Al)}<sub>2</sub> (3).

#### 4.2.2 Ring opening polymerization.

Typical polymerization procedures in the presence of one equivalent of benzyl alcohol (Table 4, run 1) are as follows. A toluene solution of **3** (0.010 mmol, 1.0 mL toluene) and BnOH (0.010 mmol) were added into a Schlenk tube in the glove-box at room temperature. The solution was stirred for 2 min, and then  $\epsilon$ -caprolactone (2.5 mmol) along with 1.5 mL toluene was added to the solution. The reaction mixture was then placed into an oil bath pre-heated to the required temperature, and the solution was stirred for the prescribed time. The polymerization mixture was then quenched by addition of an excess of glacial acetic acid (0.2 mL) into the solution, and the resultant solution was then poured into methanol (200 mL). The resultant polymer was then collected on filter paper and was dried *in vacuo*. Figure 17 and 18 are  $^1\text{H}$  NMR of  $\epsilon$ -caprolactone before and after ring opening polymerization. Peaks around 4.17 ppm have been gone after ring opening polymerization and peaks around 4.00 ppm have shown, which indicate the conversion of monomer to polymer.

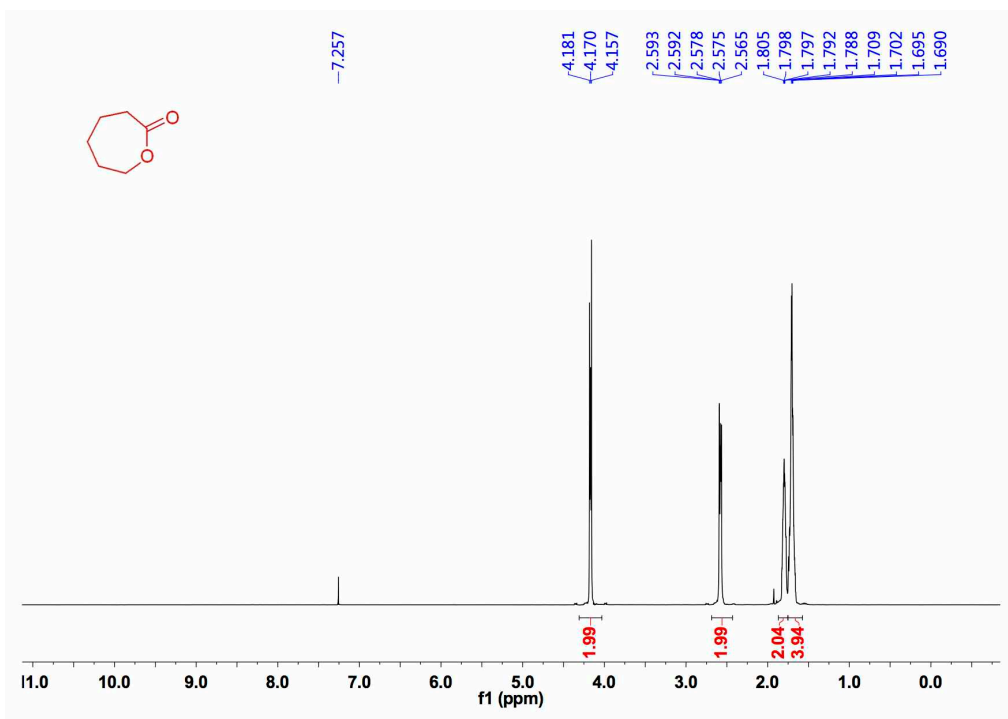


**Figure 17.**  $^1\text{H}$  NMR of  $\epsilon$ -caprolactone.

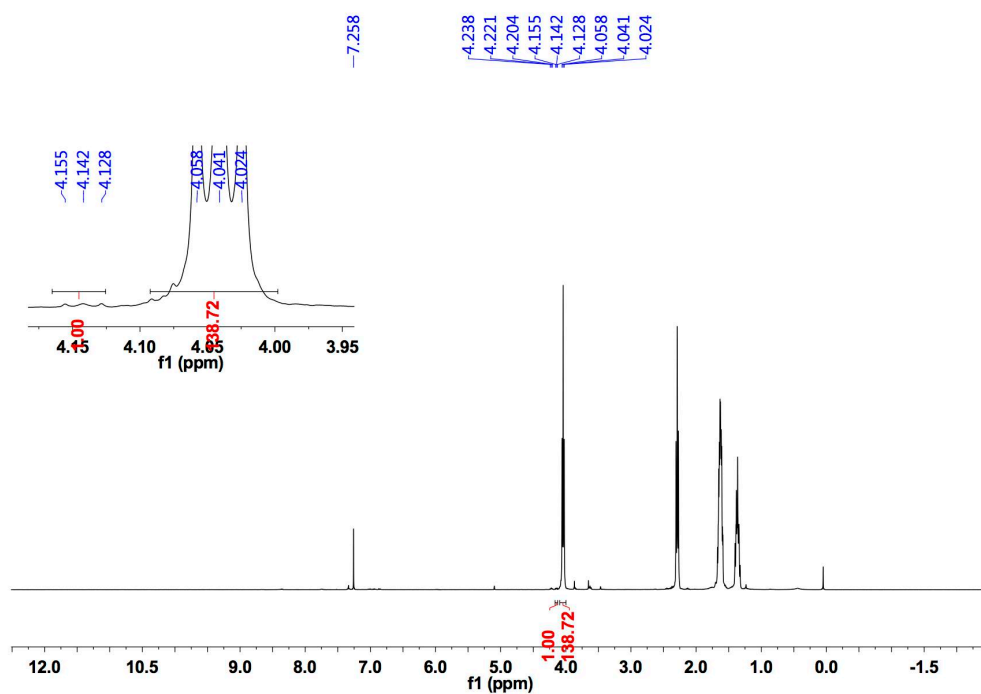


**Figure 18.**  $^1\text{H}$  NMR of  $\epsilon$ -caprolactone after ring opening polymerization using **1** 80°C for 30 minutes.

### 4.2.3 Crystallography

Crystal data for **3** were collected on a Stoe IPDS2 diffractometer using  $1^\circ$   $\omega$ -scans. A face index correction was applied.

Structures were solved by direct methods and refined by full matrix least squares on  $F^2$ . H atoms were included in a riding model except for H(6) in **1**, H(1) in **3**, for which coordinates were freely refined. Hydrogen atom  $U_{\text{iso}}$  values were constrained to be 120 % of that of the carrier atom except for methyl, ammonium, and hydroxyl-H (150 %). CCDC 986715, 986716, and 986717 contain the supplementary crystallographic data for this paper. These data can be obtained free of charge via (please use the link below) by e-mailing [data\\_request@ccdc.cam.ac.uk](mailto:data_request@ccdc.cam.ac.uk), or by contacting: The Cambridge Crystallographic Data Centre, 12 Union Road, Cambridge.CB2 1EZ,UK. Fax: +44(0)1223-336033. [www.ccdc.cam.ac.uk/data\\_request/cif](http://www.ccdc.cam.ac.uk/data_request/cif)

### 4.3. Organotungsten complexes of calix[6 and 8]arenes

#### 4.3.1 Synthesis of calixarene.

##### 4.3.1.1 Synthesis of calix[8]arene

A slurry prepared from 10 g (0.067 mol) of *p*-*tert*-butylphenol, 3.5 g (ca. 0.11 mol) of paraformaldehyde, and 1.0 mL (0.01 mol) of 10 *N* sodium hydroxide in 60 mL of xylene were placed in a 250 mL, round-bottomed, three-necked flask fitted with a Dean–Stark water collector and a gas connector. The air in the flask was replaced with nitrogen by Schlenk technique, and the stirred contents of the flask are heated to reflux. The reaction mixture was refluxed for about 4 h. The mixture is allowed to cool to room temperature, and the precipitate was removed by filtration. After that the crude product was washed, in succession, with 40mL portions of toluene, ether, acetone, and water and is then dried under reduced pressure. It was dissolved in *ca.* 160 mL of boiling chloroform. The chloroform is concentrated to *ca.* 120 mL, the solution is cooled to room temperature, and the precipitate was collected by filtration, isolated yield 10.8 g, 88 %.

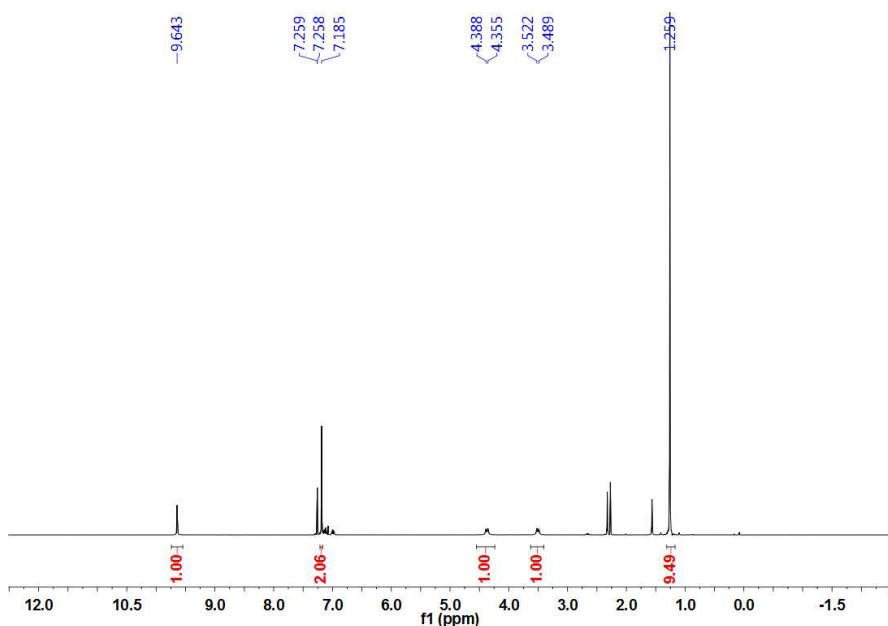


**Figure 19.**  $^1\text{H}$  NMR of Calix[8]arene.

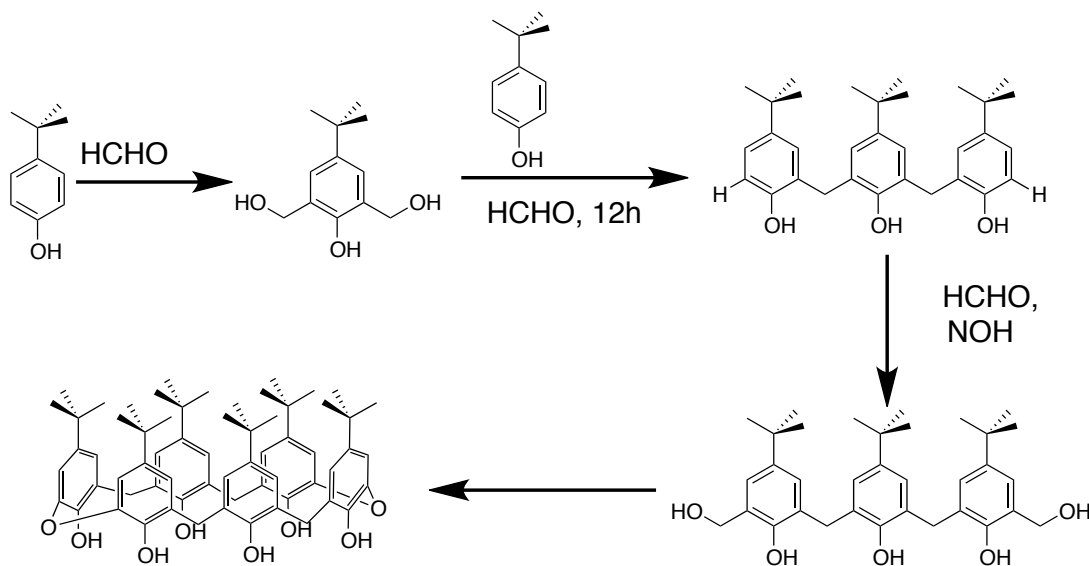


#### 4.3.1.2 Synthesis of cali[6]arene

A 200mL, three-necked, round-bottomed flask equipped with a nitrogen inlet. To the flask 10 g (0.665 mol) of *p-tert*-butylphenol, 13.5 mL of 37 % formalin solution (1.8 mol of HCHO), and 15 g (0.227 mol) of potassium hydroxide pellets was added. Heating and stirring begun, and after 15 min nitrogen was blown across the reaction mixture at a brisk rate and out through the condenser on top of the Dean–Stark trap; the reaction mixture was heated and stirred for 2 h. As the reaction progresses, the originally clear solution turned bright lemon yellow and, as water is removed, the reaction mixture eventually changes to a thick, golden-yellow mass. During this period some frothing occurred, and the reaction mixture expanded somewhat before shrinking to the original volume. Xylene (100 mL) is now added to the flask to dissolve the semisolid mass and gave a yellow solution that is brought quickly to reflux by increasing the temperature of the heating mantle. After 30 min a precipitate began to form, and the colour of the reaction mixture changes from yellow to orange. Refluxing is continued for 3 h, the heating mantle was removed, and the mixture was allowed to cool to room temperature. The mixture was filtered, and the precipitate was washed with xylene and dried on a Büchner funnel to yield 10.5–11.0 g of crude, colourless product. This material was powdered, placed in an Erlenmeyer flask, dissolved in 250 mL of chloroform (not completely soluble), and treated with 80 mL of 1 *N* hydrochloric acid. After 10–15 min the stirred solution turned yellow to light orange; stirring was continued for an additional 10 min, and the mixture is transferred to a separating funnel. The chloroform layer was drawn off, the aqueous layer was extracted with an additional 25 mL of chloroform, and the combined chloroform extracts were washed once with water and dried over magnesium sulfate. Magnesium sulfate was removed by filtration, the chloroform solution was concentrated to ca. 100 mL by boiling, and 100 mL of hot acetone was added to the boiling chloroform solution. The mixture was allowed to cool and is then filtered, isolated yield 7.5 g, 71 %.

#### 4.3.1.3 Synthesis of *p-tert*-butyltetrahomodioxacalix[6]areneH<sub>6</sub>

In order to make the tetrahomodioxacalix[6]arene, Reaction of 3-[3-[3-Hydroxymethyl]-5-*tert*-butylsalicyl]-5-*tert*-butylsalicyl-5-*tert*-butyl-2-hydroxybenzyl alcohol in xylene was needed. To make 3-[3-[3-Hydroxymethyl]-5-*tert*-butylsalicyl]-5-*tert*-butylsalicyl-5-*tert*-butyl-2-hydroxybenzyl alcohol the procedures are as below.



**Scheme 29.** Schematic retranlation of synthesis tetrahomodioxacalix[6]arene.

The first step for making 2,6-bis-hydroxymethyl-4-*tert*-butylphenol takes 7 days of reaction time. This compound was prepared by a slight modification of a literature procedure.<sup>1</sup> To a solution of NaOH (2.0 g, 0.05 mol) in H<sub>2</sub>O (18 mL) was added 4-*tert*-butylphenol **1** (7.5 g, 0.05 mol), the suspension was slightly heated to give a clear solution. The solution was cooled to 0 °C and 37% formaldehyde (7.5 mL, 0.1 mol) was added drop wise under stirring. The mixture was stirred at room temperature for seven days. To complete the precipitation, NaCl (8.5 g) was added and the precipitate was filtered off and suspended in 100 mL of H<sub>2</sub>O. The suspension was cooled and 5 % aq HCl was added. The resulting white suspension was extracted four times with CH<sub>2</sub>Cl<sub>2</sub> and the

combined organic phases were dried ( $\text{Na}_2\text{SO}_4$ ). The crude product was column chromatographed [ $\text{SiO}_2$ , eluent AcOEt/petroleum ether 40–60 degree (gradient 1:80 to 1:10)] to afford 2,6-bis-hydroxymethyl-4-*tert*-butylphenol **2** (7.3 g, 68 %). Then *p-tert*-butylphenol was dissolved in toluene, treat with *p*-toluenesulfonic acid, and slowly add **2** after reflux. After reacting for 18 h a white powder was afforded. Instead of recrystallizing from toluene, wash with cold toluene four more times. Yield 40.12g (86 %) of a white powder **3**.  $^1\text{H}$  NMR ( $\text{CDCl}_3$ ) 6.65-7.40 (m, 10, *ArH* and *OH*), 3.9 (s, 4,  $\text{CH}_2$ ), 1.26 (2 s, 27, *t*Bu).

A mixture of **3**, HCHO, NaOH, and methanol was heated at 50 °C (+- 3 degrees) for 24 h in an atmosphere of  $\text{N}_2$ . After cooling and diluting with 300 mL of water, the mixture was acidified with 50 mL of cold 10 N HCl, and a white solid was removed by filtration. This was dissolved in  $\text{CHCl}_3$ , and stirred with 100 mL of 1 N HCl, and the organic layer was separated, dried over anhydrous  $\text{Na}_2\text{SO}_4$ , and evaporated to give a sticky mass, which, when triturated with petroleum ether, gave 11.9 g (98 %) of a white solid **4**, mp 140-142.5 °C.  $^1\text{H}$  NMR ( $\text{CDCl}_3$ ) 6.86-7.30 (m, 6H, *ArH*), 4.74 (s, 4H,  $\text{COH}_2$ ), 3.88 (s, 4H,  $\text{CH}_2$ ), 1.26 (m, 27H, *t*Bu).

Then the mixture of **4** (10.0 g, 18.7 mmol) and xylene (40 mL) was heated at 120 °C and magnetically stirred under a nitrogen atmosphere for 8 h heating the cooled reaction mixture was filtered and the solid washed twice with xylene, then obtain the *p-tert*-butyltetrahomodioxacalix[6]arene $\text{H}_6$ .

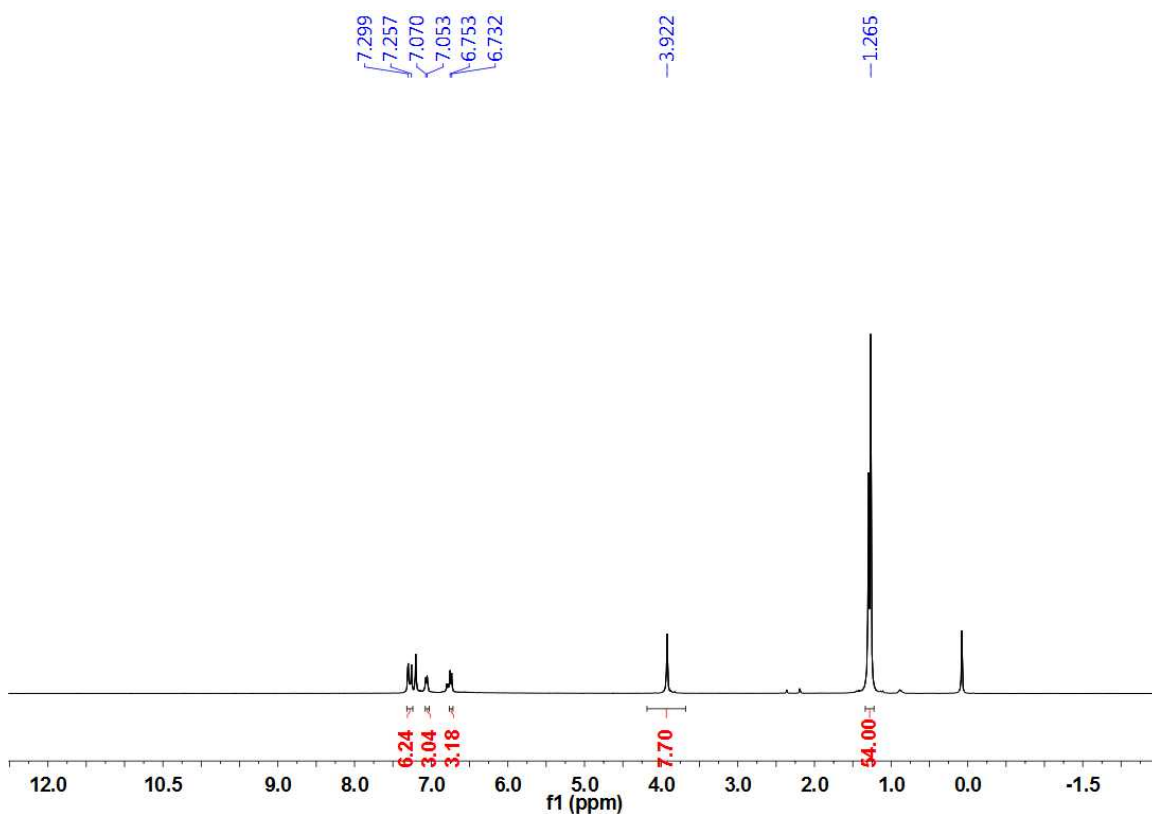
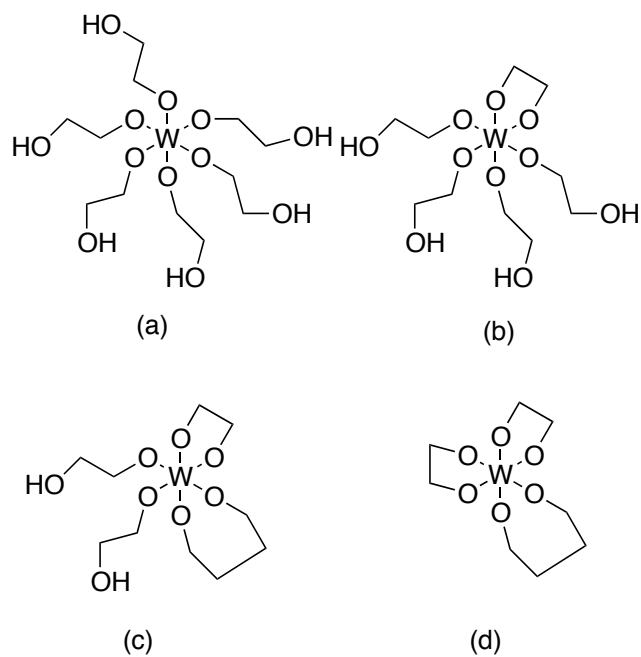


**Figure 20.**  $^1\text{H}$  NMR of *p-tert*-butyltetrahomodioxacalix[6]areneH<sub>6</sub>

#### 4.3.2 Synthesis of [W(eg)<sub>3</sub>]

The precursor [W(eg)<sub>3</sub>] was prepared via the modification method of Lehtonen and Sillanpää.<sup>2</sup> 5g of tungsten acid was added to 30ml of ethylene glycol. The reaction was heated at 150 °C for 16 h instead of 30 min. After that, the ethylene glycol was removed *in-vacuo*, the residue was extracted into hot (brought to reflux with a heat gun) chloroform (100 ml). White solid has been obtained after chloroform removed *in-vacuo*. The reaction turned from yellow solution to white solution after 30 min. However, when stopped reaction after 30 min, no eg was attached **(a)**. After 3 h, only one eg is attached **(b)**. 2 eg after 8 h **(c)**. Finally have W(eg)<sub>3</sub> **(d)** after 16 h when solution turned to white and sometime with a slight light blue coloration.



**Scheme 30.** Schematic representation of  $W(eg)_3$  (**d**) and its by-products (**a**), (**b**) and (**c**).

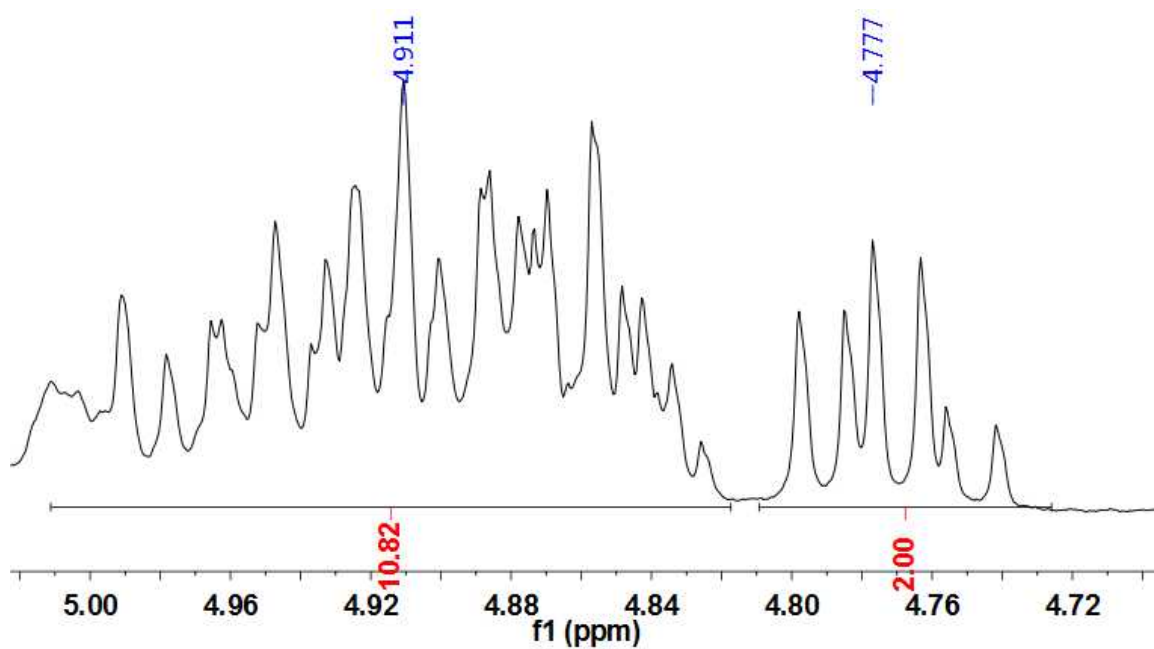


**Figure 21.** Partial  $^1H$  NMR of  $W(eg)_3$  indicates 12 H are observed for  $OCH_2$ .

### 4.3.3 Synthesis of Tungstocalixarene complexes

#### 4.3.3.1 Synthesis of $\{[W(eg)_2]_2p\text{-tert-butylcalix}[6]\text{areneH}_2\} \cdot \text{MeCN}$ (2)

Toluene (30 ml) was added to a Schlenk containing *p-tert-butylcalix*[6]*areneH*<sub>6</sub> (1.40 g, 1.44 mmol) and  $[W(eg)_3]$  (1.40 g, 2.91 mmol) and activated molecular sieves. After refluxing for 12 h, the volatiles were removed *in-vacuo*, and the residue was extracted into hot (brought to reflux with a heat gun) acetonitrile (30 ml). Prolonged standing (2-3 days) at ambient temperature afforded red prisms. Yield 1.06 g, 44.9 %.

#### 4.3.3.2 Synthesis of $\{1,2-[W(eg)_2]_2p\text{-tert-butylcalix}[8]\text{areneH}_4\} /$

#### $\{1,3-[W(eg)_2]_2p\text{-tert-butylcalix}[8]\text{areneH}_4\} (4a)/(4b) \cdot 3.5\text{MeCN}$

Toluene (30 ml) was added to a Schlenk containing *p-tert-butylcalix*[8]*areneH*<sub>8</sub> (1.00 g, 0.78 mmol) and  $[W(eg)_3]$  (1.11 g, 3.10 mmol) and activated molecular sieves. After refluxing for 12 h, the volatiles were removed *in-vacuo*, and the residue was extracted into hot (brought to reflux with a heat gun) acetonitrile (30 ml). Prolonged standing (2-3 days) at ambient temperature afforded red prisms. Yield 1.27 g, 79.4 %.

#### 4.3.3.3 Synthesis of $\{[WO(eg)]_2p\text{-tert-butyltetrahomodioxacalix}[6]\text{areneH}_2\}$ (5)

Toluene (30 ml) was added to a Schlenk containing *p-tert-butyltetrahomodioxacalix*[6]*areneH*<sub>6</sub> (0.50 g, 0.49 mmol) and  $[W(eg)_3]$  (0.36 g, 1.01 mmol). After refluxing for 12 h, the volatiles were removed *in-vacuo*, and the residue was extracted into hot (brought to reflux with a heat gun)

acetonitrile (30 ml). Prolonged standing (2-3 days) at ambient temperature afforded red prisms. Yield 0.56 g, 69.1 %. Elemental analysis calculated for **5**, C<sub>72</sub>H<sub>92</sub>O<sub>14</sub>W<sub>2</sub> (sample dried *in-vacuo* for 12 h): C 56.0, H, 6.0 %; Found C 55.6, H 6.1%. IR (nujol mull, KBr): 3170 bw, 1635 w, 1304 s, 1155 m, 1077 m, 965 m, 892 m, 846 w, 770 m, 723 s. Mass Spec (EI): 1269 (M<sup>+</sup> - W(O)(eg)). <sup>1</sup>H NMR (C<sub>6</sub>D<sub>6</sub>, 500 MHz) δ: 7.52 (m, 2H, arylH), 7.28 (m, 2H, arylH), 7.22 (m, 2H, arylH), 7.16 (m, 2H, arylH), 7.00 (m, 2H, arylH), 6.86 (m, 2H, arylH), 5.63 (m, 4H, OCH<sub>2</sub>), 5.20 (m, 4H, OCH<sub>2</sub>), 4.97 (m, 2H, OCH<sub>2</sub>), 4.88 (m, 4H, OCH<sub>2</sub>), 4.78 (m, 2H, OCH<sub>2</sub>), 3.96 (overlapping d, 4H, *endo*-CH<sub>2</sub>), 3.74 (overlapping d, 4H, *exo*-CH<sub>2</sub>), 2.06 (s, CH<sub>3</sub>CN), 1.24 (m, 54H, C(CH<sub>3</sub>)<sub>3</sub>).

#### 4.3.4 Ring opening polymerization.

Typical polymerization procedures in the presence of one equivalent of benzyl alcohol (Table 2, run 1) are as follows. A toluene solution of **3** (0.010 mmol, 1.0 mL toluene) and BnOH (0.010 mmol) were added into a Schlenk tube in the glove-box at room temperature. The solution was stirred for 2 min, and then ε-caprolactone (2.5 mmol) along with 1.5 mL toluene was added to the solution. The reaction mixture was then placed into an oil bath pre-heated at 110 °C, and the solution was stirred for the prescribed time (24 h). The polymerization mixture was then quenched by addition of an excess of glacial acetic acid (0.2 mL) into the solution, and the resultant solution was then poured into methanol (200 mL). The resultant polymer was then collected on filter paper and was dried *in vacuo*.

### 4.3.5 Crystallography

Data collected on a Bruker APEX 2 CCD diffractometer at Daresbury SRS station 9.8. The *tert*-butyl groups at C(92) and C(114) are disordered over two sets of positions. The MeCNs in the calixarene caviies were well defined and were modelled as point atoms. Platon squeeze was used to model two other MeCN molecules per unit cell (half per complex molecule) as diffuse electron density. Analysis of electron density peaks suggested the presence of two additional MeCNs in the asymmetric unit, probably at low occupancy or significantly disordered. The two large residual electron desity peaks close to two of the four unique tungsten centres could result from pseudo c symmetry or a less than ideal adsorption correction. For **4**: Data collected on a Bruker APEX 2 CCD diffractometer at Daresbury SRS station 9.8. The *tert*-butyl groups at C(92) and C(114) are disordered at C(18), C(29), C(40) and C(51) with methyl groups split over two sets of positions. One MeCN was 50/50 disordered over a centre of symmetry.



#### 4.4 Reference

1. (a) B. Dhawan, C. D. Gutshe, *J. Org. Chem.*, 1983, **48**, 1536-1539; (b) B. Masci, *J. Org. Chem.*, 2001, **66**, 1497-1499
2. A. Lehtonen, R. Sillanpaa, *Polyhedron*, 1994, **13**, 2519-2524.

## Appendix

### Crystallographic data for complexes **1**, **2** and **3** (Chapter 2.).

Identification code	<b>1</b>	<b>2</b>	<b>3</b>
Chemical formula	C <sub>22</sub> H <sub>38</sub> Al <sub>4</sub> N <sub>2</sub> O <sub>2</sub>	C <sub>24</sub> H <sub>46</sub> Al <sub>4</sub> N <sub>2</sub> O <sub>2</sub> ·C <sub>7</sub> H <sub>8</sub>	C <sub>24</sub> H <sub>46</sub> Al <sub>4</sub> N <sub>2</sub> O <sub>2</sub>
Formula weight	470.46	594.68	502.55
Temperature K	150(2)	150(2)	150(2)
Radiation MoK $\alpha$ , wavelength/ Å	0.71073	0.71073 Å	0.71073 Å
Crystal system, space group	monoclinic, P21/n	monoclinic, P21/n	triclinic, P-1
a/ Å	8.7510(7)	7.1092(4)	7.3610(9)
b/ Å	15.3173(12)	21.2450(12)	10.0951(12)
c/ Å	10.1026(8)	12.3300(7)	10.6561(14)
$\alpha$ /°	90	90	103.037(10)
$\beta$ /°	90.133(2)	92.839(2)	95.097(10)
$\gamma$ /°	90	90	96.205(10)
V/ Å <sup>3</sup>	1354.17(19)	1859.98(18)	761.67(16)
Z	2	2	1
Calculated density Mg m <sup>-3</sup>	1.154	1.085	1.096
Absorption coefficient $\mu$ / mm <sup>-1</sup>	0.19	0.15	0.17
F(000)	504	644	272
Crystal colour	colourless	colourless	colourless
Crystal size	0.61 × 0.30 × 0.09 mm <sup>3</sup>	0.73 × 0.11 × 0.07	0.36 × 0.19 × 0.17
Reflections for cell refinement	6528	6768	5427
Data collection method	Bruker SMART 1000 CCD Diffractionmeter $\omega$ rotation with narrow frames	Bruker SMART 1000 CCD Diffractionmeter $\omega$ rotation with narrow frames	Stoe IPDS2 Diffractionmeter $\omega$ rotation with 1° frames.
$\theta$ range for data collection	2.4 to 28.8°	2.5 to 28.4°	2.0 to 29.2
Index ranges	h -11 to 11, k -20 to 19, l -13 to 13	h -9 to 9, k -28 to 27, l -15 to 16	h -10 to 8, k -13 to 13, l -14 to 14
Completeness to $\theta = 26.00^\circ$	100.0 %	99.9 %	98.4 %
Intensity decay	0 %	0 %	0 %
Reflections collected	11499	15849	7591
Independent reflections	3228 (Rint = 0.0206)	4408 (Rint = 0.0192)	3999 (Rint = 0.0586)
Reflections with $F^2 > 2\sigma$	2703	3453	2412
Absorption correction	semi-empirical from equivalents	semi-empirical from equivalents	face-indexed (Tomba method)
Min. and max. transmission	0.892 and 0.983	0.896 and 0.989	0.9784 and 0.9564
Structure solution	direct methods	direct methods	direct methods
Refinement method	Full-matrix least- squares on F <sup>2</sup>	Full-matrix least- squares on F <sup>2</sup>	Full-matrix least- squares on F <sup>2</sup>
Weighting parameters a, b	0.052, 0.3059	0.0486, 0.7440	0.051, none
Data / restraints / parameters	3228 / 0 / 157	4408 / 52 / 235	3999 / 2 / 154
Final R indices [ $F^2 > 2\sigma$ ]	R1 = 0.033, wR2 = 0.097	0.039 0.107	0.041 0.093
R indices (all data)	R1 = 0.0416, wR2 = 0.0977	0.0592 0.1367	0.0780 0.1026
Goodness-of-fit on F <sup>2</sup>	1.08	1.03	0.859
Largest and mean shift/su	0.001 and 0.000	0.001 and 0.000	0.001 and 0.000
Largest diff. peak and hole/ e Å <sup>-3</sup>	0.3 and -0.22	0.31 and -0.20	0.351 and -0.254

Crystallographic data for complexes **1-5** (Chapter 3.).

Formula	$C_{70}H_{82}O_{11}W_2$	$C_{74}H_{96}O_{14}W_2 \cdot 1.5$	$C_{92}H_{112}O_{12}W_2$	$C_{96}H_{124}O_{16}W_2 \cdot 3.5 \text{ MeCN}$	$C_{72}H_{92}O_{14}W_2 \cdot 0.83 \text{ PhMe, MeCN}$
Compound	<b>1</b>	<b>2</b>	<b>3</b>	<b>4a/b</b>	<b>5</b>
Formula weight (g mol <sup>-1</sup> )	1471.09	1638.78	1777.52	2045.34	1663.05
Crystal system	Monoclinic	Triclinic	Monoclinic	Triclinic	Monoclinic
Space group	<i>C2</i>	<i>P</i> $\bar{1}$	<i>P2<sub>1</sub>/c</i>	<i>P</i> $\bar{1}$	<i>P2<sub>1</sub>/c</i>
Unit cell dimensions					
<i>a</i> (Å)	23.4741(8)	14.4323 (7)	12.2109(2)	14.8901(11)	19.7129(9)
<i>b</i> (Å)	12.0721(4)	22.4200 (12)	34.2259(5)	17.5516(13)	13.6419(7)
<i>c</i> (Å)	16.8073(5)	25.5537 (13)	20.5984(3)	22.0164(16)	31.4289(16)
$\alpha$ (°)	90	100.6758 (6)	90	112.02119(9)	90
$\beta$ (°)	116.734(4)	90.5674 (7)	92.226(1)	105.3910(10)	104.805(5)
$\gamma$ (°)	90	108.4771(6)	90	93.0486(10)	90
<i>V</i> (Å <sup>3</sup> )	4253.7(2)	7685.6(7)	8602.2(2)	5067.2(6)	8171.3(7)
<i>Z</i>	2	4	4	2	4
Calculated density (Mgm <sup>-3</sup> )	1.149	1.416	1.373	1.341	1.352
Adsorption coefficient (mm <sup>-1</sup> )	2.747	2.67	2.730	2.331	2.871
Transmission factors (max., min)	0.6096, 0.5031	0.924, 0.617	0.7719, 0.6112	0.933, 0.679	0.5975, 0.4796
Crystal size (mm)	0.29 × 0.24 × 0.22	0.20 × 0.09 × 0.03	0.20 × 0.15 × 0.10	0.18 × 0.08 × 0.03	0.30 × 0.20 × 0.20
$\theta_{\text{max}}$ (°)	26.37	30.9	26.37	28.00	28.56
Reflections measured		97130		60220	18607
Unique reflections, <i>R</i> <sub>int</sub>	6695, 6695, 0.0258	51563, 0.045	17552, 17552, 0.0536	31223, 0.0443	18607, 0.0453
Reflections with $F^2 > 2\sigma(F^2)$	5824	42481	14374	20519	12892
Number of parameters	362	1768	979	1435	814
<i>R</i> <sub>1</sub> , <i>wR</i> <sub>2</sub> [ $F^2 > 2\sigma(F^2)$ ]	0.0364, 0.0841	0.057, 0.145	0.0387, 0.0738	0.0763, 0.158	0.0552, 0.1246
GOOF	1.024	1.04	1.067	1.113	1.050
Largest difference peak and hole (e Å <sup>-3</sup> )	1.296 and -0.645	9.10 and -3.26	1.329 and -0.872	1.318 and -2.295	1.034 and -0.884